2013

RNA Interference of CTLA4 in Human Leukaemia T Cells

Ralitsa Vassileva
Technological University Dublin

RNA interference of CTLA4 in human leukaemia T cells

Ralitsa Vassileva

PhD

Dublin Institute of Technology

2013

RNA interference of CTLA4 in human leukaemia T cells

Ralitsa Vassileva, MSc

A thesis submitted for the degree of Doctor of Philosophy

Dr. Jacinta Kelly, Dr. James Curtin

School of Biological Sciences

Dublin Institute of Technology

2013

Abstract

The activation of naive T cells is essential for the initiation of the adaptive immunity. One promising approach to overcome immunological tolerance involves augmenting endogenous T cell-mediated immunity by interrupting the T cell down-regulatory pathways.

In this project a gene therapy delivery system to overexpress small interfering RNA was used to silence the inhibitory signals induced by CTLA4. A small hairpin RNA duplex designed to silence expression of CTLA4 was successfully cloned into a plasmid. A stably transfected T cell line that is expressing constitutively the CTLA4 siRNA has been developed as a model to understand the role of CTLA4 in functional assays. The expression of the mature siRNA in this new cell line was confirmed upon optimization of a real-time quantification by a stem loop RT-PCR method and the downregulation of CTLA4 was detected at the protein and RNA level. The generated cell lines were used to study the role of CTLA4 in T cell activation pathways. It was determined that CTLA4 crosslinking downregulated IL-2 production in the control cell lines. However, silencing of CTLA4 abrogated this effect in the cell line expressing the CTLA4 siRNA. These results suggested that it is possible to modulate T cell activation using RNA interference for CTLA4. CTLA4 crosslinking in combination with CD3 and CD28 ligation did not seem to have an effect on the phosphorylation of ERK or other proteins, which take part in the proximal T cell signaling, like ZAP-70, Lck, SLP-76 and LAT. However, it was found that the c-Jun N-terminal kinase (JNK) activation is up-regulated in the control cell lines. In the stable cell line with silenced CTLA4 expression such effect was not

observed, thus suggesting a role of CTLA4 as a negative regulator in T cell activation via the up-regulation of JNK.

I certify that this thesis which I now submit for examination for the award of Doctor of Philosophy, is entirely my own work and has not been taken from the work of others, save and to the extent that such work has been cited and acknowledged within the text of my work.

This thesis was prepared according to the regulations for postgraduate study by research of the Dublin Institute of Technology and has not been submitted in whole or in part for another award in any other third level institution.

The work reported on in this thesis conforms to the principles and requirements of the DIT's guidelines for ethics in research.

DIT has permission to keep, lend or copy this thesis in whole or in part, on condition that any such use of the material of the thesis be duly acknowledged.

Signature Date

Acknowledgements

I would like to thank to the Graduate Research School, the School of Biology and the supervisors Dr. Jacinta Kelly and Dr. James Curtain for the PhD position.

I would like to thank Dr. Fergus Ryan for the useful advice regarding all molecular biology based experiments and for his help during the daily fight with DIT facilities.

Many, many thanks to Dr. Mike Freeley (TCD) for all the helpful protocols, reagents, advice and discussions regarding all immunological assays and for letting me use their lab facilities.

I am very grateful to the post-grad students and technicians at the School, especially Daireen.

Thanks for Internet and Google!

A big hug for the "Coombe family": Antonin, Caterina, Tomasz, Matteo, Catarina, Francesco, Julia, Pierre, Tina, Maite, Leandro, Alexandre, Vanda, Fabiola, Adam, Dee and Domenico.

Abbreviations

AP-1/2	clathrin-associated adaptor complex 1/2
AP-1	activating protein 1
APC	antigen presenting cells
ARF-1	adenosine diphosphate ribosylation factor-1
CD3	Cluster of differentiation 3
CD28	Cluster of differentiation 28
CMV	Cytomegalovirus
CTLA4	cytotoxic T lymphocyte antigen-4
DAG	diacylglycerol
DC	dendritic cells
DNA	Deoxyribonucleic acid
ERK	extracellular signal-regulated kinase
Gads	Grb2 related adaptor protein
GFP	Green fluorescence protein
Grb2	growth factor receptor-bound protein
IDO	indoleamine 2,3-dioxygenase
IL-2	Interleukin 2
IP_3	inositol (1,4,5) trisphosphate
IS	Immunological synapse
ITAM	immunoreceptor tyrosine-based activation motifs
Itk	IL-2 inducible T-cell kinase
JNK	cJun N-terminal kinase
LAT	linker for activated T cells
Lck	Lymphocyte-specific protein tyrosine kinase
MAPK	mitogen activated protein kinase
MCS	Multiple cloning site
MHC	major histocompatibility complex
miRNA	micro RNAs

mRNA	messenger RNA
NFAT	nuclear factor of activated T cells
NF-κB	nuclear factor-κB
PBMCs	peripheral blood mononuclear cells
PCR	Polymerase chain reaction
PI-3K	phosphoinositide 3-kinases
PI-4,5 P_2	phosphatidylinositol-4,5 bisphosphate
PKB/Akt	protein kinase B
PKC	protein kinase C
PLC-γ	phospholipase C
PLD	phospholipase D
PMA	Phorbol 12-Myristate 13-Acetate
RISC	RNA-induced silencing complex
RNA	Ribonucleic acid
RNAi	RNA interference
RT-PCR	Reverse transcription polymerase chain reaction
Scr	scrambled
SHP-1/2	Src-homology region 2 domain-containing phosphotase-1/2
shRNA	short-hairpin RNA
si	silencing
siRNA	short-interfering RNA
SLP-76	SH2 domain-containing leukocyte protein of 76kd
SMAC	supramolecular activation cluster
Sos	son of sevenless
TCR	T cell receptor
TGN	*trans* Golgi Network
Tregs	T regulatory cells
ZAP-70	Zeta-chain-associated protein kinase 70
3'UTR	3'untranslated region

Table of Contents

Table of Figures

1. Introduction

1.1 Adaptive immunity

Adaptive immunity describes a specific immune response against a particular molecular pattern. It is triggered by cells of the innate immune system like macrophages and dendritic cells (DC) in peripheral lymphoid tissues. There antigens are presented to and recognized by lymphocytes, the cells that mediate the adaptive immune response. B lymphocytes mediate humoral immunity that involves the production of antibodies in response to an antigen. T lymphocytes are responsible for cell-mediated immunity. During its development each lymphocyte generates a unique antigen receptor by somatic gene recombination [1]. The mature naïve lymphocytes enter the bloodstream. The initiation of the adaptive immune response occurs during their circulation through peripheral lymphoid organs such as lymph nodes, spleen and the mucosal lymphoid tissues. Activated antigen presenting cells (APCs) that have encountered and processed an antigen migrate there to meet and activate the naïve lymphocytes. Upon recognition of their specific antigen naïve lymphocytes proliferate and differentiate into effector cells that are actively involved in the elimination of that pathogen. However, this process can take several days before an effect occurs [2]. Another important function is the development of immunological memory which consists of long-lived subsets of the effector cells able to respond rapidly if they encounter the same antigen again [3].

1.2 T cell activation

T cells are activated by the antigen-specific binding between the T cell receptor (TCR) and the peptide-bound major histocompatibility complex (MHC) expressed on APCs like

B cells, dendritic cells and macrophages. A successful activation is dependent also on the interaction between a number of costimulatory and accessory receptors and their ligands which are assembled in a particular way in the contact zone between the T cell and the APC. This contact zone is called the immunological synapse (IS) [4, 5]. The assembly of signaling molecules on the inner leaflet of the T cell membrane is known as supramolecular activation cluster (SMAC). Interactions between adhesion molecules, such as LFA-1 and ICAM-1, determine the initial formation of the IS. Later, according to the kinetic segregation theory, these large molecules together with phosphatases (e.g. CD45) migrate laterally to an outer ring to form the peripheral SMAC. Another group of receptors (e.g. TCR, CD3, MHC, CD28, CD80, CD86) and signaling molecules (e.g. Lck, Fyn, PKCθ, Zap-70) are concentrated in the central zone known as cSMAC [5, 6]. The signaling mediated by the TCR and the costimulatory receptors that results in the activation of T cells involves the activation of three important families of transcription factors: nuclear factor of activated T cells (NFAT), activating protein 1 (AP 1) and nuclear factor-κB (NF-κB). These transcription factors bind to the promoter region of the IL-2 gene and drive its transcription. IL-2 is a cytokine which is produced by the activated T cells. It binds to the IL-2 receptor expressed on the same cells and promotes their proliferation and differentiation [7]. The TCR consists of α and β chains that bind to the ligand, and the CD3 ε, γ and δ and the TCR ζ subunits that are responsible for the signaling [8]. One of the first events that mark the T cell activation is the induction of Src family kinases Lck and Fyn. These phosphorylate the immunoreceptor tyrosine-based activation motifs (ITAMs) that are present in the intracellular domains of the signaling TCR subunits [9]. Upon binding to the phosphorylated ITAMs the protein tyrosine kinase

ZAP-70 is phosphorylated [10]. Two adapter proteins: linker for activated T cells (LAT) and SH2 domain-containing leukocyte protein of 76kd (SLP-76) are able than to associate with ZAP-70 and contribute to the signaling. These adapter proteins lack any intrinsic enzymatic activity, however, they contain several tyrosine-based motifs which upon phosphorylation serve as docking sites for other signaling proteins. Such proteins are PLC-γ1, Grb2, PI-3 kinase, Itk and Gads [11]. The phosphorylation of phospholipase C (PLC) γ1 leads to its activation. PLC-γ1 cleaves phosphatidylinositol-4,5 bisphosphate (PI-4,5-P_2) into inositol (1,4,5) trisphosphate (IP_3), important for Ca^{2+} release from the endoplasmic reticulum and diacylglycerol (DAG), important for protein kinase C (PKC) activation [8]. The increased levels of Ca^{2+} in the cell are important for the activation of calcineurin. Calcineurin is a phosphatase that dephosphorylates members of the NFAT family allowing their translocation to the nucleus and binding to sites of the IL-2 promoter [12]. T cells express several isoforms of the PKC family. PKC θ is the only isoform that can localize to the immunological synapse and is involved in the activation of transcription factors like NF-κB [13, 14]. Another pathway that affects the metabolism of phosphoinositide lipids is mediated by phosphoinositide 3-kinases (PI 3-K). The triggering of this pathway in lymphocytes is associated with the involvement of costimulatory signals, cytokines and chemokines. The intracellular domain of the co-stimulatory receptor CD28 contains motifs that serve as binding sites for several proteins mediating downstream signaling. Upon binding to CD28 and activation, PI-3K phosphorylates the D3-hydroxyl position of the inositol ring, thereby converting PI-4,5-P_2 and PI-4-P to PI-3,4,5-P_3 and PI-3,4-P_2, respectively [15]. The resulting phospholipids can bind to the plextrin homology (PH) domain of PLC-γ1, Tec, PDK-1, protein kinase B

(PKB/Akt) and serve as an anchor to the plasma membrane for these proteins [16]. Another protein important for the activation of the IL-2 promoter is Ras. Ras is activated by the guanine nucleotide exchange factor son of sevenless (SOS) which is associated via the adaptor protein growth factor receptor-bound protein (Grb2) to LAT [17]. Other groups have shown also the ability of Grb2 to bind to CD28, thus potentiating IL-2 production [18]. Once activated Ras initiates the activation of several pathways mediated by the mitogen activated protein kinase (MAPK) family. The extracellular signal-regulated kinase (ERK) cascade which belongs to this family plays an essential role in the phosphorylation of transcription factors like c-Fos and c-myc [19]. The cJun N-terminal kinase (JNK) cascade is also a member of the MAPK family and is important for the transcriptional regulation of Jun proteins. Members of the Jun and Fos proteins combine in the nucleus to form AP-1 dimers that contribute to the regulation of the IL-2 gene [20]. Another transcription factor required for IL-2 production is NF-κB. The NF-κB signaling complex resides in the cytosol and its activation leads to the release of transcription factors c-Rel, RelB, RelA (p65), p50 and p52 in the nucleus where they can bind to the CD28 response element in the IL-2 promoter [21]. Another target is the bcl-xL promoter, which indicates a role of NF-κB signaling in cell survival [22]. It has been suggested that both NF-κB and JNK activation are dependent on CD28 costimulation [23]. A schematic representation of the main signaling pathways involved in T cell receptor signaling is shown on figure 1.1.

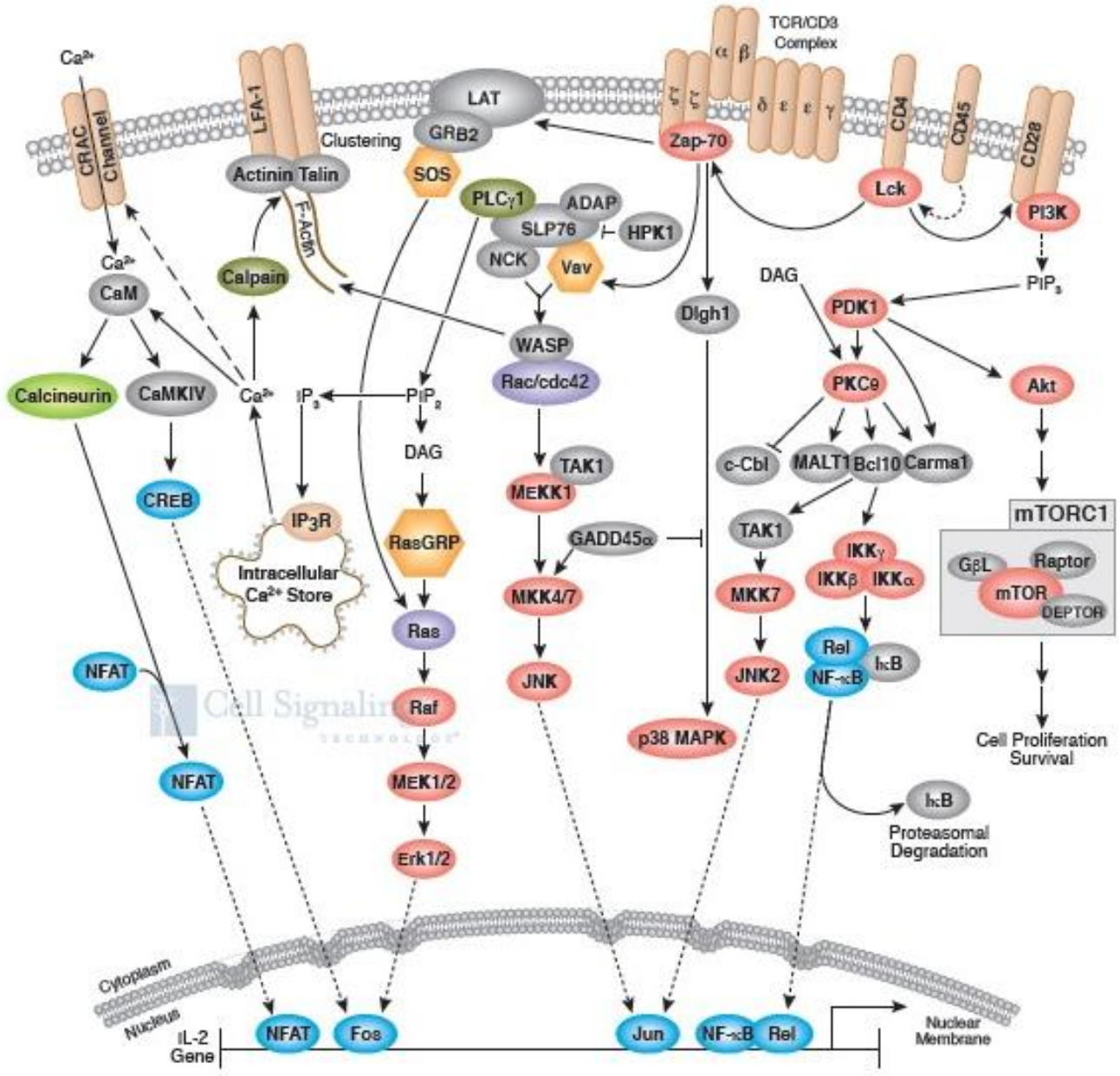

Cell Signaling Technology

Figure 1.1 T cell receptor signalling.

TCR signalling is initiated upon binding of the peptide/MHC complex to the TCR/CD3 complex. The signalling pathways mediated by the TCR and costimulatory receptor CD28 result in activation of transcription factors (NFAT, Fos, Jun, NF-κB) that bind to the promoter of the IL-2 gene and induce its expression.

1.3 CTLA4

The balance of stimulatory and inhibitory signals is crucial to maximise protective immune responses while maintaining immunological tolerance and preventing autoimmunity. CD28 and cytotoxic T lymphocyte antigen-4 (CTLA4/ CD152) are the two homologous members of the immunoglobulin superfamily that are the key receptors for this regulation via positive and negative costimulation. The essential inhibitory role of CTLA4 was demonstrated by the phenotype of CTLA4-deficient mice that died of a lymphoproliferative disease within 3 weeks of age [24]. This also indicates the involvement of CTLA4 in protection against autoproliferative and autoimmune disorders. In humans several CTLA4 gene polymorphism, described later, have been identified and associated with susceptibility to autoimmune diseases.

The CTLA4 gene is located on chromosome 2 in humans and on chromosome 1 in mice and consists of four exons. Four different isoforms can be generated by alternate splicing of the mRNA transcript (Fig. 1.2 A) [25]. The most characterised one is the full length protein. This type I transmembrane protein consists of three domains and a leader peptide and is expressed as a homodimer on the cell surface. The leader peptide is encoded by exon 1 and the ligand binding site by exon 2, which are both part of the extracellular region of the molecule. Exon 3 corresponds to the transmembrane domain and exon 4 to the cytoplasmatic tail [26]. Another transcript of the gene detected in humans is the soluble CTLA4 (sCTLA4) that does not contain the transmembrane region [27]. Its potential for immunomodulation has been studied and associated with autoimmune diseases [28]. However, other studies question if the protein recognised by

CTLA4 specific antibodies in human plasma is a direct product of the CTLA4 gene [29]. An additional transcript known as ligand-independent CTLA4 (liCTLA4) that consists of exon 1, 3 and 4 has been found in mouse but not in human [30].

Several CTLA4 gene polymorphisms have been described (Fig. 1.2 B). Three of them have been studied more extensively. A single nucleotide polymorphism (SNP) A/G at position 49 in the first exon leads to a change of an amino acid in the leader peptide from threonine to alanine and has been associated with susceptibility to autoimmune diseases like Graves' disease [31]. The C-318T polymorphism in the promoter region has been associated with increased CTLA4 expression. An AT dinucleotide repeat has been identified in the 3' UTR region. Exactly how these polymorphisms affect CTLA4 function and susceptibility to autoimmune diseases is still unclear.

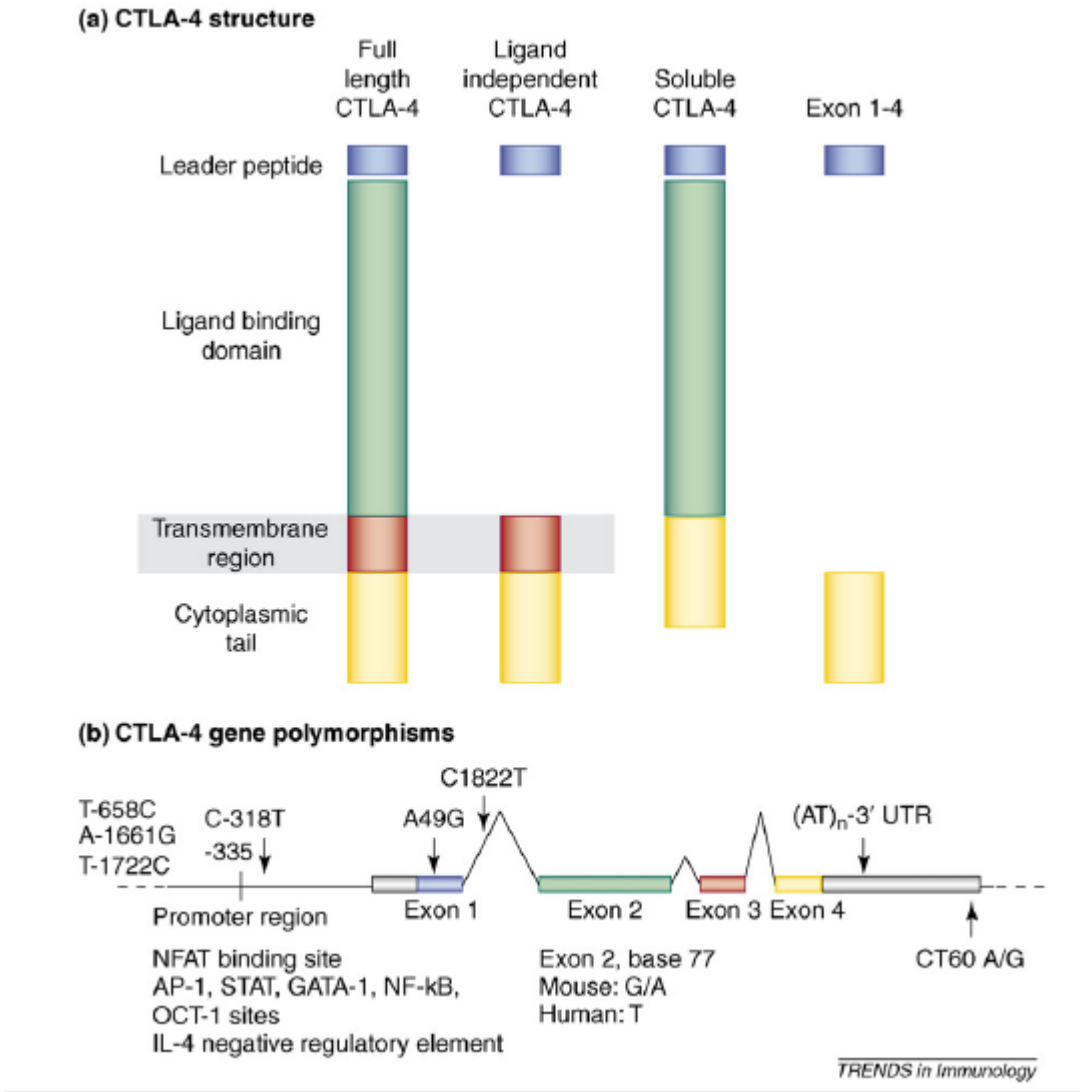

Valk *et al.*, 2008 [25]

Figure 1.2 CTLA4 structure.

The CTLA4 protein consists of a leader peptide (encoded by exon 1), a ligand binding domain (encoded by exon 2), a transmembrane domain (encoded by exon 3) and a cytoplasmic tail (encoded by exon 4). (A) CTLA4 possible isoforms: full length CTLA4 (exon 1, 2, 3 and 4); ligand independent CTLA4 (exon 1, 2 and 4, murine only); soluble CTLA4 (exon 1, 2 and 3); an isoform consisting of exon 1 and 4. (B) Gene structure of CTLA4 with identified polymorphisms. Several gene polymorphisms have been associated with autoimmune diseases.

1.3.1 CTLA4 localization and trafficking

The full length protein CTLA4 that is expressed in activated T cells has been widely studied. In naïve T cells intracellular CTLA4 is detectable at low levels and only upon stimulation the amount of the protein starts to increase steadily. However, the majority of CTLA4 is stored intracellular and surface expression does not peak until 48-72 hours after T cell activation [32]. An exception is the subset of regulatory T cells (CD4+CD25+Foxp3+) that express CTLA4 constitutively on the cell surface [33].

The majority of the protein is localized in several intracellular compartments: the *trans* Golgi network (TGN), endosomes and lysosomes [34]. The mechanism of the translocation of the molecule to the cell surface is tightly regulated and of key importance for the regulation of the immune response (Fig.1.3). So far it is considered that only when the receptor is expressed at the surface it has an impact on the T cell activation. It has been shown that the TCR-interacting molecule (TRIM) expressed in T cells and NK cell acts as a chaperone during CTLA4 trafficking to the cell surface. Newly synthesized CTLA4 binds to T-cell receptor-interacting molecule (TRIM) in the TGN promoting the formation of CTLA4-containing vesicles and their transport to the cell surface [35]. Valk *et al*. showed that CTLA4 and TRIM colocalize in the TGN but not on the cell surface or in endosomes. Downregulation of TRIM by short-hairpin RNA inhibited CTLA4 surface expression and restricted it to the TGN, while the expression of TCR and CD28 was unaffected. However, the mild phenotype of TRIM-deficient mice suggests that there are other proteins that compensate the absence of TRIM [36]. The externalisation of CTLA4 is also dependent on the activity of guanosine triphosphatases (GTPase), adenosine

diphosphate ribosylation factor-1 (ARF-1) and phospholipase D (PLD). ARF family GTPases and PLD are associated with the budding of vesicles at the Golgi apparatus [37]. Clathrin adapter heterotetrameric complexes AP-1 and AP-2 are involved in the selective recognition and recruitment of proteins into coated pits. AP-2 is known to mediate the endocytosis of multiple receptors that contain specific internalisation signals such as tyrosin-based motifs in their cytoplasmic domains [38]. The cytoplasmic tail of CTLA4 has a homology to CD28 and contains a Gly-Val-Tyr-Val-Lys-Met (GVYVKM) motif for AP-2 binding. Upon dephosphorylation of the tyrosine residue (Y201) in this sequence, AP-2 binding to CTLA4 mediates its internalisation to endosomal and lysosomal compartments [39]. Within the same sequence, however, the YVKM motif, when phosphorylated, represents a binding site for PI3K, SHP-2 and PP2A [40, 41]. Members of the Src family tyrosine kinases Fyn and Lck associate with the TCR and co-receptor complex and phosphorylate the tyrosine residues on CD3 and ζ chain of the TCR ITAMs, allowing ZAP-70 to bind and promoting T cell activation [42]. Lck and Fyn can also phosphorylate the YVKM motif of the CTLA-4 receptor, allowing binding of PI3K or SHP-2 to CTLA4, preventing AP-2 binding, which promotes its surface retention [43]. In this way phosphorylation and dephosphorylation of Y201 could regulate the balance between CTLA4 trafficking and signalling. In contrast, AP-1 binds to Golgi-associated CTLA4 via the same non-phosphorylated GVYKM motif as AP-2. The AP-1 complex is structurally similar to the AP-2 complex, but is localised in the TGN. When it associates with CTLA4, it mediates the shuttling from the TGN to endosomal and lysosomal compartments for degradation [39].

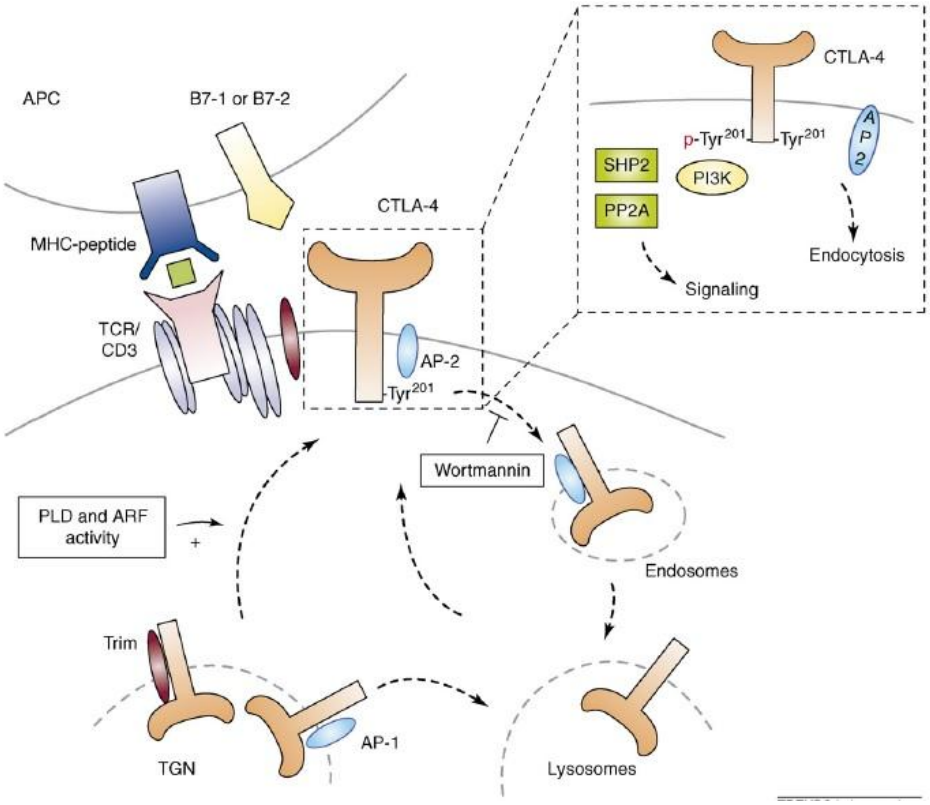

Valk *et al*., 2008 [25]

Figure 1.3 CTLA-4 trafficking.

Newly synthesised CTLA4 can bind to the transmembrane protein TRIM in the TGN which mediates cell surface expression. Phospholipase D (PLD) and GTPase ADP ribolysation factor-1 (ARF) activity also promote CTLA4 externalisation. On the other hand, CTLA4 in TGN can also bind to clathrin-adaptor protein 1 (AP-1) which mediates its transport to lysosomal compartments. Surface expression of CTLA4 is stabilised by phosphorylation at the tyrosine 201 of the cytoplasmic tail, which represents a binding site for PI3K, SHP2 and PP2A. Clathrin-adaptor protein 2 (AP-2) can bind to the dephosphorylated tyrosine 201 and mediate CTLA4 internalisation.

1.3.2 CTLA-4 mediated signalling

The exact mechanism by which CD28 and CTLA-4 transmit their respective signals is still being investigated. Both receptors have structural similarity, but opposing effect on T-cell immunity. CD28 and CTLA-4 share the same ligands, CD80 (B7-1) and CD86

(B7-2) which are expressed on APCs. CD86 is constitutively expressed on dendritic cells, macrophages and B cells and is further upregulated upon activation. CD80 is absent from resting cells and is expressed only on activated APCs [44]. CD80 is expressed as a dimer and it is suggested that the molecule has stronger affinity to its ligands compared to the monomer CD86 [45]. Since CTLA4 is also expressed as a dimer this allows a bivalent binding to CD80 and the building of a lattice like network, which is considered to be the strongest possible interaction between the costimulatory molecules and their ligands [45]. Different studies provide evidence that CD80 and CD86 have distinct abilities to induce T cell stimulation and identify CD80 as the major ligand for CTLA4. Experiments with T cells stimulated with transfectants expressing either CD80 or CD86 revealed that CD80 is a more potent costimulator inducing initial cell division than CD86. Upon consequent expression of CTLA4 however the T cells divided at a slower rate, which could be reversed by the addition of a blocking CTLA4 antibody to the cultures [46].

It is considered that CTLA4 can influence both T cell immune responses through cell extrinsic and intrinsic pathways. Cell extrinsic models include the secretion of soluble CTLA4 (sCTLA4), capturing/removing of ligands from APC by CTLA4, the production of indoleamine 2,3-dioxygenase (IDO) and the involvement of Treg cells [27, 47-49]. The cell intrinsic mechanisms include the competition with CD28 for the same ligands, the role of associated phosphatases, blockade of lipid-raft expression and microcluster formation and direct negative signalling [50-52].

One of the suggested models is that once present in the IS CTLA4 outcompetes CD28 due to its stronger affinity and avidity for the same ligands. A lot of studies have focused to investigate a mechanism mediated directly through the cytoplasmatic tail of the

protein. CTLA4 lacks an immunoreceptor tyrosine-based inhibitory motif (ITIM) that is found in other inhibitory receptors and, therefore, it requires association with further signalling molecules. Two phosphatases, SHP-2 and the serine/threonine phosphatase PP2A have been reported to associate with CTLA4 (Fig.1.4) [40, 50]. SHP-2 targets phosphotyrosine residues, whereas PP2A dephosphorylates serine and threonine residues. It has been described that CTLA4 can be found in a complex together with CD3ζ and SHP-2 [53]. The direct interaction between SHP-2 and the signalling molecule CD3ζ is thought to be a mechanism by which CTLA4 downregulates TCR signalling. Confirming this hypothesis is the observation that CD3ζ is hyperphosphorylated in CTLA4 knockout mice [50]. However, mutations in the tyrosine residues in the CTLA4 cytoplasmatic tail associated with binding to SHP-2 did not confirm involvement of this phosphotase in the negative signalling.

PP2A, on the other hand, interacts with the cytoplasmic tail of human CTLA4 through two motifs, the lysine rich motif centred at lysine 155 and the tyrosine residue 182 [40]. This phosphatase has been described as a negative regulator for ERK and JNK. At the same time there are reports describing an inhibition in the kinase activity of these proteins after the engagement of CTLA4, which indicates that PP2A might have a role as a mediator for the downstream effects of the receptor [54]. Furthermore, it has been shown that T cells from CTLA4-deficient mice show higher levels of ERK activity upon stimulation [55]. It also has been reported that CTLA-4 inhibits cell cycle progression and activation of transcription factors NF-κB, NFAT, and AP-1 [56].

Another model suggests that CTLA4 interferes with raft aggregation mediated by TCR and CD28 [52]. These lipid rafts appear upon TCR ligation and CD28 costimulation and

represent platforms that carry signalling proteins on the cell surface [57]. The inhibition of this rafts expression by CTLA4 was associated with reduced presence of phospho-LAT in the domains [52]. In this model, the two costimulatory molecules CD28 and CTLA-4 would target the same event in opposing ways: by simply regulating the availability of crucial signal molecules that are required for effective TCR signalling.

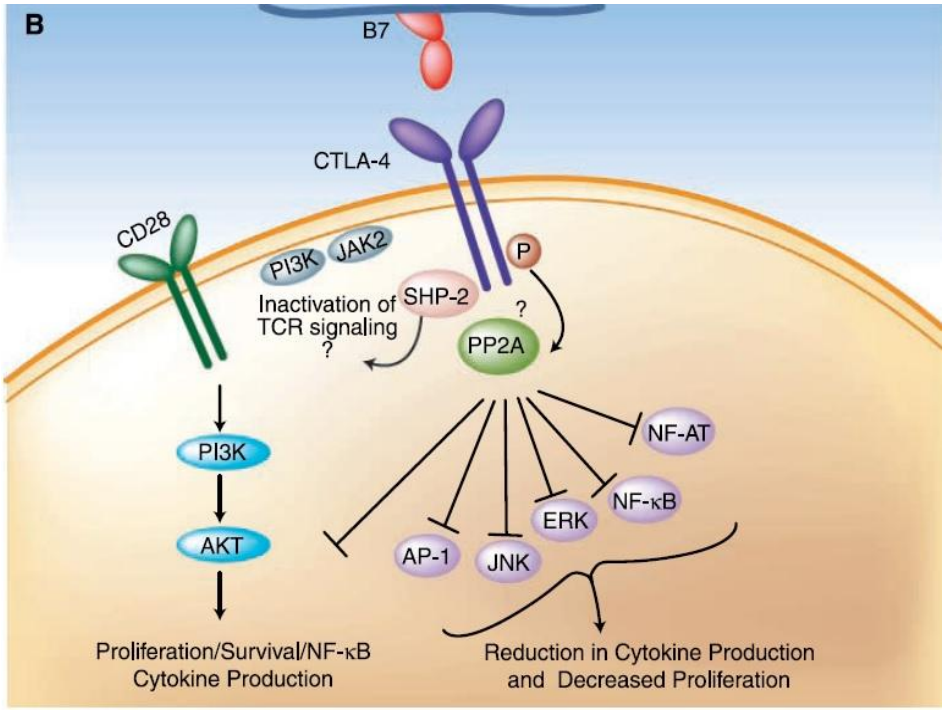

Hodi, 2007 [58]

Figure 1.4 CTLA4 mediated signalling.

CTLA4 binds with higher affinity than CD28 to its ligands the B7 molecules, also known as CD80 and CD86. It mediates inhibitory effects on downstream signalling events possibly via phosphatases like PP2A and SHP-2. This could result in downregulation of transcription factors like JNK, ERK, NF-κB and NFAT leading to decreased cytokine production and proliferation.

The involvement of CTLA4 in the blockage of microcluster formation in T cells represents another way of interfering with the TCR signalling. Microclusters containing important mediators, such as TCR, ZAP-70, SLP-76 and Gads form shortly after TCR ligation. It has been shown that CTLA4 blocks ZAP-70 microcluster formation and that this block occurred concurrently with a loss of calcium mobilization needed for T cell proliferation [52].

Several models describing cell-extrinsic mechanisms of CTLA4 function have been suggested. Tregs represent around 10% of peripheral CD4+ T cells and are important for maintenance of self-tolerance and control of antigen specific responses [59, 60]. This CD4+CD25+ subset is characterised by expression of significant levels of CTLA-4 on the surface and the transcription factor FoxP3. Genetic mutations in FoxP3 result in the development of lethal autoimmune and autoproliferative diseases [61]. It has been shown that Tregs play a role in the suppression of immune responses to pathogens, tumours and transplants [62, 63]. Still it is not fully understood which factors and pathways are responsible for the up-regulated expression and role of CTLA4 in Tregs. It has been shown that CTLA4 expressed on Tregs may trigger induction of IDO in DCs, which will have immunosuppressive effects in the local environment [64]. Another mechanism of action would be the direct induction of a negative signal to the responder T cell via the ligation of CTLA4 on Tregs with CD80 expressed on the responder T cell [65]. Other groups have demonstrated that specific deletion of CTLA4 in FoxP3+ Tregs in mice impairs the Treg-mediated down-regulation of CD80 and CD86 expression on DCs and leads to enhanced tumour immunity [66].

Indoleamine 2,3-dioxygenase (IDO) catabolises tryptophan, leading to localised tryptophan depletion and inhibition of T cell proliferation [67]. Some models indicate that CTLA4-Ig is able to induce IDO production in APC, which will eventually inhibit T cell activation, however, others do not confirm the link between CTLA4-Ig and IDO induction [68].

Another possible extrinsic mechanism is the CTLA4-mediated trans-endocytosis of CD80 and CD86. In the past couple of years the group of D.M. Sansom reported in several studies about the depletion of ligands by CTLA4. Live cell imaging of CTLA4+CHO cells incubated with CD86-GFP+ CHO cells showed depletion of GFP from the membrane of the donor cells and an increase in GFP was detected in the CTLA4+ cells. Evidence of co-localisation of CD86 and CTLA4 was also found in cultures using activated T cells together with monocyte-derived DC. Furthermore, this effect was inhibited upon addition of blocking anti-CTLA4 antibody [47].

1.3.3 Blockade of CTLA4 as a potential immunotherapy

Immunotherapy is one of the most recent approaches to treat cancer since it is less toxic compared to standard cancer treatments like radiation, chemotherapy and surgery. The potential of the modulation of the immune system as a way to treat and prevent diseases was recognized early and led to the eradication of several severe infectious diseases like diphtheria, polio, measles and mumps [69]. Passive immunotherapies do not stimulate a patient's immune system to "actively" respond to a disease in the way a vaccine does. They usually are comprised of antibodies or other immune system components that are made outside of the body (i.e. in the laboratory) and administered to patients to provide immunity against a disease, or to help them fight off an infection. The administration of

monoclonal antibodies (mAb) is the most widely used form of passive cancer immunotherapy today.

The identification of CTLA4 as a major inhibitory receptor led to the suggestion that its blockade would lead to unopposed CD28 activation of T cells and would suppress or/and deplete the activity of Tregs. The improvement of antitumour immunity using antibodies against CTLA4 has been investigated in numerous animal models. Allison *et al.* have demonstrated that the injection of anti-CTLA4 leads to rejection of a variety of immunogenic tumours [70]. Studies in preclinical models have shown that antibody-mediated blockade of CTLA4 on Tregs in combination with Gvax (GM-CSF secreting cellular vaccine) is not sufficient to induce an antitumour response. Only a synergistic effect provided by the blockade of CTLA4 on both T effector and T regulatory cells is able to induce maximal antitumor activity in mouse melanoma [71]. Another tumour vaccine combining CTLA4 blockade with irradiated B16 expressing the Flt3 ligand induced rejection of melanoma pre-implanted 3 days before vaccination in mice models [72].

Several antibodies against human CTLA4 have been developed and two of them ipilimumab and tremelimumab have entered clinical trials. These drugs are being tested in combination with chemotherapy also in prostate, lung and pancreatic cancer [73]. But most of these trials were completed in patients with advanced melanoma. Some of the patients treated with ipilimumab showed some improvement in the response against tumours and their life span was extended [74]. Grade III/IV autoimmune toxicities like dermatitis, colitis were seen in the patients upon treatment with both antibodies [75] [76]. These results show that such therapy is able to break tolerance against cancer antigens but

also against self-antigens or commensal flora which may hinder the utilisation of such antibodies in cancer treatments. A repeated administration of high doses of the antibodies is necessary to maintain an effective concentration in the organism, which makes this therapy very expensive and can contribute to the observed toxicities in patients. Another important issue for the assessment of such therapies and the measurement of drug efficacy is the choice of evaluation time points. The response to agents that block immune checkpoints like CTLA4 is often delayed and observed months after the initial administration compared to chemotherapies where responses occur within weeks [77].

An alternative to the usage of blocking antibodies to modulate CTLA4 signalling would be the impediment of CTLA4 expression at the RNA level. This can be achieved by an approach called RNA interference and has been already applied in mouse T cells to "knock down" expression [78].

1.4 RNA interference

The RNAi pathway was discovered by Fire and Melo in 1998 in studies using *C.elegans* for which they were awarded the Nobel prize in physiology in 2006 [79]. RNA interference (RNAi) is a mechanism that controls sequence-selective suppression of gene expression in a wide range of organisms. It is involved in a variety of functions including growth, development, neuronal patterning and cellular metabolism. The RNAi pathway is initiated by the production of small RNAs (20-30 nucleotides) which encode sequences complementary to target transcripts. The binding to the small RNAs leads to translational repression and/or cleavage of the target mRNA [80]. Two of the main classes of small regulatory RNA that has been identified in both plants and animals are the short-

interfereing RNAs (siRNA) and micro RNAs (miRNAs). Both types are generated from long double –stranded RNA (dsRNA) that are produced in, or introduced to the cells, followed by processing by ribonuclease Dicer [81].

The siRNAs can derive from the replication of RNA viruses, transcription of convergent genes, transposons, self-annealing transcripts or experimental transfection. The prime molecule involved in siRNA generation is Dicer, an RNase III type endonuclease that cleaves the long dsRNA molecules to form 19-25 nt long siRNA duplexes with 3' two-nucleotide overhangs [81]. The siRNA duplex is unwound by Argonaute proteins, a protein family recruited by Dicer (Fig. 1.5). The guide strand that mediates the silencing is then incorporated into the RNA-induced silencing complex (RISC). In addition to Dicer and a member of the Argonaute proteins, the RISC-loading complex may also contain other proteins [82]. The complex then associates with the target mRNA that has complementary sequence to the guide strand of the siRNA and catalyses the cleavage of the mRNA. The term "siRNA" is usually referred to small RNAs that derive from exogenously added constructs, whereas "miRNA" is usually used for the endogenous generated small RNAs.

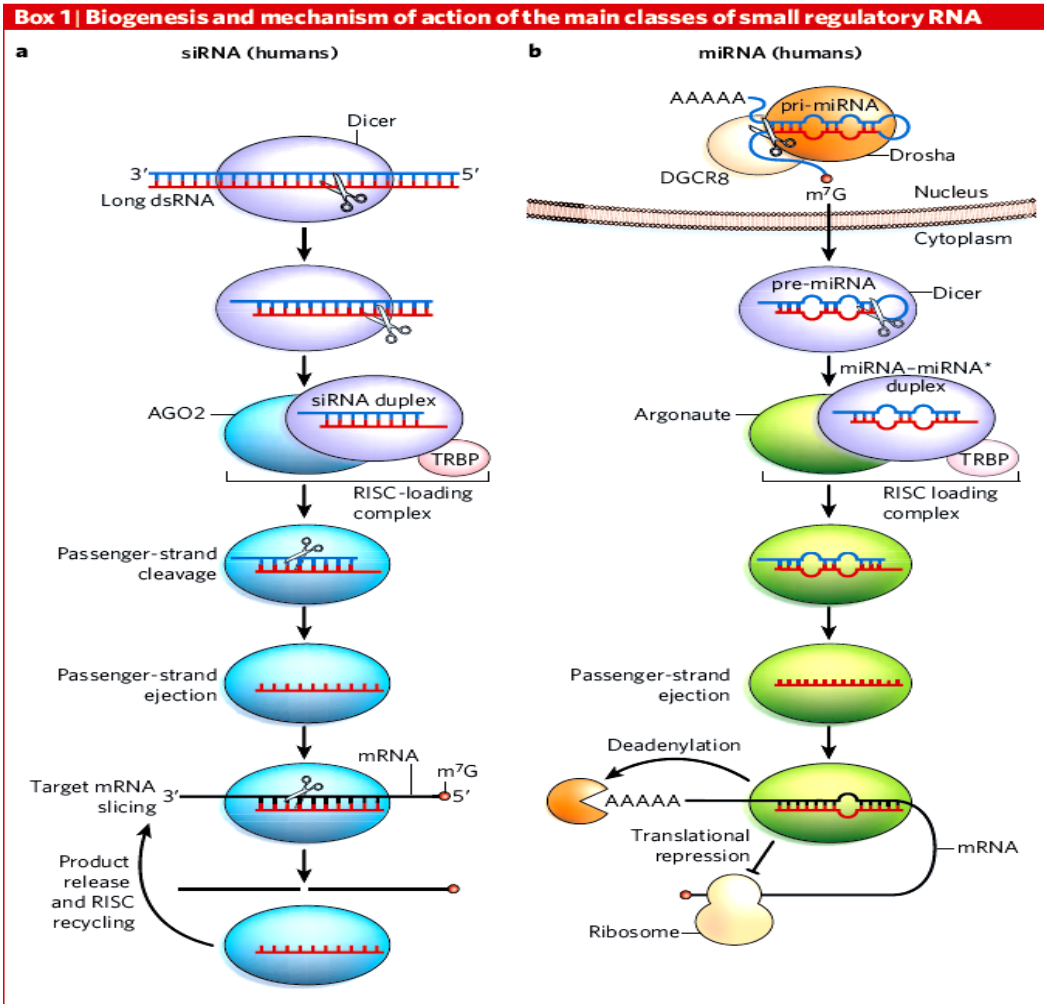

Doudna, A *et al*.,2009[83]

Figure 1.5 Biogenesis and mechanism of action of siRNA and miRNA.

(A) Long dsRNAs is introduced in the cytoplasm and recognized by the endonuclease Dicer. Upon cleavage, the resulting ~ 20-nucleotide dsRNAs are incorporated into the RISC complex which contains members of the Argonaute protein family. The passenger strand is cleaved and the guide strand can associate with the complementary mRNA, mediating cleavage or translational repression. (B) shRNAs are designed to follow the cellular machinery and microRNAs maturation pathway. miRNAs are transcribed in the nucleus as pri-miRNA, contaning stem-loop structures, 5` cap and 3` poly-A tail. They are processed by endonuclease Drosha in association with DGCR8. The resulting pre-miRNAs are characterized by a hairpin structure and 2-nucleotide overhangs at the 3`end. Upon transportation into the cytoplasm they are recognized by Dicer complex and follow the pathway of siRNAs described in (A).

miRNAs are ~19-23 nt long single-stranded RNAs generated from single-stranded transcript having local-hairpin structure. They are transcribed from endogenous miRNAgenes or introns of protein coding genes as primary transcripts (pri-miRNAs), containing ~65-70 nt stem-loop structures. Pri-miRNAs are usually transcribed by RNA Polymerase II and therefore possess 5' cap and 3' poly-A tail [84]. The transcripts are then recognized and processed in the nucleus by the endonuclease Drosha in association with DGCR8 which remove the 5' cap and 3' poly-A tail [85]. The resulting pre-miRNAs have a hairpin structure and are characterized by two nucleotides overhangs at the 3' end and a 5' phosphate group. The nuclear transport protein, Exportin-5, carries the pre-miRNA with the help of Ran-GTPase to the cytoplasm, where it is further processed by Dicer [86]. Upon cleavage of the pre-miRNA Dicer loads the miRNA duplex into the RISC complex. The passenger strand is removed and degraded and the guide strand remains incorporated in the complex. The binding of the mature miRNA to the target can then repress translation or direct degradation of the mRNA. Animal miRNA usually target the 3' untranslated region of the mRNA and have incomplete base pairing, in contrast to siRNAs that have perfect complementarity to their targets [87].

The RNA interference is widely applied to study reverse genetics and different "tools" have been developed to knockdown target genes using the RNAi pathway. It has been observed that chemically synthesized dsRNA can mediate gene silencing in mammalian cells [80]. Short hairpin RNA (shRNA) transcribed by Polymerase III promoters like U6 and H1 and incorporated into viral or bacterial vectors have shown to trigger long term silencing both in vitro and in vivo [88]. Another system called shRNA-miR utilizes the hairpin structure from an endogenous miRNA gene in which the mature miRNA

sequence in pre-miRNA is replaced with the target sequence and the expression is under the control of a Polymerase II promoter [89].

1.4.1 Detection of small RNAs

Since the discovery of the RNAi pathway hundreds of miRNAs have been identified in the genome of animals and plants [90, 91]. Furthermore, it has been shown that expression of small RNAs could be tissue-specific, developmental stage-specific or disease-specific [92, 93]. Therefore, the accurate detection and quantification of small RNA is very important for the study of the role of miRNA. However, the small size of ~ 20 nucleotides and sometimes the low abundance make the analysis of miRNA profiling quite challenging. Several methods for detection have been developed. Among them is northern blotting with radio-labeled or digoxigenin (DIG) labeled probes [94, 95]. Cloning, microarray hybridization and real-time PCR analysis were also utilized to detect expression of small RNAs [96, 97]. Chen *et al*. describe a real-time PCR quantification method of mature miRNA by stem-loop PCR. A stem-loop RT primer binds sequence-specific to the 3' portion of miRNA molecule and is reverse transcribed. Next, the RT product is quantified using conventional TaqMan PCR that includes miRNA-specific forward primer, universal reverse primer and dye-labeled TaqMan probes (Fig. 1.6) [97]. This assay offers several advantages such as high sensitivity, specificity and better quantification which are important for the detection of low abundant miRNAs during miRNA profiling. It allows high throughput and can be completed much quicker than methods based on cloning and northern blotting.

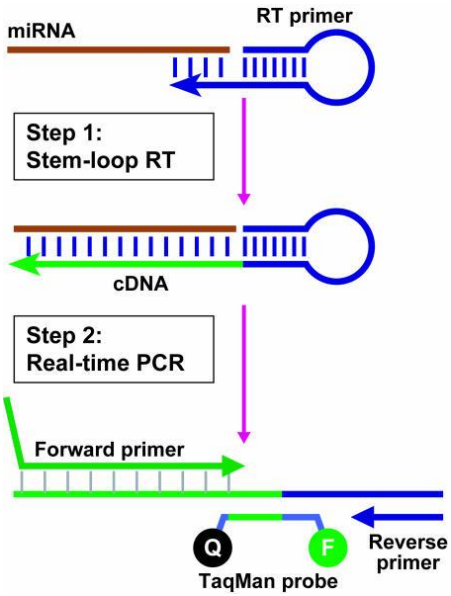

Chen *et al.*, 2005[97]

Figure 1.6 Schematic representation of TaqMan miRNA assay.

The first step of the assay is the reverse transcription of the mature miRNA using a stem-loop RT primer that binds specifically to the 3` portion of the miRNA molecule. The second step is the detection and quantification of the RT product using a miRNA-specific forward primer, miRNA-specific TaqMan probe and a universal reverse primer that binds to the sequence of the stem-loop RT primer used for the reverse transcription.

Hypothesis

CTLA4 is identified as a negative regulator of T cell activation. However, the exact mechanism of function is still not well understood. Despite that, it is already a potential target for therapeutic intervention. Antibodies blocking the CTLA4 : CD80/86 interaction have been used in cancer therapies to lower the threshold of T cell activation and potentially to induce antitumour response. Therapies based on the administration of antibodies are associated with several disadvantages that were described in the introduction. An alternative approach to the blocking of CTLA4 using antibodies could be the knock-down of the protein at the RNA level using RNA interference.

In this project it was investigated if CTLA4 expression could be silenced using vectors expressing CTLA4-specific shRNA generated via molecular cloning and evaluated in transfected cells. The effect of CTLA4 downregulation on T cell activation was studied by investigation of the expression of signaling molecules and cytokine production upon antibodies-mediated stimulation using a human leukaemia T cell model.

Aims

- Construct an expression vector encoding CTLA4 specific shRNA and test silencing efficacy in T cells
- Generate a stable cell line encoding the CTLA4 specific shRNA; test silencing efficacy and shRNA expression
- Investigate the role of CTLA4 downregulation on T cell activaion

2. Chapter 1 - Generation and validation of an shRNA approach to silence expression of CTLA4

2.1 Methods

2.1.1 Use of pCTLA4-Flag vector

Initially, the efficacy of the generated different vectors encoding shRNA against CTLA4 was tested in co-transfection experiments. Since HeLa cells do not express endogenous CTLA4, co-transfection with pCTLA4-Flag (a gift from G. Ruberti [98]) was performed. The coding sequence of CTLA4 was cloned in the multiple cloning site of pcDNA3 backbone downstream of a human CMV promoter and a Flag-coding sequence was introduced between the first and second exon of CTLA4. A map of the vector is shown in figure 6.1. in appendix II. Thus the fusion of the two sequences allows the detection of CTLA4 expression using a monoclonal anti-Flag antibody [98].

2.1.2 Construction of pBSU6siCTLA-4 / pBSU6scrCTLA-4

A shRNA expressing vector was used to achieve RNA interference. The small hairpin constructs were designed, chemically synthesized (Sigma) and cloned downstream of the U6 promoter in a modified Bluescript vector.

A sequence complementary to the CTLA4 mRNA that can potentially silence CTLA-4 (siCTLA4-F and siCTLA4-R) was determined using Dharmacon software (siDESIGN

Center, Thermo Scientific).The design was modified further according to Xu, Z [99] recommendations to create a hairpin loop, poly A tail and a PmeI and PstI flanking restriction sites, so that the construct can be inserted into a pBSU6 vector (a gift from Xu,Z [99]). A map of the plasmid is shown in figure 6.2. in appendix II. The choice of the restriction sites allows directional cloning in the vector since PmeI creates a blunt end of the insert and PstI – a sticky end. This pair of oligonucleotides (Sigma) was labeled siCTLA4-F and siCTLA4-R (Table 2.1). Another pair of oligonucleotides (Sigma), a scrambled control, was designed by exchanging 4 nucleotides in the sequence complementary to CTLA4 (scrCTLA4-F and scrCTLA4-R) and modified further in the same way (Table 2.1). The two pairs of oligonucleotides (Sigma) were annealed in a thermocycler. Single stranded complementary oligos (Sigma) were mixed at a 1:1 molar ratio. The tubes were heated for 5 min at 95°C followed by gradual cooling (-1°C/1min), incubation at 60°C for 30 min and further gradual cooling (-1°C/1min) to 4°C. 5µg of pBSU6 plasmid DNA [99] were linearized by incubation with PmeI and PstI (New England Biolabs) restriction enzymes at 37°C for 2h. To avoid re-ligation the plasmid DNA was dephosphorylated with Alkaline Phosphatase for 1h at 37°C. The linearized plasmid was gel purified before being used in the ligation reaction. Vector DNA and the diluted annealed oligonucleotides were mixed at 1:5 ratio, with 2µl of 10xLigation buffer, 1µl T4Ligase (Roche) and water up to 20µl. After incubation at room temperature overnight 9µl of the ligation reaction were used to transform competent XL-10 *E.coli*. Upon successful transformation and isolation of the plasmid DNA, the samples were sequenced using primers T7 (forward) and T3 (reverse) for the Bluescript backbone by MWG Operon, UK.

Oligonucleotide	Sequence 5'-3'
siCTLA4-F	GGCAACGGAACCCAGATTTATTCAAGAGATAAATCTGGGTTCCGTTGC TTTTTCTGCA
siCTLA4-R	GAAAAAGCAACGGAACCCAGATTTATCTCTTGAATAAATCTGGGTTCC GTTGCC
scrCTLA4-F	GGAAACTGAACCCAGCTTGATTCAAGAGATCAAGCTGGGTTCAGTTTC TTTTTCTGCA
scrCTLA4-R	GAAAAAGAAACTGAACCCAGCTTGATCTCTTGAATCAAGCTGGGTTC AGTTTCC

Table 2.1 Oligonucleotides sequences used to generate small hairpin structures.

2.1.3 Construction of pCIneo siCTLA-4 / pCIneo scrCTLA-4

To develop a cell line stably expressing the shRNA of interest the plasmid used for transfection should contain a resisitance marker that would allow selection in mammalian cells. Therefore, the shRNA together with the U6 promoter were excised from the Bluescript backbone and inserted into a pCIneo vector (Promega) encoding the neomycine resistance gene. A vector map of pCIneo (Promega) is shown in figure 6.3. in appendix II. The U6 promoter shRNA cassette from the pBSU6siCTLA-4 and pBSU6scrCTLA-4 vector was excised using PCR. Primers (shCTLA4 Fr and shCTLA4 Rev, Table 2.2) flanking the cassette were designed using Primer 3 Plus software. The shCTLA4 Rev primer was further modified to contain the BamHI (G'GATC_C) sequence at the 5' end so that upon PCR amplification the product would contain an

additional BamHI restriction site. Due to this modification the two primers shCTLA4 Fr and shCTLA4 Rev had different length, resulting in different melting temperature Tm. Therefore, the optimal annealing temperature for the PCR amplification was tested using a range from 55°C to 66°C (data shown in figure 6.5. in appendix II). Upon amplification the DNA was purified using phenol/chloroform. The samples were then digested with BamHI (New England Biolabs) for 2h at 37°C generating sticky ends on both sites of the DNA fragment. 5µg of pCIneo plasmid DNA were linearized by incubation with BamHI (New England Biolabs) restriction enzyme at 37°C for 2h, followed by dephosphorylation with Alkaline Phosphatase for 1h at 37°C. Both the linearized vector and the insert DNA were gel purified. The quality of the DNA was checked on 1% agarose gel before setting up the ligation reaction. Insert and vector DNA were mixed in 1:1 or 3:1 ratio together with 2µl of 10xLigation buffer, 1µl T4Ligase (Roche) and water up to 20µl. After incubation at 12°C overnight 9µl of the ligation reaction were used to transform competent XL-10 *E.coli*.

2.1.4 Construction of pCTLA4-Flag siCTLA4 / pCTLA4-Flag scrCTLA4

To confirm the silencing effect of the chosen shRNA sequence, the shRNA cassette was cloned into the pCTLA4-Flag vector (figure 6.1., appendix II. To generate the insert DNA the same strategy was applied as described before (2.2.2). 5µg of pCTLA4-Flag plasmid DNA [98] were digested with BglII (New England Biolabs) 37°C for 2h, followed by dephosphorylation with Alkaline Phosphatase for 1h at 37°C. Both the linearized vector and the insert DNA were gel purified. The quality of the DNA was

checked on 1% agarose gel. The U6 shRNA cassette was inserted in the BglII restriction site of pCTLA4-Flag since restriction with BamHI and BglII results in the generation of compatible ends. Ligation reaction was set up as described before, followed by transformation of competent XL-10 *E.coli.*

2.1.5 Construction of pBSU6neo siCTLA4 / pBSU6neo scrCTLA4

To develop a plasmid that would allow generation of a stable cell line, the neomycin resistance gene from the pCIneo vector was inserted into the pBSU6 siCTLA4 and into its corresponding control pBSU6 scrCTLA4. A third vector pBSU6neo was developed and used as an additional control for the transfection experiments.

The neo cassette was excised from the pCIneo vector (Promega) using PCR. Primers (Neo Promega Fr and Neo Promega Rev, Table 2.2) flanking the cassette were designed adding additional NotI restriction sites (GC'GGCC_GC) on both ends and upon amplification the DNA was purified using phenol/chloroform. The sample was then digested with NotI (New England Biolabs) for 2h at 37°C generating sticky ends on both sites of the DNA fragment. 5µg of pBSU6siCTLA4 and pBSU6scrCTLA4 plasmid DNA were linearized by incubation with BamHI restriction enzyme (New England Biolabs) at 37°C for 2h, followed by dephosphorylation with Alkaline Phosphatase for 1h at 37°C. Both linearized vectors and the insert DNA were gel purified and the quality of the DNA was checked on 1% agarose gel. The neo cassette was inserted in the NotI restriction site of pBSU6siCTLA4 and pBSU6scrCTLA4. The ligation reactions were set up as described before and a transformation of competent XL-10 *E.coli* was performed.

Oligonucleotide	Sequence 5'-3'	Annealing T (°C)	Product (bp)
shCTLA4 Fr	CCACCCCATTGACGTCA	58	550
shCTLA4 Rev	GTTCAGGATCCGACCATGATTACGCCAA		
Neo Promega Fr	GATATGCGGCCGC GTGCGGTATTTCACA	55	1444
Neo Promega Rev	CAATTGCGGCCGC TGTACTGAGAGTGCA		

Table 2.2 Sequences of primers used in PCR reactions.

The annealing temperature used in the PCR reaction and the expected product size are indicated for each pair of primers. shCTLA4 Rev was modified to contain the sequence of the BamHI restriction site (underlined). Neo Promega Fr and Neo Promega Rev were both modified to contain the sequence of the NotI restriction site (underlined).

2.1.6 Preparation of competent XL-10 E.coli

10 ml of LB Broth (Appendix I) were inoculated with XL-10 *E.coli* (DIT, Daireen Caffrey) from frozen stock. The cells were grown overnight in orbital incubator at 37°C and 200 rpm. 25 ml of LB Broth were inoculated with 1 ml of the overnight culture and the incubation was continued for further 2.5-3h until the mid-log phase ($A_{600} \approx 0.45$). The flask was incubated on ice for 10 min followed by centrifugation at 3000 rpm, 4°C for 10 min. The pellet was resuspended in 10 ml ice cold 0.1M $CaCl_2$ solution (Appendix I) and incubated on ice for 30 min. The cells were pelleted as described above, resuspended in 10 ml ice cold 0.1M $CaCl_2$ solution (Appendix I) and incubated on ice for 10 min. After centrifugation at 3000 rpm, 4°C for 10 min the pellet was resuspended in 0.5 ml 0.1M $CaCl_2$ solution (Appendix I). The cells were incubated on ice for 1h. Aliqouts of 100µl were used for transformation or frozen at -80°C for further use in 0.1M $CaCl_2$/ 15% Glycerol.

2.1.7 Transformation of competent cells

5-50 ng of plasmid DNA, 9 µl of ligation reaction or 2 µl of TOPO TA ligation reaction were transferred to 100µl of competent XL-10 *E.coli*. Incubation on ice for 1h was followed by heat shock for 90 sec at 42°C in pre-warmed water bath. The cells were immediately transferred on ice for further 2 min. 1 ml of SOC medium (Appendix I) was added followed by incubation at 37°C for 1h. The cells were plated at different volumes on LB agar (Appendix I) plates containing 50 µg/ml ampicillin and incubated overnight at 37°C.

To analyse the XL-10 *E.coli* transformed with TOPO TA ligation reaction the cells were spread on LB agar (Appendix I) plates containing 50 µg/ml ampicillin and 40 µl of 40 mg/ml X-gal in dimethylformamide (DMF) and incubated at 37°C overnight. White and light blue colonies were further analysed for the presence of the insert.

2.1.8 Plasmid Mini-prep

A single colony was picked from a freshly streaked selective plate and inoculated in 3ml of LB Broth (Appendix I) containing 50 µg/ml ampicillin. The cells were incubated overnight at 37°C while shaking at 200 rpm. Plasmid mini - prep was performed using a kit from Fermentas according to the manufacturer instructions. The bacterial culture was harvested by centrifugation at 8000 rpm in a microcentrifuge for 2 min at room temperature. The supernatant was removed and the cells were resuspended by vortexing in 250 µl of resuspension solution containing RNase A. Upon addition of 250 µl of lysis

buffer (Fermentas) the tube was inverted several times until the solution becomes viscous. 350 µl of neutralization solution were added and mixed by inverting. The samples were centrifuged for 5 min at 12000 g, room temperature. The supernatant was transferred to the GeneJET spin column and centrifuged for 1 min at 12000 g. The flow-through was discarded and 500 µl of wash solution were added to the column. The samples were centrifuged for 1 min at 12000 g and the washing step was repeated. After discarding the flow-through an additional centrifugation step was performed to avoid any residual ethanol in the plasmid DNA. The GeneJET spin column was placed in a new eppendorf tube. 50 µl of elution buffer were added to the column, followed by incubation for 2 min at room temperature. The purified plasmid DNA was eluted after centrifugation for 2 min at 12000 rpm. The samples were further analyzed by restriction digestion and/or stored at -20°C.

2.1.9 Plasmid Maxi-prep

Plasmid Maxi-prep was used to isolate sufficient amount of high quality plasmid DNA that was used for transfections.

200-300 ml of LB Broth (Appendix I) containing 50 µg/ml ampicillin were inoculated with 2-3 ml bacterial culture and incubated overnight at 37°C while shaking at 200 rpm. Plasmid maxi – prep was performed using a kit from Roche following the manufacturer instructions. The cells were pelleted by centrifugation for 10 min at 4000 g, 4°C. The supernatant was discarded and the pellet was resuspended in 12 ml Suspension buffer containing RNAse A. The samples were transferred to a 50 ml Falcon tube and 12 ml of Lysis buffer was added. The solution was mixed by inverting and incubated at room

temperature for 3 min. Upon addition of 12 ml cold Neutralization buffer the samples were mixed by inverting and incubated on ice for 5 min, which results in precipitation of the solution. The lysate were cleared by filtration and the flow-through was collected into a new tube. The column was placed into a 50 ml Falcon tube and equilibrated with 6 ml of Equilibration buffer. The samples were loaded on the column and the column was emptied by gravity flow. Afterwards, two washing steps with 16 ml of washing buffer each were performed. The column was then transferred into a new collection tube and the DNA was eluted in 15 ml pre-warmed (50°C) Elution buffer. 11 ml of isopropanol were added and the samples were centrifuged at 15000 g, 4°C for 30 min. The supernatant was discarded and the plasmid DNA was washed with 4 ml 70% ice cold ethanol. After centrifugation for 10 min at 15000g, 4°C the pellet was air dried for 5-10 min and resuspended in 50-300 µl of TE buffer (Appendix I). The concentration and quality of the DNA was estimated and the samples were stored at -20°C.

2.1.10 Cell culture and transient transfection of HeLa cells

HeLa cells were used as a model in co-transfection experiments to evaluate the generated constructs.

The human HeLa cell line was maintained at 37°C in 5% CO_2 in RPMI 1640 (Lonza) containing 10% FCS (Lonza), 100 U/ml penicillin, 0.1 mg/ml streptomycin (Sigma) and 2mM L-Glutamine (Sigma). Cells were grown to confluence before being trypsinised with 2% trypsin solution for 3-4 min at 37°C. 15 ml of complete RPMI medium was added to the cell suspension to inactivate trypsin. The cell suspension was pelleted at 1200 rpm for 8 min, room temperature and cells were split 1:10 in a new culture flask.

For transfections cells were seeded at $4x10^5$ cells/well in 2 ml of medium in 6-well plates and incubated overnight to allow adhesion. 3 µl of FuGENE HD transfection reagent (Roche) or GeneJuice (Novagen) transfection reagent and 1µg of plasmid DNA were added to 100 µl of serum-free RPMI (Lonza) medium, vortexed briefly and incubated at room temperature for 15 min to allow complex formation. The mixture was added dropwise to the cells over the entire surface of the well. The cells were incubated for another 24-48h at 37°C in 5% CO_2. After the incubation time the medium was discarded and the plate was washed with PBS. The cells were trypsinised for 3 min with 300µl trypsin, followed by inactivation with 1 ml complete medium. The cell suspension was transferred in a new eppendorf tube, pelleted at 1500 rpm for 5 min and washed once with PBS. Transfection efficiency was analyzed with X-gal assay, when the cells were transfected with pCMV-SPORT (DIT) or immunofluorescence, when the cells were transfected with pmaxGFP (Lonza). When the cells were transfected with pCTLA4-Flag (a gift from G. Ruberti [98], figure 6.1. in appendix II) alone or in combination with shRNA expressing constructs the samples were analysed using Western blot or Real-time PCR to detect CTLA4 expression.

2.1.11 Stable transfection of HeLa and clones selection

$4x10^5$ cells/well in 2 ml of medium in 6-well plates and incubated overnight to allow adhesion. Cells were transfected as described above with 1µg of plasmid DNA (pCTLA4-Flag). 24h post-transfection the cells were transferred into 100mm dishes and incubated in media containing 200 µg/ml G418 (Roche). The cells were incubated for 3 weeks in media containing G418 (Roche) that was changed every 3-4 days so that only cells that expressed the neomycin resistance gene encoded by the plasmid could survive.

Individual clones were picked and transferred to a new culture dish. To analyse the clones protein and RNA were extracted and the protein lysate were tested for the expression of CTLA4 with anti-Flag antibody in western blot. CTLA4 expression was also analysed using real-time PCR with qCTLA4 Fr and qCTLA4 Rev (Table 2.4).

2.1.12 Staining of HeLa cells with X-gal

HeLa cells transfected with plasmid DNA contaning the β-galactosidase gene were stained with X-gal solution to estimate the transfection efficiency. After the incubation period the cells were washed twice with 2 ml PBS. They were fixed by adding 1 ml of 0.25% glutaraldehyde in PBS to each well. Upon incubation for 15 min the cells were washed three times with 2 ml PBS. 500µl/well of staining solution was added and the plates were incubated at 37°C for 1.5-3h until transfected cells were stained blue. Samples were analysed using brightfield microscopy.

2.1.13 Immunofluorescence

Immunofluorescence was used to check transfection efficiency in cells transfected with pmaxGFP (Lonza). HeLa cells were grown on coverslips in 6 well plates. The cells were transfected with 1 µg pmaxGFP plasmid DNA (Lonza). After the incubation period the media was discarded and the cells were washed twice with 2 ml PBS. They were fixed by adding 1 ml of 4% PFA in PBS (Appendix I) to each well and incubation at room temperature for 15 min. After two washing steps for 5 min each with 2ml PBS the membrane was permeabalized by adding 1 ml of 0.1% Triton-X-100 in PBS (Appendix I) for 5 min. After the incubation time the cells were counterstained with 1ml propidium

iodide solution for 5 min at room temperature. Upon incubation the cells were washed twice with PBS. The coverslips were transferred and mounted on microscope slides. GFP expression was studied on a fluorescence microscope.

Jurkats transfected with pmaxGFP plasmid DNA were incubated in plates. The plates were centrifuged at 1000 rpm for 5 min. Then the cells were analysed for GFP expression on an inverted fluorescence microscope.

2.1.14 Protein extraction

The cells were pelleted in eppendorf tubes by centrifugation at 1300rpm for 5 min at room temperature. The pellet was washed once with 1 ml PBS. The cells were resuspended in 50-100µl of RIPA buffer (appendix I) or cell lysis buffer [100] and mixed by vortexing. The samples were incubated on ice for 20 min and mixed by vortexing every 5 min to ensure lysis. After centrifugation for 20 min at 12000g, 4°C the supernatant containing the protein lysate was transferred to a new tube that was stored at -80°C. Protein concentration was estimated using Bradford assay.

2.1.15 Bradford assay

Bradford protein assay was used to estimate the protein concentration. The protein concentration in solutions depends on the change in absorbance in Coomassie Brilliant Blue G-250 dye (BioRad) upon binding of the protein. For the standard curve six 2-fold serial dilutions were performed starting with a top concentration of 0.5 mg/ml BSA in H_2O. Protein lysates were diluted with H_2O when necessary. 10µl of each sample and each standard dilution, including a blank (H_2O) were added in duplicates to a 96-well

plate. 200µl of 1x dye reagent (BioRad) (5x dye reagent diluted 4:1 with H_2O) were added to each well and incubated at room temperature for 5 min. Absorbance was measured at 595nm. The blank value was subtracted from the measured values. Protein concentration was estimated according to the values obtained for the BSA standard curve.

2.1.16 Western blot

20-30 µg of protein samples that were previously boiled for 5 min in 1x loading buffer were loaded on 12% resolving / 5% stacking gel. The gels were run in ATTO gel electrophoresis system in 1x Running buffer (appendix I) at 100V/ 45mA for about 2h until the loading dye had reached the bottom of the gel. After electrophoresis the gel system was disassembled and the stacking gel was cut out and discarded. 2 pieces of Whatmann 3MM filter paper and 1 piece of nitrocellulose membrane were cut just the same size as the gel and soaked in ice cold 1x transfer buffer (appendix I) for 2 min together with 2 pads. The "sandwich" was placed in the tank filled with ice-cold 1x transfer buffer with the gel closer to the cathode (-) and the membrane closer to the anode (+) to ensure that the negatively charged proteins will transfer in the correct direction on the membrane. The transfer was done at 100 V for 70 min. Afterwards the membrane was blocked in 5% blocking buffer (appendix I) for 1h at room temperature on a shaking incubator. It was washed 3 times for 5 min each in 1xWashing buffer (appendix I) followed by incubation overnight at 4°C with the primary antibody diluted in 3% blocking buffer. Afterwards the membrane was washed 5 times for 5 min each in 1xWashing buffer. It was incubated for 1h at room temperature on a shaker with the secondary HRP-conjugated antibody (Sigma), previously diluted in 3% blocking buffer.

An ECL kit (Thermo Scientific) was used for protein detection according to the manufacturers' instructions. In a dark room 1 ml chemiluminiscent substrate was mixed with 1 ml of hydrogen peroxide and added dropwise to the membrane so that the solution covered the whole surface. After 5 min incubation the membrane was placed in the developing cassette and exposed to an X-ray film (Kodak, X-OMAT, Sigma) between 3 sec and 45 min. The X-ray film was then developed in a film processor.

2.1.17 Stripping and re-probing of the membrane

For some Western blots the same membrane was used to analyse protein expression of several proteins. Therefore, upon initial detection, the membrane was re-probed with another primary and secondary antibodies and analysed as described above (2.1.16). This was done when the expected size of the second protein was not too close to the one that was initially detected. When the sizes of the expected protein bands were too close or the same, the membrane was first stripped and then re-probed. The membrane was incubated in stripping buffer (Appendix I) in pre-heated water bath at 65°C for 30 min. The stripping buffer (Appendix I) was discarded and the membrane was washed at least 10 times for 5 min each with TBST buffer (Appendix I) at room temperature. Afterwards, the membrane was incubated in blocking buffer (Appendix I) for 1 h at room temperature and could be re-probed again with primary and secondary antibodies.

2.1.18 DNA purification of PCR product

DNA from the PCR products that were used in the molecular cloning was purified from the remaining reagents used in the PCR reaction that could possibly interfere with the following ligation reaction and transformation of the bacterial cells. 100 µl of the PCR reaction were transferred into 1.5 ml Eppendorf tube upon PCR amplification. 1 volume of phenol/chloroform/isoamyl alcohol was added and the tube was vortexed for 30 sec. Upon centrifugation for 1 min at 12 000 rpm at 4°C the upper layer was transferred into a new tube. 1 volume of chloroform was added and the tube was vortexed for 30 sec. Upon centrifugation for 1 min at 12 000 rpm at 4°C the upper layer was transferred into a new tube. 350 µl of 100% ethanol were added and mixed by inverting. Upon incubation for 5 min on ice the tube was centrifuged for 5 min at 12 000 rpm at 4°C. The supernatant was discarded and the pellet was washed with 500 µl ice cold 70% ethanol. Upon centrifugation for 5 min at 12 000 rpm at 4°C the pellet DNA was resuspended in 18 µl H_2O. The DNA samples were stored at -20°C or subjected to restriction digest.

2.1.19 Gel electrophoresis

All PCR products and plasmid DNA preparations were analyzed on 1% agarose gels. All gels were run at 120V for 40-80 min. The bands were visualized using ethidium bromide staining (0.5µg/ml ethidium bromide dissolved in gel). Low melt agarose (Invitrogen) was used whenever it was necessary to purify the DNA fragment out of the gel.

2.1.20 DNA purification from agarose gel

The linearised DNA fragments deriving from the digested plasmids used for the molecular cloning were separated on a gel and purified from it, before being used in the ligation reaction. DNA was loaded on low-melt agarose gel and the gel was run for 1-2h until the different fragments were separated. The extraction and purification of the DNA fragments was performed with QIAquick Gel Extraction Kit (Qiagen) according to manufacturers' instructions. The DNA bands were visualized under UV light and the fragment was excised from the gel with a scalpel. The gel slice was weighted and transferred to a microcentrifuge tube. 300μl of Buffer QG were added to each 100μg of gel and the tubes were incubated at 50°C for 10 min. To help dissolve the gel, the tubes were mixed by vortexing every 2-3 min. Upon solubilization 1 gel volume isopropanol was added to the sample and mixed. The sample was loaded on QIAquick spin column that was previously inserted in a 2ml collection tube. After centrifugation for 1 min at 13000rpm, the flow-through was discarded. 0.5ml of Buffer QG were added to the column to remove all traces of agarose and the column was centrifuged for 1 min at 13000rpm. To wash the DNA bound to the column, 0.75ml of Buffer PE were added and the samples were centrifuged again. The flow-through was discarded followed by an additional centrifugation step for another minute to allow removal of any residual ethanol that is contained in the Buffer PE. The column was then placed in a new tube and 45μl of water was added to it. After incubation for 1 min the DNA was eluted by centrifugation for 1 min at 13000rpm. To analyze the DNA 5μl of the sample was loaded on a gel. The extracted DNA fragments were stored at -20°C.

2.1.21 RNA extraction

Total RNA extraction from cultured cells was carried out with High Pure RNA Isolation Kit (Roche). The assay was performed according to manufacturers' instructions. The cells (1-3x10^6 cells) were resuspended in 200µl PBS and 400µl of Lysis/-Binding Buffer were added to them. After vortexing for 20sec the sample was transferred to a High Pure Filter Tube that was previously inserted into a collection tube. The sample was centrifuged at 8000g for 30sec and the flow-through was discarded. 500µl of Wash Buffer I were added to the column and spun at 8000g for 30sec. After discarding the flow-through again, the column was washed by adding 500µl of Wash Buffer II and centrifuged at 8000g for 30 sec. An additional washing step with 200µl of Wash Buffer II was performed and the sample spun at 12000g for 2 min. The column was inserted into a new tube and the RNA was eluted by adding 50µl of Elution buffer to the column and spinning at 8000g for 1 min. The concentration of the RNA was estimated and the samples were stored at -80°C.

2.1.22 DNase treatment

DNase treatment was performed to remove any DNA contamination that might be present in the RNA sample and could interfere in the following gene expression analyses using RT-PCR or Real-time PCR. 3µg of total RNA were DNase treated in a total volume of 20µl. To the RNA sample were added 2µl of 10x Buffer (Roche), 0.5µl DNase (Roche), 0.15µl of RNase Inhibitor (Roche) and water up to 20µl. The samples were incubated for 18 min at 37°C in a heat block. To stop the reaction 1 µl of 0.2M EDTA was added followed by incubation for 10 min at 75°C. The RNA was used then for cDNA synthesis or stored at -80°C.

2.1.23 Reverse transcriptase of RNA

mRNA was reverse transcribed into cDNA which was used to analyse expression of CTLA4 and GAPDH. 1µg of DNase treated total RNA was used for the reverse transcriptase reaction in a total volume of 20µl. 1µg of RNA was added to a tube together with 0.7 µl of oligo(dT) (100µM) Primers (Roche) and the mixture was made up to 13µl using DEPC-treated water. The sample was heated to 65°C for 10 min and then immediately transferred on ice. After brief centrifugation 4µl of 5xRT buffer, 2µl of dNTP mix (10mM), 0.5µl of RNase Inhibitor and 0.5µl of Reverse transcriptase (20U/µl) (Roche) were added to the tube. The sample was incubated at 55°C for 30 min in a heat block. The cDNA was stored at -20°C until being analyzed with PCR or Real-time PCR.

2.1.24 PCR

PCR was used to amplify DNA fragments used in the cloning strategies and to confirm expression of genes using the cDNA as a template.

All PCR reactions were performed using Taq DNA Polymerase (Roche) in a final volume of 25µl. The reaction contained 2.5µl of 10xPCR reaction buffer with 15mM $MgCl_2$, 0.5µl of dNTP mix (10mM), 2µl of forward primer (10µM), 2µl of reverse primer (10µM), 200-500ng DNA, 0.2µl Taq Polymerase (1U/µl) and water up to 25µl. A non-template control was included in each run. The following steps were performed in a thermal cycler: an initial 5 min denaturation step at 94°C, followed by a cycle of 30 sec at 94°C, an annealing step for 1 min at 55-62°C (depending on primers, Table 2.4), 1 min at

72°C and final elongation step of 5 min at 72°C. 30-35 cycles were used before the samples were cooled down to 4°C. 10µl of product were used for the analysis on agarose gel.

2.1.25 Real-time PCR

Real-time PCR was carried out on reverse transcribed cDNA using SYBR Green I Master mix (Roche) using the LightCycler 480 PCR System (Roche). Primers specific for CTLA4 (qCTLA4 Fr, qCTLA4 Rev) and GAPDH (qGAPDH mix) genes are listed in Table 2.3. PCR was performed according to manufacturer's instructions using the following protocol: preincubation at 95°C for 5 min, followed by 45 cycles of 95°C for 10 sec, 62°C for 10 sec and 72°C for 10 sec; melting curve analysis at 95°C for 5 sec, 65°C for 1 min, 95°C for 5 continuous acquisition/$^{\circ}$C and final cooling step to 4°C. All samples were carried out in triplicate and a negative control with no cDNA template was included in each run. The relative quantification of the target gene expression was determined using the $2^{-\Delta\Delta Ct}$ method and GAPDH was used for normalization.

Oligonucleotide	Sequence 5'-3'	Annealing T (°C)	Product (bp)
GAPDH Fr	ACCACAGTCCATGCCATCAC	58	452
GAPDH Rev	TCCACCACCCTGTTGCTGTA		
CDS CTLA4 Fr	GGCACAAGGCTCAGCTGA	60	343
CDS CTLA4 Rev	ATGGCCCTCAGTCCTTGGA		
Neo Fr	CTTCTCGAGCCTTGGCTA	60	550
Neo Rev	GCGATAAGGATCCGCGTA		
gCTLA4 Fr	CAGTGTTCTTCCTGCCACAA	60	592
gCTLA4 Rev	ATCTGGGTTCCGTTGCCTAT		
qCTLA4 Fr	CTCAGCTGAACCTGGCTACC	62	138
qCTLA4 Rev	CTGCTGGCCAGTACCACAG		

Table 2.3 Sequences of primers used in the PCR and RT-PCR assays in this study.

The specific annealing temperature used in the PCR reaction and expected size of the PCR product are indicated for each primer pair. Primers (Sigma) were designed using the Primer 3 Plus software.

2.1.26 Data analysis and statistics

Data analysis was performed using Microsoft Excel (2007) and GraphPad Prism. Differences between experimental groups were assessed with unpaired t-test or one-way ANOVA, followed by Tukey post-test and two-way ANOVA, followed by Bonferroni post-test for experiments with more than two subgroups. Results were represented as mean ± SEM. Differences were considered statistically significant if $P < 0.05$.

2.2 Results

2.2.1 Optimisation of transfection efficiency in HeLa cells

To optimize the transfection efficacy in HeLa cells a series of transfection experiments were performed using two different transfection reagents – GeneJuice (Novagen) and FuGENE HD (Roche). Varying ratios of DNA amount (µg) vs transfection reagent (µl) have also been tested. The cells were transfected with pCMV-SPORT (provided by Daireann Caffrey) which expresses the reporter gene β-galactosidase and the transgene expression was determined by X-gal staining. Analysis of the images determined that the optimal ratio for transfection of HeLa cells is 1µg DNA: 3µl of transfection reagent. No difference was observed comparing the two transfection reagents (Fig.2.1).

A)

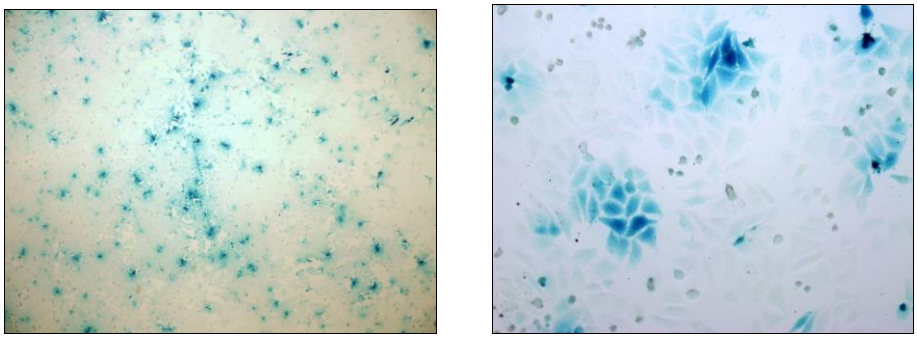

B)

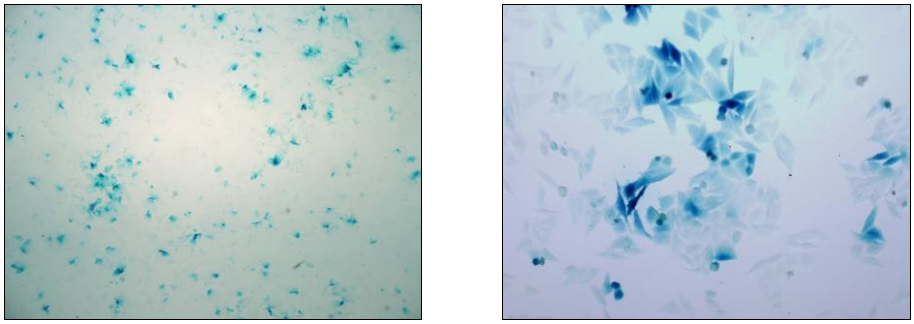

Figure 2.1 Transgene expression of β-galactosidase in HeLa cells.

(A) HeLa transfected with pCMV-SPORT and FuGENE HD (Roche). (B) HeLa transfected with pCMV-SPORT and GeneJuice (Novagen). Magnification: 40x images on the left; 200x images on the right.

The results were further confirmed in transfection experiments using pmaxGFP™ plasmid DNA (Lonza) (Fig. 2.2).

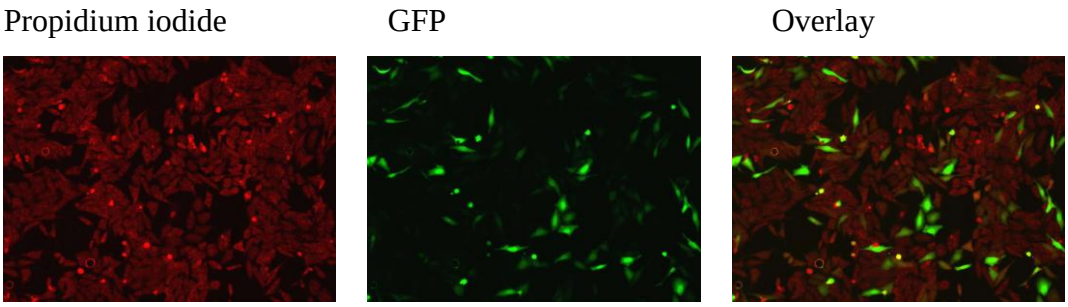

Figure 2.2. Transgene expression of GFP in HeLa cells.

The cells were transfected with 1µg pmaxGFP and 3µl of FuGENE HD transfection reagent. Transfection efficacy was determined after 24h by immunofluorescence. Magnification 200x.

2.2.2 Optimisation of transfection conditions for pCTLA4-Flag in HeLa cells

In this project several vectors that contain shRNA sequences specific for silencing of human CTLA4 were developed. HeLa cells were used to test the efficacy of silencing of the different constructs because of the consistently high transient transfection rate in this cell line. To estimate the lowest amount of plasmid DNA needed to induce CTLA4 expression, HeLa cells were transfected with different amounts of pCTLA4-Flag. At 24h post-transfection the expression of CTLA4 was detected via Western blot with an anti-Flag antibody and β-Actin was used as a loading control. It was determined that 0.2µg of pCTLA4-Flag DNA were sufficient to induce well detectable CTLA4 expression in the HeLa cells that was reproducible in the different experiments (Fig.2.3).

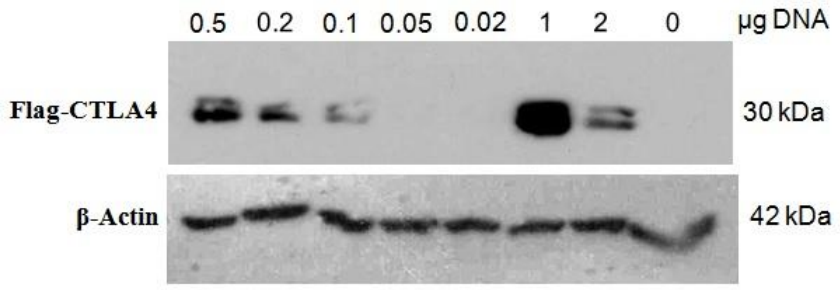

Figure 2.3. Transgene expression of pCTLA4-Flag in HeLa cells.

The cells were transfected with different amounts of pCTLA4-Flag. An empty Bluescript plasmid was used to ensure that the total amount of transfected DNA was 1µg except for lane 7. 24h post-transfection CTLA4 expression was detected by Western blot. Data are representative of two different experiments performed. The membrane was re-probed with anti-β-Actin antibody.

2.2.3 Construction and characterisation pBSU6 siCTLA4 and pBSU6 scrCTLA4

To generate a vector expressing shRNA silencing CTLA4, chemically synthesized oligonucleotides were cloned into the multiple cloning site of pBSU6 vector downstream of the U6 promoter (Fig. 2.4 A). The complementary oligonucleotides were designed to build a hairpin encoding a sequence that would silence CTLA4. The ends of the oligonucleotides were adapted to the PmeI and PstI restriction sites in the MCS of the vector thus allowing directional cloning. Two constructs were developed: one encoding the CTLA4 specific sequence and a control encoding a scrambled version of it. Upon successful ligation the newly generated plasmids containing the insert lacked the restriction sites between PmeI and PstI. Another important feature of the new plasmids is that the PmeI restriction site that generates a blunt end is being destroyed and the PstI

restriction site that generates a sticky end remains. Restrictions of the generated plasmids and the original vector pBSU6 using PmeI and EcoRI were performed to confirm that (Fig. 2.4 B). The restriction with EcoRI did not linearise the generated vectors pBSU6 siCTLA4 and pBSU6 scrCTLA4 since this restriction site was present only once between PmeI and PstI in the multiple cloning site (MCS) of the original plasmid. As expected the digestion with PmeI was also not successful in the vectors containing the insert and the samples on the gel looked like the ones from the undigested plasmid loaded as a control. The lack of a PmeI restriction site confirmed that only a single copy of the hairpin sequence was inserted. On the contrary, the restriction of pBSU6 with PmeI and EcoRI resulted in linearization of the plasmid evident as one single sharp band on the gel. Another hypothetical possibility would be the insertion of three copies of the hairpin structure in the linearised plasmid, which would have resulted into a successful PmeI restriction and a failed EcoRI digest. This case was not observed in the tested samples. Surprisingly, in the undigested control DNA samples distinct bands were visible on the gel around 3.5 Kbp together with circular and the supercoiled DNA in the upper part of the gel. These bands were observed in all negative controls during the testing of the transformed clones. They were also present in all samples where a control digest was performed with an enzyme that was not supposed to cut the construct (data shown in figure 6.4., appendix II). It is not clear why multiple bands are visible in the negative controls. However, there is still a clear difference on all gel images in the appearance between the successful digested and linearised constructs and the undigested samples. To further ensure that the plasmids encoded the right sequences, the DNA of the generated constructs was sequenced (MWG Operon, UK) (Fig.2.4 C).

A)

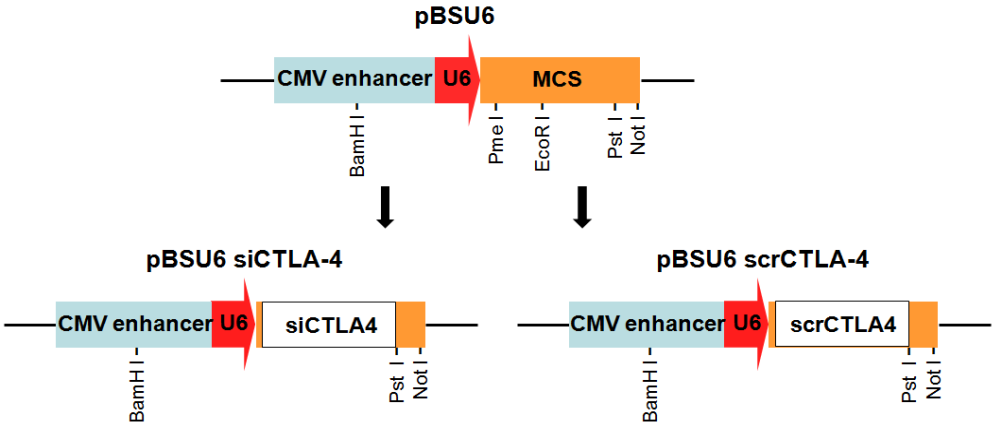

B)

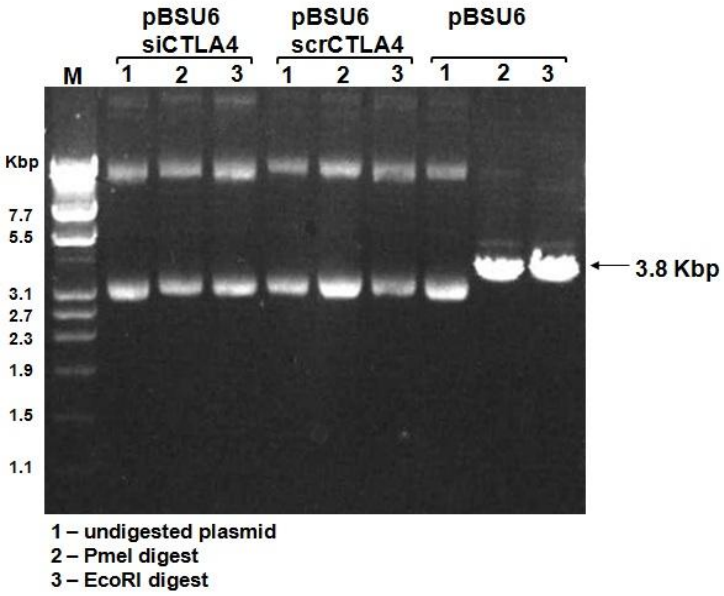

1 – undigested plasmid
2 – PmeI digest
3 – EcoRI digest

C)

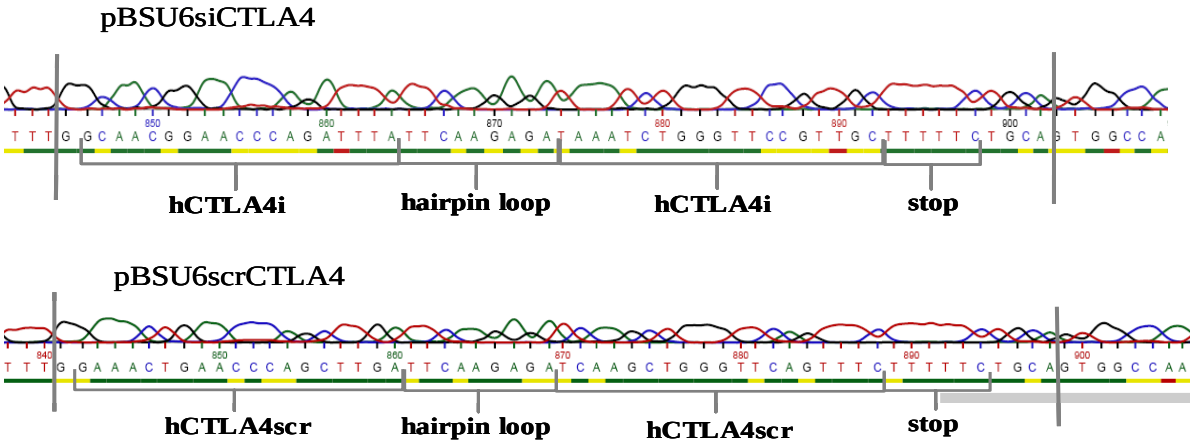

Figure 2.4 Schematic representation of the generation of pBSU6 siCTLA-4 and pBSU6 scrCTLA-4.

(A) Schematic diagram of pBSU6, pBSU6 siCTLA4 and pBSU6 scrCTLA-4 showing a part of the plasmid and indicating the orientation of the promoter and the position of the restriction enzymes used for the cloning. (B) Gel electrophoresis and restriction map analysis of the generated pBSU6 siCTLA4 and pBSU6 scrCTLA4 compared to pBSU6. Lanes are as follows: 1. undigested plasmid; 2. PmeI digest; 3. EcoRI digest (C) Sequenced DNA samples from pBSU6 siCTLA4 and pBSU6 scrCTLA4. The following features are indicated: siRNA duplex used to silence CTLA4 and the corresponding scrambled version; hairpin loop and termination signal for Pol III Polymerase.

The knockdown efficiency of the shRNA was first evaluated in transient co-transfection in HeLa cells using Western blot. 24h-post transfection CTLA4 expression was detected at similar levels in the samples transfected with pCTLA4-Flag in combination with pBSU6scrCTLA4 or the empty vector pBSU6. In contrast, no or reduced CTLA4 expression was observed in the HeLa cells transfected with the pBSU6siCTLA4 and pCTLA4-Flag. The membrane was re-probed with anti-β Actin antibody to confirm equal loading (Fig. 2.5).

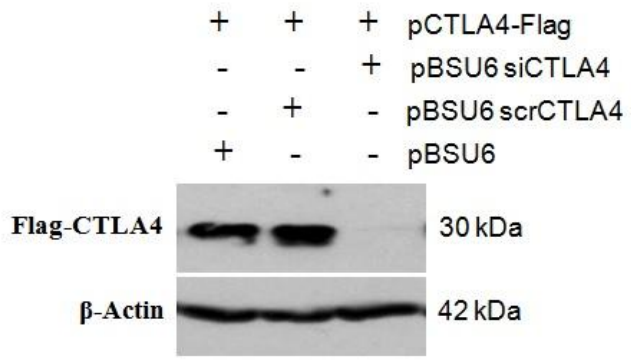

Figure 2.5. Downregulation of CTLA4 expression in HeLa cells following transfection with pBSU6 siCTLA4.

The cells were co-transfected with 0.2μg of pCTLA4-Flag and 0.8μg of pBSU6, or pBSU6 scrCTLA4 or pBSU6 siCTLA4. Western blot analysis of CTLA4 expression was performed 24h post-transfection. The membrane was re-probed with anti-β-Actin antibody used as a loading control. Data are representative of three different experiments performed.

2.2.4 Construction and characterisation of pCIneo siCTLA4 and pCIneo scrCTLA4

To develop a cell line stably expressing the shRNA of interest the plasmid used for transfection should contain a resisitance marker that would allow selection in mammalian cells. Therefore, the shRNA together with the U6 promoter were excised from the Bluescript backbone and inserted into a pCIneo vector encoding the neomycine resistance gene (vector map is shown on figure 6.3., appendix II). Primers (shCTLA4 Fr and shCTLA4 Rev (Table 2.2)) were designed to PCR amplify the shRNA cassette generating an additional BamHI restriction site. Another BamHI restriction site, already present in the Bluescript vector, was used to adapt both ends of the insert. Since the BamHI site in

the pCIneo vector is not located in the MCS, it was possible to insert another gene of interest downstream of the CMV promoter (Fig. 2.6 A). A restriction digest with PstI was performed to confirm the successful cloning and the orientation of the insert in the newly generated constructs. Two PstI restriction sites were already present in the empty pCIneo vector so that the insert of the shRNA cassette results in the introduction of a third PstI restriction site in the new plasmids (Fig. 2.6 B). The sizes of the resulting fragments in the new constructs upon digestion with PstI are 1.8 Kbp, 1.1 Kbp and 3 Kbp. The sizes of the resulting fragments upon digestion with BamHI are 0.47 Kbp and 5.47 Kbp. To allow better separation of the larger fragments the gel shown on figure 2.6 B was run at 120V for 1.5h. At this timepoint, however, the small 0.47 Kbp fragments that were previously visible (lane 2: pCIneo siCTLA4 and lane 2: pCIneo scrCTLA4) have run out of the gel. On figure 6.6. (Appendix II) is shown an additional picture of the testing of different clones with several restriction enzymes where the gel was run for a shorter period of time and the small 0.47 Kbp fragment is still visible.

A)

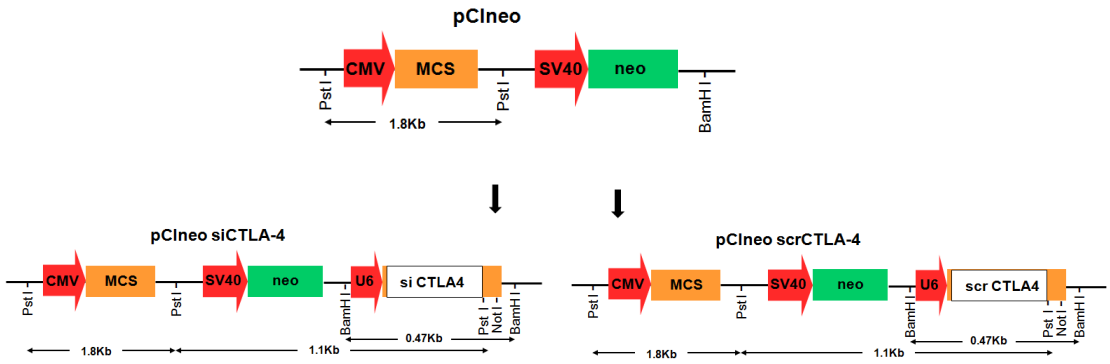

B)

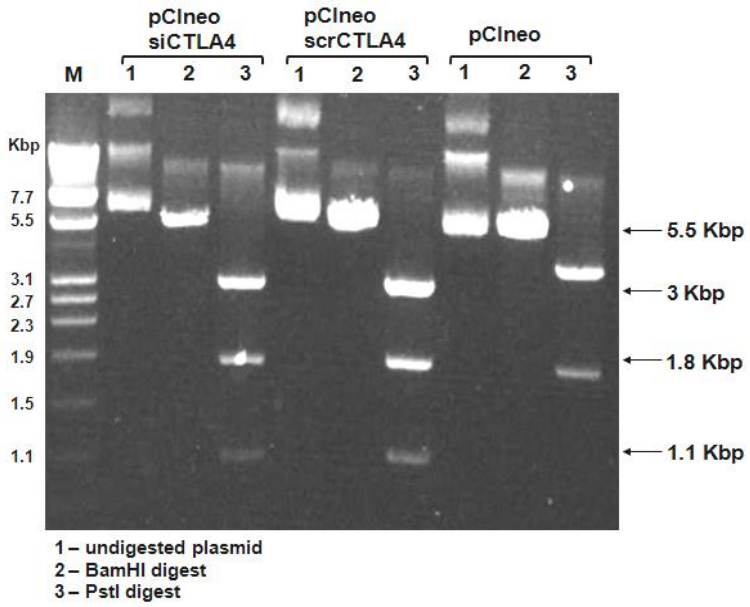

Figure 2.6. Schematic representation of the generation of pCIneo siCTLA4 and pCIneo scrCTLA4.

(A) Schematic diagram of pCIneo, pCIneo siCTLA4 and pCIneo scrCTLA4 showing a part of the plasmid and indicating the orientation of the promoters and the position of the restriction enzymes used for the cloning. (B) Gel electrophoresis and restriction map analysis of the generated pCIneo siCTLA4 and pCIneo scrCTLA4 compared to pCIneo. Lanes are as follows: 1. undigested plasmid; 2. BamHI digest; 3. PstI digest.

The knockdown efficiency of the generated constructs was evaluated in transient co-transfections with pCTLA4-Flag. Western blot analysis of total cellular extracts 24h after transfection showed no expression of CTLA4 in the samples transfected with pCIneo siCTLA4. However, it was not possible to detect CTLA4 also in the HeLa cells treated with the pCIneo scrCTLA4 control. The membrane was re-probed with anti-β Actin antibody to confirm equal loading (Fig. 2.7).

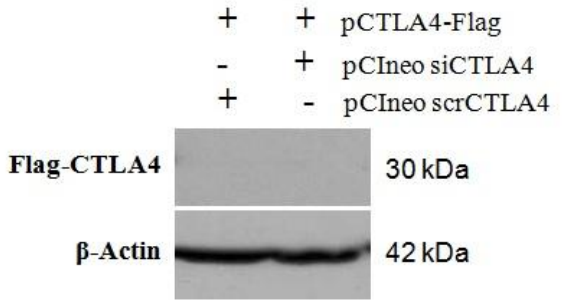

Figure 2.7. Downregulation of CTLA4 expression in HeLa cells following transfection with pCIneo siCTLA4.

The cells were co-transfected with 0.2µg of pCTLA4-Flag and 0.8µg of pCIneo siCTLA4 or pCIneo scrCTLA4. Western blot analysis of CTLA4 expression was performed 24h post-transfection. The membrane was re-probed with anti-β-Actin antibody used as a loading control. Data are representative of a minimum of three different experiments performed.

2.2.5 Construction and characterisation of pCTLA4-Flag siCTLA4 and pCTLA4-Flag scrCTLA4

To confirm the silencing effect of the chosen shRNA sequence, the shRNA cassette was cloned into the pCTLA4-Flag vector and the expression levels of CTLA4 in transfected HeLa cells were compared. The shRNA cassette including the U6 promoter was excised from the Blusecript plasmids by PCR amplification using the primers shCTLA4 Fr and shCTLA4 Rev (Tale 2.2). Since there are two BamHI restriction sites present in the pCTLA4-Flag vector, it was impossible to use the same enzyme to linearise the plasmid. However, BglII and BamHI restrictions have compatible ends and therefore, a unique BglII restriction site present in pCTLA4-Flag was used to linearise the vector (Fig. 2.8 A). The generated constructs were digested with EcoRI and PstI to confirm the successful cloning and the orientation of the insert. The resulting fragments in the new plasmids are 3.5 Kbp, 2.3 Kbp and 1 Kbp. A digestion of pCTLA4-Flag vector with EcoRI and PstI results in separation of two fragments: 2.3 Kbp and 4.1 Kbp (Fig. 2.8 B).

A)

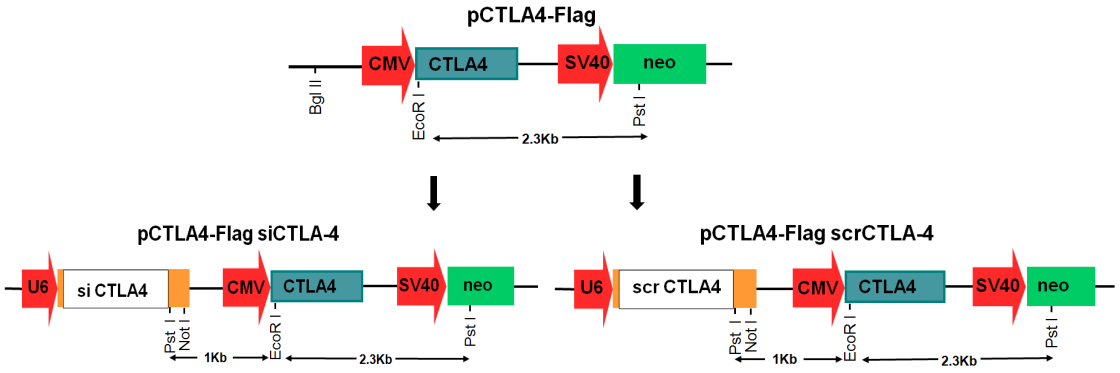

B)

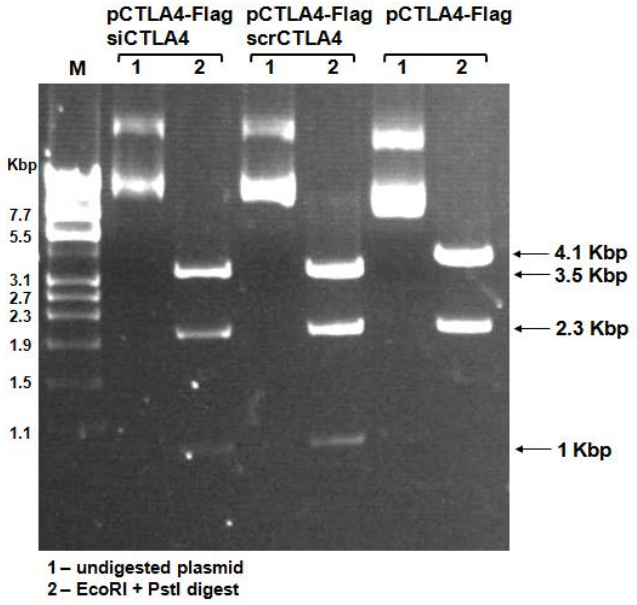

Figure 2.8. Schematic representation of the generation of pCTLA4-Flag siCTLA4 and pCTLA4-Flag scrCTLA4.

(A) Schematic diagram of pCTLA4-Flag, pCTLA4-Flag siCTLA4 and pCTLA4-Flag scrCTLA4 showing a part of the plasmid and indicating the orientation of the promoters and the position of the restriction enzymes used for the cloning. (B) Gel electrophoresis and restriction map analysis of the generated pCTLA4-Flag siCTLA4 and pCTLA4-Flag scrCTLA4 compared to pCTLA4-Flag. Lanes are as follows: 1. undigested plasmid; 2. EcoRI +PstI digest.

The knockdown efficiency of the generated constructs was evaluated in transient transfections with the new plasmids. Western blot analysis of total cellular extracts 24h after transfection showed no significant silencing effect. High levels of CTLA4 expression were observed in the samples transfected with pCTLA4-Flag siCTLA4 and the ones treated with pCTLA4-Flag scrCTLA4. The membrane was re-probed with anti-β Actin antibody to confirm equal loading (Fig. 2.9).

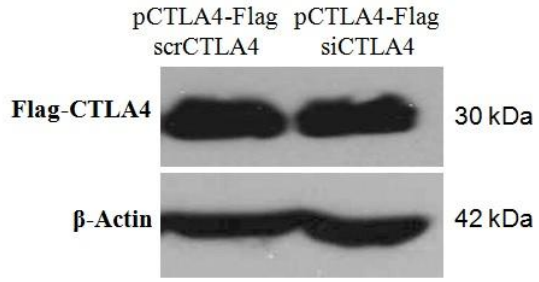

Figure 2.9. Detection of CTLA4 expression in HeLa cells following transfection with pCTLA4-Flag siCTLA4.

The cells were transfected with 1µg of pCTLA4-Flag siCTLA4 or pCTLA4-Flag scrCTLA4. Western blot analysis of CTLA4 expression was performed 24h post-transfection. The membrane was re-probed with anti-β-Actin antibody used as a loading control. Data are representative of a minimum of three different experiments performed.

2.2.6 Construction and characterisation of pBSU6neo siCTLA4 and pBSU6neo scrCTLA4

The cloning of the shRNA into pCIneo and pCTLA4-Flag did not seem to mediate downregulation, however, the first construct containing the shRNA in the Bluescript backbone (pBSU6 siCTLA4) showed a strong silencing effect. Therefore, to develop a plasmid that would allow generation of a stable cell line, the neomycin resistance gene was inserted into this plasmid and into its corresponding control pBSU6 scrCTLA4. A third vector pBSU6neo was developed and used as an additional control for the transfection experiments. The neomycin cassette including the neomycin gene, the SV-40 promoter and the poly-A tail was excised from the pCIneo vector with PCR amplification using primers (Neo Promega Fr and Neo Promega Rev (Table 2.2)) that generated NotI restriction sites on both ends of the plasmid. The cassette was then inserted into the NotI restriction site present in the MCS of pBSU6 downstream of the inserted shRNA sequence (Fig. 2.10 A). A restriction digest with BamHI was performed to confirm the successful cloning and the orientation of the insert in the newly generated constructs. The BamHI restriction site just before the poly-A tail of the neomycin gene added a second restriction site in the new plasmids (Fig. 2.10 B). It also gives information about the direction of the inserted sequence. The size of the neomycin cassette is about 1.5 Kbp and the size of the empty pBSU6 is 3.8 Kbp. If the poly-A tail of the neomycin gene is downstream the shRNA cassette, two fragments will result upon restriction with BamHI: one that is 0.51 Kbp and another one that is 4.8 Kbp. If the SV-40 promoter from the neomycin cassette is downstream of the shRNA cassette, the resulting fragments would be 1.8 Kbp and 3.5 Kbp. The small 0.51 Kbp fragments are not easy to distinguish in

figure 2.10 B. Therefore, the contrast and brightness of the lower part of the picture were enhanced and it was presented separately as figure 2.10 C. The resulting larger 4.8 Kbp fragments in the new constructs (lane 2 for pBSU6neo siCTLA4, pBSU6neo scrCTLA4 and pBSU6neo) are clearly visible and easy to compare with the linearized empty vector pBSU6 (lane 2), which confirms the presence of the insert and determines that the poly-A tail of the neomycin gene is downstream the shRNA cassette.

A)

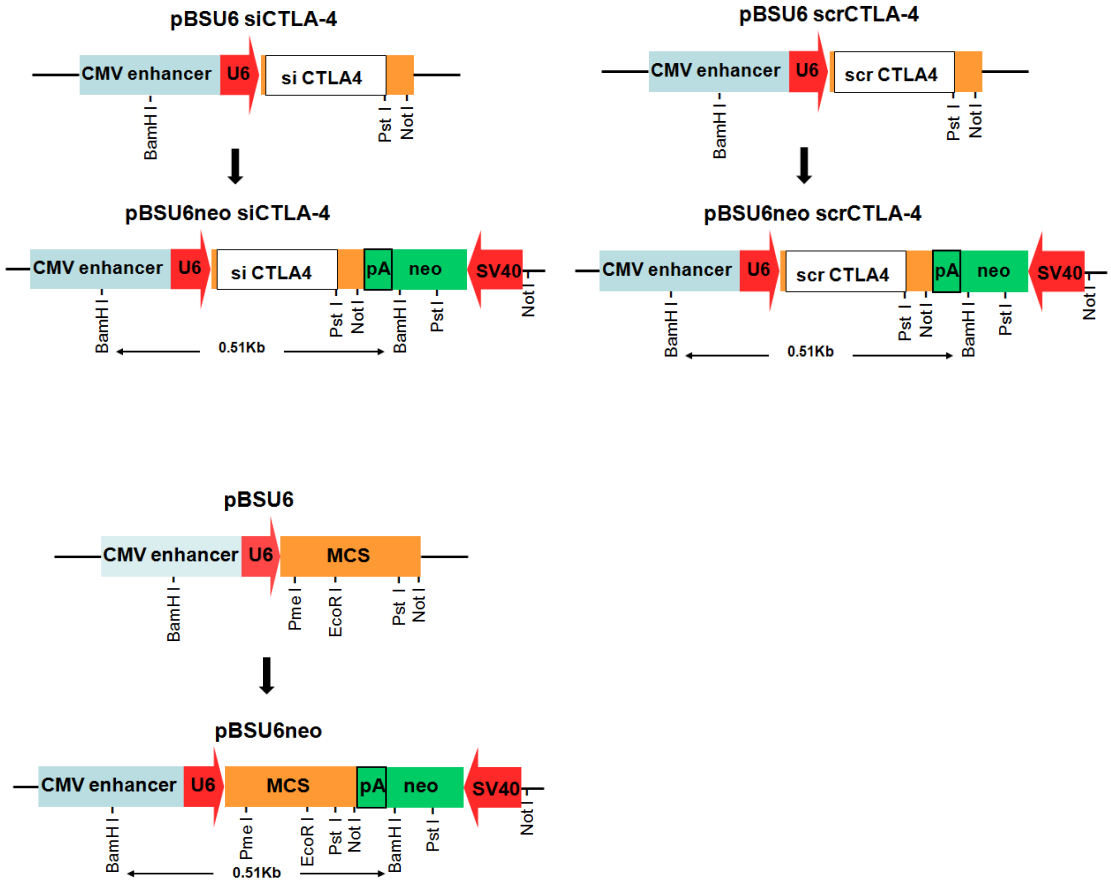

B)

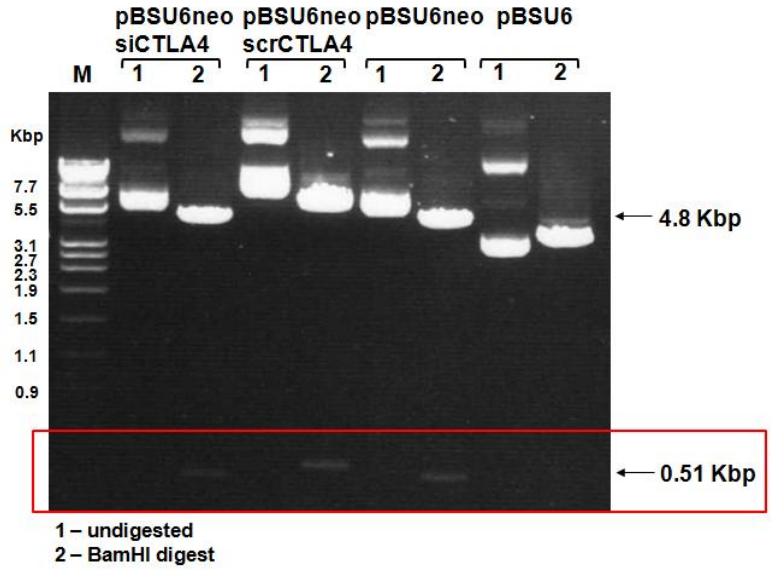

C)

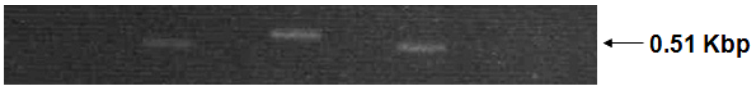

Figure 2.10. Schematic representation of the generation of pBSU6neo siCTLA4 and pBSU6neo scrCTLA4.

(A) Schematic diagram of pBSU6 siCTLA4, pBSU6 scrCTLA4 and pBSU6 and pBSU6neo siCTLA4, pBSU6neo scrCTLA4 and pBSU6neo showing a part of the plasmid and indicating the orientation of the promoters and the position of the restriction enzymes used for the cloning. (B) Gel electrophoresis and restriction map analysis of the generated pBSU6neo siCTLA4, pBSU6neo scrCTLA4 and pBSU6neo compared to pBSU6. Lanes are as follows: 1. undigested plasmid; 2. BamHI digest. (C) showing the lower part of the gel with adjusted brightness and contrast.

The knockdown efficiency of the generated constructs was evaluated in transient co-transfections with pCTLA4-Flag. Western blot analysis of total cellular extracts 24h after transfection showed significantly reduced expression levels of CTLA4 in the samples transfected with pBSU6neo siCTLA4. In contrast, it was possible to detect similar level of expression in the HeLa cells treated with the controls pBSU6neo scrCTLA4 or pBSU6neo. The membrane was re-probed with anti-β Actin antibody to confirm equal loading (Fig. 2.11).

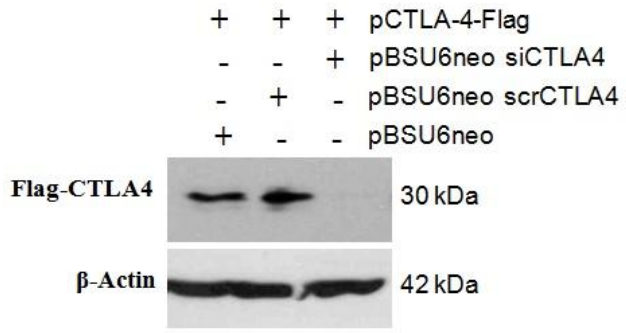

Figure 2.11. Downregulation of CTLA4 expression in HeLa cells following transfection with pBSU6neo siCTLA4.

The cells were co-transfected with 0.2μg of pCTLA4-Flag and 0.8μg of pBSU6neo, pBSU6neo scrCTLA4 or pBSU6neo siCTLA4. Western blot analysis of CTLA4 expression was performed 24h post-transfection and β-Actin was used as a loading control. Data are representative of a minimum of three different experiments performed.

Real-time PCR is a quantitative method used to study gene expression. Therefore, the silencing efficiency of pBSU6neo siCTLA4 was further investigated using this technique. It was determined that the CTLA4 expression induced by pCTLA4-Flag was reduced more than 75% in the HeLa cells transiently co-transfected with pBSU6neo siCTLA4 and pCTLA4-Flag at 5:1 ratio compared to controls (Fig. 2.12).

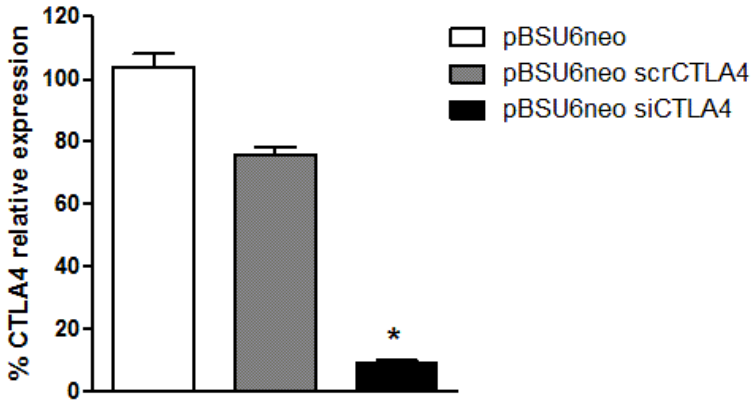

Figure 2.12. Knockdown of CTLA4 expression in HeLa cells.

The cells were co-transfected with 0.2µg of pCTLA4-Flag and 0.8µg of pBSU6neo siCTLA4, pBSU6neo scrCTLA4 or pBSU6neo. The relative expression of CTLA4 was determined by Real-time PCR analysis 24h post transfection. The relative quantification of the target gene expression was determined using the $2^{-\Delta\Delta Ct}$ method and GAPDH was used for normalization. Expression levels were analysed relative to the sample transfected with pBSU6neo set as 100%.*P< 0.05 indicates significance in relation to pBSU6neo and pBSU6neo scrCTLA4. Statistical analysis was performed using one-way ANOVA followed by Tukey post-test. Columns represent the means of triplicates ± SEM.

2.2.7 Establishing Hela stable transfected with pCTLA4-Flag

HeLa are an easy to handle cell line and show high transfection efficiency compared to Jurkats or PBMCs. Originally, it was planned to develop other constructs encoding sequences to silence CTLA4. Therefore, to facilitate their characterization and to avoid variability that may occur in co-transfection, a HeLa cell line stably transfected with pCTLA4-Flag was developed. HeLa were transfected with the plasmid and selected for neomycin resistance for 3 weeks. Colonies derived from single clones were grown and tested for CTLA4 expression. Figure 2.13 shows several samples where CTLA4

transcripts were determined by Real-time PCR. Surprisingly, in none of the twelve tested samples was possible to detect CTLA4 by Western blot using the anti-Flag antibody. In only six of the samples expression was detectable using the more sensitive Real-time PCR despite the neomycin resistance of all selected clones.

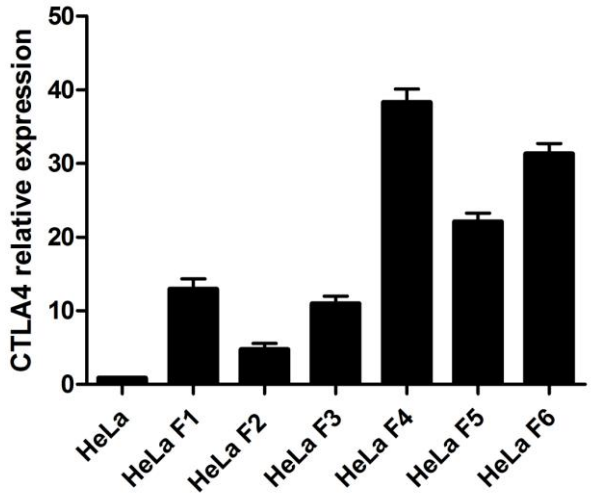

Figure 2.13. CTLA4 expression in stable transfected HeLa.

RNA from untransfected HeLa cells and selected clones transfected with pCTLA4-Flag (marked as F1-F6) was isolated and reverse transcribed to cDNA. Expression of CTLA4 was detected by real-time PCR. Expression levels were analysed relative to controls of untransfected HeLa and normalized to GAPDH expression. Columns represent the means of triplicates ± SEM.

The HeLa F4 cell line showed the highest expression levels of CTLA4 from the tested clones in the Real-time PCR experiments and was used further in the study. HeLa F4 cells were transfected with pBSU6neo, pBSU6neo scrCTLA4 and pBSU6neo siCTLA4 to estimate if the levels of CTLA4 expression would be affected. Using relative quantification, it was determined that the CTLA4 expression in the sample transfected with pBSU6neo siCTLA4 was significantly decreased over 60% compared to the control transfected with pBSU6neo (Fig.2.14). A slight decrease of about 20% was observed also

in the sample transfected with pBSU6neo scrCTLA4. These data correspond to the results obtained from the transient co-transfections confirming the efficacy of the generated plasmid pBSU6neo siCTLA4 to silence CTLA4. It also suggests that the generated cell line HeLa F4 could be used as a model to investigate other plasmids developed to modify CTLA4 gene expression.

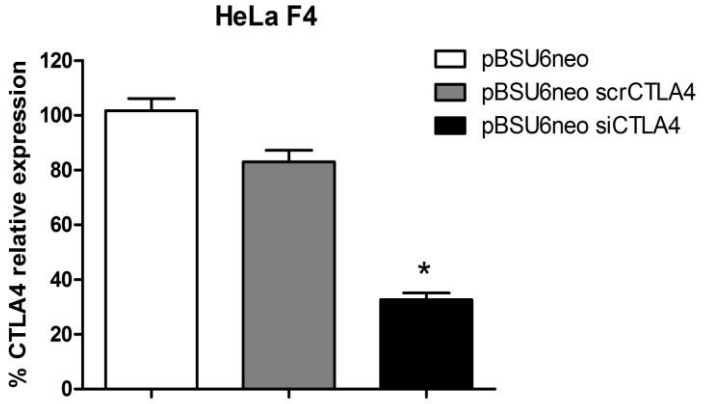

Figure 2.14. CTLA4 expression in HeLa F4 transfected with pBSU6 neo, pBSU6neo scrCTLA4 or pBSU6neo siCTLA4.

HeLa F4 cells were transfected with 1µg of pBSU6neo, pBSU6neo scrCTLA4 or pBSU6neo siCTLA4. CTLA4 expression was determined by real-time PCR analysis 24h post transfection. The relative quantification of the target gene expression was determined using the $2^{-\Delta\Delta Ct}$ method and GAPDH was used for normalization Expression levels were analysed relative to the sample transfected with pBSU6neo set as 100%.*P< 0.05 indicates significance in relation to pBSU6neo. Statistical analysis was performed using one-way ANOVA followed by Tukey post-test. Columns represent the means of triplicates ± SEM.

3. Chapter 2 – Generation and validation of stable cell lines expressing CTLA4 specific shRNA

3.1 Methods

3.1.1 Cell culture and stimulation of Jurkat cells

The human T cell line Jurkat was maintained at 37°C, 5% CO_2 in RPMI 1640 (Lonza) containing 10% FCS (Lonza), 100 U/ml penicillin, 0.1 mg/ml streptomycin (Sigma) and 2mM L-Glutamine (Sigma). Cells were split 1:15 every 3 days to maintain a concentration of 0.1-1.5 x 10^6 cells/ml.

To induce CTLA-4 expression in Jurkats, 3 x 10^6 cells/ well in 6 well plates were stimulated with 40ng/ml PMA (Phorbol 12-Myristate 13-Acetate) (Sigma) and 1µM ionomycin (Sigma) for 48-72h [101]. The presence of CTLA-4 was investigated with Western blot and/or RT-PCR. For antibodies-mediated stimulation 96-well plates were coated overnight at 4°C with 0.35 µg/well anti-mouse IgG (Sigma) in sterile PBS. Unbound antibodies were removed carefully and the wells were washed with PBS. The wells were then coated with a solution of 0.65 µg/well anti-CD3 (BD Pharmingen); 0.065 µg/well anti-CD28 (Ancell); 0.65 µg/well anti-CTLA4 (BD Pharmingen) or pre-mixed combination in sterile PBS and incubated overnight at 4°C. Unbound antibodies were removed carefully and the wells were washed with PBS. Cells were plated at a concentration of 8 x 10^5 cells/ml in RPMI (Lonza) for the indicated times. For stimulation

in 24-well plates the amount of antibodies was following: 0.65 µg/well anti-mouse IgG; 1.3 µg/well anti-CD3; 0.13 µg/well anti-CD28; 1.3 µg/well anti-CTLA4 [100].

3.1.2 Isolation and stimulation of PBMC

PBMCs containing T cells were used in some experiments as a positive control when CTLA4 expression was tested.

Whole blood was diluted 1:1 with PBS. 3 ml of Histopaque-1077 (Sigma) was added into a 12ml tube. 6ml of the diluted blood sample was added carefully dropwise, so that it would build a second layer in the tube. The sample was centrifuged at 1300 rpm for 30 min at room temperature. The upper layer containing the plasma and the pellet containing the erythrocytes and granulocytes were discarded. The intermediate layer containing the mononuclear cells was transferred into a new tube. The cells were pooled and washed twice with 10ml PBS. The pellet was resuspended in 2-5 ml complete RPMI (Lonza) and the cell number was estimated. The PBMC were further cultured in complete RPMI (Lonza) at 37°C, 5% CO_2.

To induce CTLA4 expression in PBMC, 3-4 x 10^6 cells/ well in 6 well plates were stimulated with 5ng/ml PMA (Sigma) and 0.5µM ionomycin (Sigma) for 48-72h. The presence of CTLA4 was investigated with Western blot and/or RT-PCR.

3.1.3 Transient transfection of Jurkats

Several attempts were made to transfect Jurkats using liposome-based transfection reagents (Fugene HD (Roche) and GeneJuice (Novagen)) with plasmids encoding the reporter gene β-galactosidase (pCMV-SPORT) or GFP (pmaxGFP). However, attempts to visualize the expression of the reporter genes of interest as in the transfected HeLa

(Fig.2.1 and Fig.2.2) failed (Fig. 6.7., appendix II) suggesting that the transfection was not successful. For transfections cells were plated at $5x10^5$ cells/ml in 2 ml of medium in 6-well plates. 3 µl of FuGENE HD transfection reagent (Roche) and 1µg of plasmid DNA were added to 100 µl of serum-free medium, vortexed briefly and incubated at room temperature for 15 min to allow complex formation. The mixture was added dropwise to the cells over the entire surface of the well. The cells were incubated for another 24-48h at 37°C in 5%CO_2. After the incubation time the transfection efficiency was analyzed with X-gal assay or immunofluorescence. However, attempts to visualize the expression of the reporter genes of interest failed suggesting that the transfection was not successful.

Therefore, transient transfection was also performed using electroporation and the Amaxa Nucleofector Kit V (Lonza) according to the manufacturer instructions. $1x10^6$ cells were resuspended in 100 µl of Nucleofector Solution V together with 2 µg of DNA and the suspension was transferred into certified cuvette. The cells were transfected using Nucleofector Program X-01 for Nucleofector I Device. 500 µl of antibiotics-free medium was added to the cuvette and the cell suspension was transferred into prepared 12-well plate (final volume 1.5 ml media/well). Samples were incubated for 24h at 37°C in 5% CO_2 before gene expression was analysed by immunofluorescence.

3.1.4 Stable transfection of Jurkats and clones selection

With the development of a stable transfected Jurkat cell line would be avoided the variability in the results that could be caused by the low transient transfection efficiency in this cell line. To generate stable transfected clones $1x10^6$ cells were transfected with plasmid DNA encoding the neomycine gene (pBSU6neo siCTLA4, pBSU6neo

scrCTLA4 or pBSU6neo) by electroporation as described above. 24h post transfection the cell suspension was transferred to media containing 700 µg/ml G418 (Roche). The cells were selected for 2 weeks and media was changed every 3-4 days. Stable cell clones were selected using limited dilution. The cells were resuspended at 10 cells/ml and 100 µl were plated in 96-well plates. After approximately 3 weeks colonies derived from the individual clones were visible and were further propagated. DNA samples were tested for the presence of the plasmid in the genome. To test the expression of CTLA4, $3x10^6$ cells were stimulated with PMA/ionomycin for 3 days. Then the RNA was extracted and CTLA4 expression was detected by RT-PCR. IL-2 levels in the supernatants were determined using ELISA.

3.1.5 DNA extraction

DNA extraction was performed to isolate DNA from cells which was used in PCR amplification. Cells were resuspended in 200µl PBS and 300µl of cell lysis solution (appendix I) was added. 100µl of protein precipitation solution (appendix I) were added and the samples were vortexed for 15 sec. Upon centrifugation for 5 min at 12000g the supernatant was transferred into a new tube. 300µl isopropanol were added and mixed by inverting. The DNA was pelleted for 5 min at 12000g and the pellet was then washed with 500µl 70% ethanol. The DNA pellet was air dried and resuspended in 30-50µl TE buffer (appendix I). Samples were stored at -20°C.

3.1.6 IL-2 ELISA

The production of the cytokine IL-2 in stimulated cells was used as a marker for T cell activation. The amount of secreted IL-2 was detected in the supernatant of stimulated

cells and quantified using human IL-2 ELISA Ready-SET-Go kit (eBioscience). The assay was performed according to the manufacturers' instructions.

96well- ELISA plate (Corning Costar) was coated with 100µl/well of capture antibody previously diluted 1/250 in coating buffer and incubated overnight at 4°C. After incubation the plate was washed 5 times with 300µl/well Wash buffer. Unspecific binding was prevented by pipetting 200µl/well of 1x assay diluent and incubation of the plates for 1h at room temperature. After blocking the plates were washed 5 times. The standard (recombinant IL-2) and samples (supernatant of cells) were diluted using 1x assay diluent and 100µl/well were used. For the standard curve 6 2-fold serial dilutions were performed starting with a top concentration of 500pg/ml. The samples were incubated for 2h at room temperature. Upon incubation the plates were washed 5 times. 100µl/well of the detection antibody previously diluted 1/250 were added and plates were incubated for 1h at room temperature. After 5 washing steps 100µl of avidin-HRP diluted 1/250 in 1x assay diluent were added to each well and the plate was incubated for further 30min. Then the plates were washed 7 times with Wash buffer. 100µl/well TMB substrate solution was added and the plates were incubated at room temperature for 5-10 min until a colour change developed. 50µl/well stop solution (1M H_2SO_4) were added to terminate the reaction and absorbance was measured at 450nm.

3.1.7 Stem-loop RT-PCR followed by Real-time PCR (detection and quantification of mature siRNA)

Two different stem-loop RT primers designed according to Chen *et al.* [97] bind sequence-specific to the 3' portion of the mature *siCTLA4* or *scrCTLA4* and are reverse transcribed. DNase treated total RNA (150 ng) was incubated with the appropriate stem-

loop primer (Table 2.4) (0.1 µM) (Sigma) at 65°C for 5 min in a total volume of 7 µl. After cooling on ice for 2 min the following components were added: 2 µl of 5xRT buffer, 0.75 µl dNTPs mix (10mM), 0.25 µl RNase Inhibitor and 0.25 µl reverse transcriptase (Roche). Reverse transcriptase reaction was performed on thermocycler using the following protocol: incubation for 30 min at 16°C, followed by pulsed RT of 60 cycles at 30°C for 30 sec, 42°C for 30 sec and 50°C for 1 sec. To inactivate the reverse transcriptase the samples were heated at 85°C for 5 min. The cDNA was stored -20°C until being analyzed with Real-time PCR.

The resulting 70 bp large RT products then could be amplified in a Real-time PCR with a forward primer sequence-specific for the *siCTLA4* or *scrCTLA4* and a universal reverse primer (Table 2.4). The expression was quantified using a conventional SYBR Green I assay. To detect the mature *siCTLA4* and *scrCTLA4* 1 µl stem-loop RT-PCR product was amplified using siRNA-specific forward primer (1 µM), the universal reverse primer (1 µM) (Table 2.4) and SYBR Green I Master mix (Roche) on the LighCycler 480 PCR System (Roche). The reactions were incubated in a 96-well plate at 95°C for 5 min, followed by 45 cycles of 95°C for 7 sec, 62°C for 10 sec and 72°C for 7 sec; melting curve analysis at 95°C for 5 sec, 65°C for 1 min, 95°C for 5 continuous acquisition/°C and final cooling step to 4°C. All samples were run in triplicate and a negative control containing no template (RT product) was included in each run. The PCR product was visualized on a 2% agarose gel by ethidium bromide staining. The PCR fragments were also subcloned into pCR2.1-TOPO (Invitrogen) and sequenced by MWG Operon (UK) to confirm the presence of the expressed siRNA.

Oligonucleotide	Sequence 5'-3'
Stem loop siCTLA4	GTCGTATCCAGTGCAGGGTCCGAGGTATTCGCACTGGATACGACAAGCAA
Stem loop scrCTLA4	GTCGTATCCAGTGCAGGGTCCGAGGTATTCGCACTGGATACGACAAAGAA
Fr siCTLA4 sl	GCGGTAAATCTGGGTTCCG
Fr scrCTLA4 sl	GCGGTCAAGCTGGGTTCAG
Universal Rev	CAGTGCAGGGTCCGAGGT
mature *siCTLA4*	TAAATCTGGGTTCCGTTGCTT
mature *scrCTLA4*	TCAAGCTGGGTTCAGTTTCTT

Table 2.4 Oligonucleotides used for the stem-loop RT-PCR assay.

Stem loop siCTLA4 primer was used to reverse transcribe the mature *siCTLA4.* For the following Real-time PCR detection the Fr siCTLA4 sl and Universal Rev primers were used. Stem loop scrCTLA4 primer was used to reverse transcribe the mature *scrCTLA4.* For the following Real-time PCR detection the Fr scrCTLA4 sl and Universal Rev primers were used. Primers were designed according to Chen *et al*. [97].

3.1.8 TOPO TA Cloning

Cloning in pCR2.1-TOPO (Invitrogen) was performed according to the manufacturer's instructions. Briefly 2 µl of PCR product was added to 1µl salt solution, 1µl linearized vector and 2 µl H_2O and incubated for 5 min at room temperature.

3.2 Results

3.2.1 Jurkat as a model for CTLA4 investigation

Jurkat cells are a T-cell lymphoma cell line that has been widely used to study TCR signaling. However, there is a controversy in the literature if the Jurkat cells express endogenously CTLA4 [102, 103]. Therefore, it was necessary to investigate if this cell line was a suitable model for investigation of CTLA4 knockdown. Several attempts were made to determine CTLA4 expression on the protein level in Jurkats and PBMCs by Western blot. As a positive control was used a sample of HeLa cells transiently transfected with pCTLA4-Flag, where the protein was detected with the mouse monoclonal anti-Flag antibody. Samples of stimulated and unstimulated PBMCs and Jurkats were tested using a goat anti-human CTLA4 antibody (#AF-386-PB, R&D). Surprisingly, CTLA4 expression was detected only in the transfected HeLa cells (Fig. 3.1). The same membrane was re-probed with an antibody against β-Actin to ensure equal loading. The presence of bands in all the lanes confirmed that no protein degradation has occurred. Later in the course of the project another antibody from Santa Cruz was tested and the expression of the protein was successfully detected in Western blot in stimulated Jurkats (Fig.3.13).

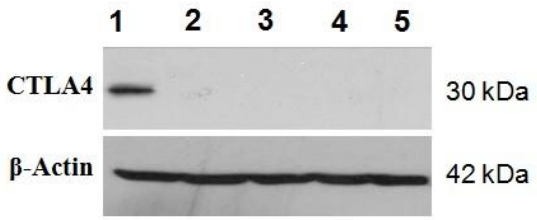

Figure 3.1. CTLA4 expression detection.

CTLA4 detection using anti-human CTLA4 Ab (R&D) in protein lysate from stimulated Jurkats and PBMCs. Lanes are loaded as follows: 1. HeLa transfected with pCTLA4-Flag; 2. Jurkat control; 3. Jurkat stimulated for 3 days with PMA/ionomycin; 4. PBMCs control; 5. PBMCs stimulated for 3 days with PMA/ionomycin.

The expression levels were further investigated and compared by RT-PCR and Real-time PCR. CTLA4 was detected at the mRNA level with reverse transcriptase PCR in the stimulated Jurkat cells (Fig.3.2 A). As a positive control stimulated PBMCs were used. The Real-time PCR experiments which allow better relative expression quantification, confirmed that CTLA4 was expressed much stronger in the transfected HeLa cells compared to stimulated Jurkats (Fig. 3.2 B). These results suggested that the transcription induced by the CMV promoter in the pCTLA4-Flag in transiently transfected HeLa cells was much stronger than the endogenously induced expression. The data from the Real-time PCR also showed that the anti-CTLA4 antibody from R&D is probably not sensitive enough to detect the weaker endogenous expression.

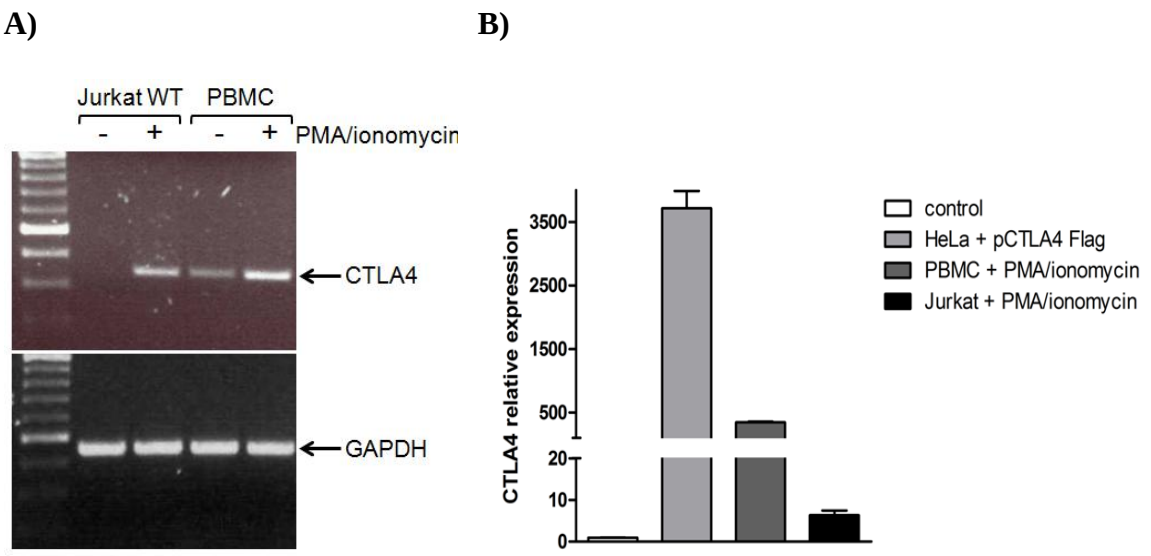

Figure 3.2. CTLA4 expression in Jurkats.

(A) Jurkat cells and PBMCs were stimulated for 3 days with PMA and ionomycin. CTLA4 expression was detected using CTLA4-specific primers in RT-PCR. GAPDH was used as a loading control. (B) CTLA4 detection in stimulated Jurkats, stimulated PBMCs, transfected HeLa cells and untransfected HeLa cells (control) by Real-time PCR. The relative quantification of the target gene expression was determined using the $2^{-\Delta\Delta Ct}$ method and GAPDH was used for normalization. Columns represent the means of triplicates ± SEM.

Next, the induction kinetics of CTLA4 expression in Jurkats was determined. Jurkats were incubated with the same amount of PMA and ionomycin over a 5-days time course. At different time points the RNA was isolated, converted to cDNA and the levels of CTLA4 were measured by Real-time PCR and normalized to that of the GAPDH transcripts. It was observed that CTLA4 expression starts no earlier than 6h upon stimulation and reaches peak levels at day 3-4 (Fig. 3.3).

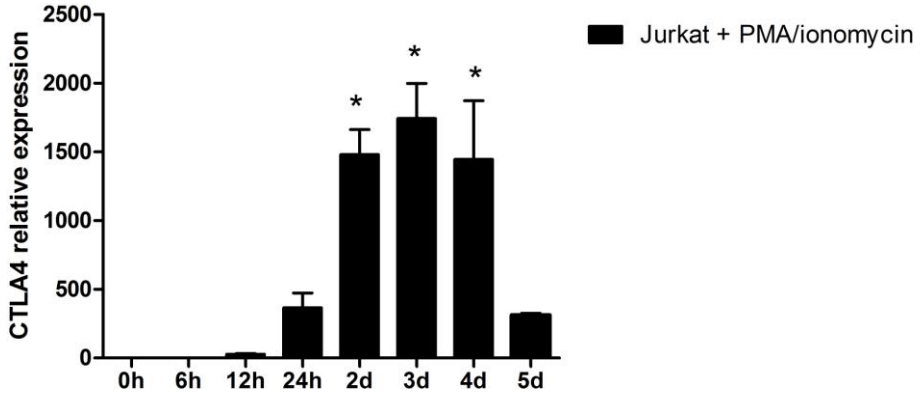

Figure 3.3. CTLA4 expression kinetics in Jurkats.

Jurkat cells were cultured in the presence of PMA and ionomycin for 0h, 6h, 12h, 24h, 2, 3, 4 and 5 days. CTLA4 expression levels were detected by Real-time PCR. The relative quantification of the target gene expression was determined using the $2^{-\Delta\Delta Ct}$ method and GAPDH was used for normalization. *P< 0.05 indicates significance in relation to unstimulated control. Columns represent the means of triplicates ± SEM. Statistical analysis was performed using one-way ANOVA followed by Tukey post-test.

One of the main characteristic effects of T-cell activation is the production of interleukin-2 (IL-2). It has been previously reported that blockade of CTLA4/ CD80, CD86 interaction increases IL-2 production by T cells [104]. Therefore, we expected to see that the induced CTLA4 knockdown in T cells will result in alteration of the produced IL-2 levels in these cells upon stimulation compared to controls. To confirm that Jurkats are a suitable model for functional studies of the CTLA4 silencing effects, the secretion of IL-2 was determined. Figure 3.4 shows the amount of IL-2 secreted in the supernatant of Jurkats and PBMCs upon stimulation with PMA and ionomycin for 3 days.

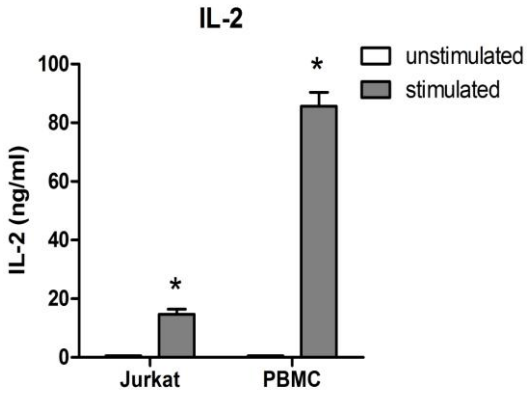

Figure 3.4. IL-2 production in stimulated Jurkats and PBMCs.

Jurkat cells and PBMCs were cultured for 3 days in the presence of PMA and ionomycin. The amount of IL-2 secreted in the supernatant was determined by ELISA. *P< 0.05 indicates significance in relation to unstimulated control. Columns represent the means of duplicates ± SEM. Statistical analysis was performed using unpaired t-test.

3.2.2 Optimisation of transfection conditions for Jurkats

Several attempts were made to transfect Jurkats using liposome-based transfection reagents (Fugene HD (Roche) and GeneJuice (Novagen)) with plasmids encoding the reporter gene β-galactosidase (pCMV-SPORT) or GFP (pmaxGFP). However, attempts to visualize the expression of the reporter genes of interest as in the transfected HeLa (Fig.2.1 and Fig.2.2) failed (figure 6.7., appendix II) suggesting that the transfection was not successful. Therefore, we tried to transfect the Jurkats using electroporation and the Amaxa® Cell Line Nucleofector Kit V recommended for this cell line. The cells were transfected with pmaxGFP vector supplied from the manufacturer (Amaxa) and analysed 24h post transfection using fluorescence microscopy. The pictures showing the transgene expression of GFP in the cells indicate the successful transfection of the Jurkats using electroporation (Fig. 3.5).

A)

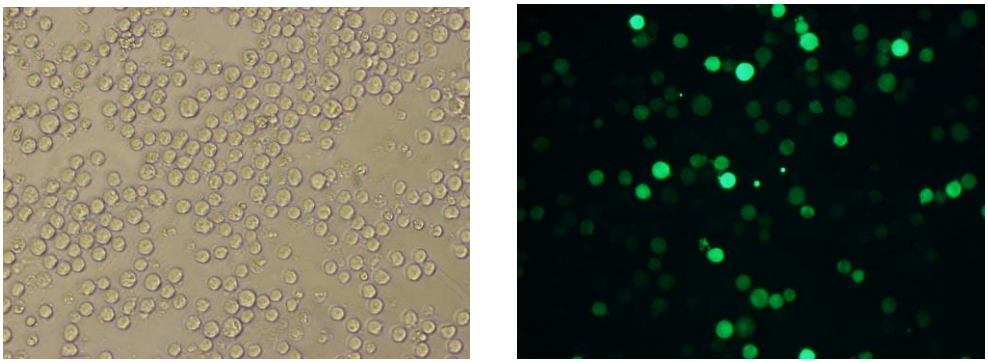

B)

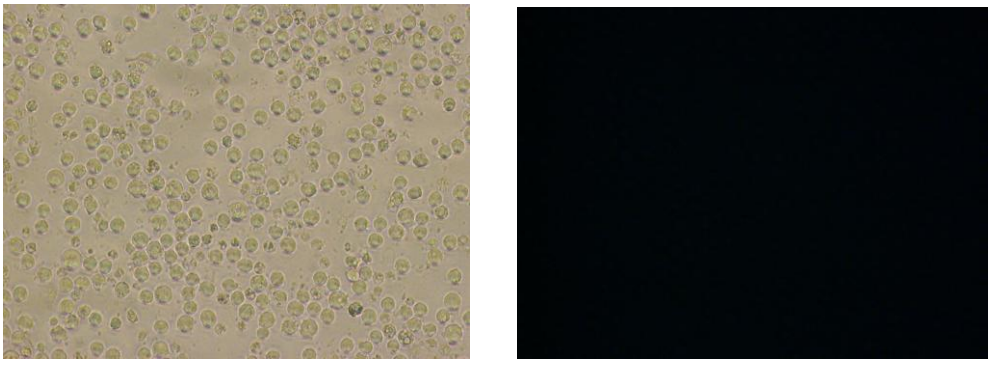

Figure 3.5. Transgene expression of GFP in Jurkats.

(A) Jurkat cells transfected using electroporation with 2 µg pmaxGFP Vector or (B) 2 µg pBSU6 vector as a negative control. 24h post transfection cells were analysed using light (left panels) and fluorescence microscopy (right panels). Magnification 200x.

3.2.3 Transient transfections of Jurkats

The efficacy of pBSU6neo siCTLA4 to downregulate the activation-induced endogenous CTLA4 expression in Jurkats was tested next. Jurkats were transiently transfected with

the plasmid and 24h later stimulated with PMA and ionomycin for 3 days. CTLA4 expression was detected using RT-PCR. To ensure that the transfection was successful, the presence of the neomycin resistance gene was detected using PCR (Fig. 3.6). The plasmids were detected in the DNA of all three transfected samples compared to the untreated control. The results presented in Fig. 3.6 B show that Jurkats transfected with the plasmid but left untreated afterwards, do not express CTLA4. This indicates that the electroporation used for the transfection of the Jurkats did not induce CTLA4 expression in the cell line. However, CTLA4 was detected upon stimulation for 3 days. Unfortunately, it was not possible to determine definitely if pBSU6neo siCTLA4 is silencing the expression of the receptor in the transiently transfected Jurkats. In some experiments a decrease was observed (Fig. 3.6 C), however, in others (Fig. 3.6 B) CTLA4 expression was detected and the levels were similar to those in the negative controls – Jurkats transfected with pBSU6neo scrCTLA4 and Jurkats transfected with pBSU6neo.

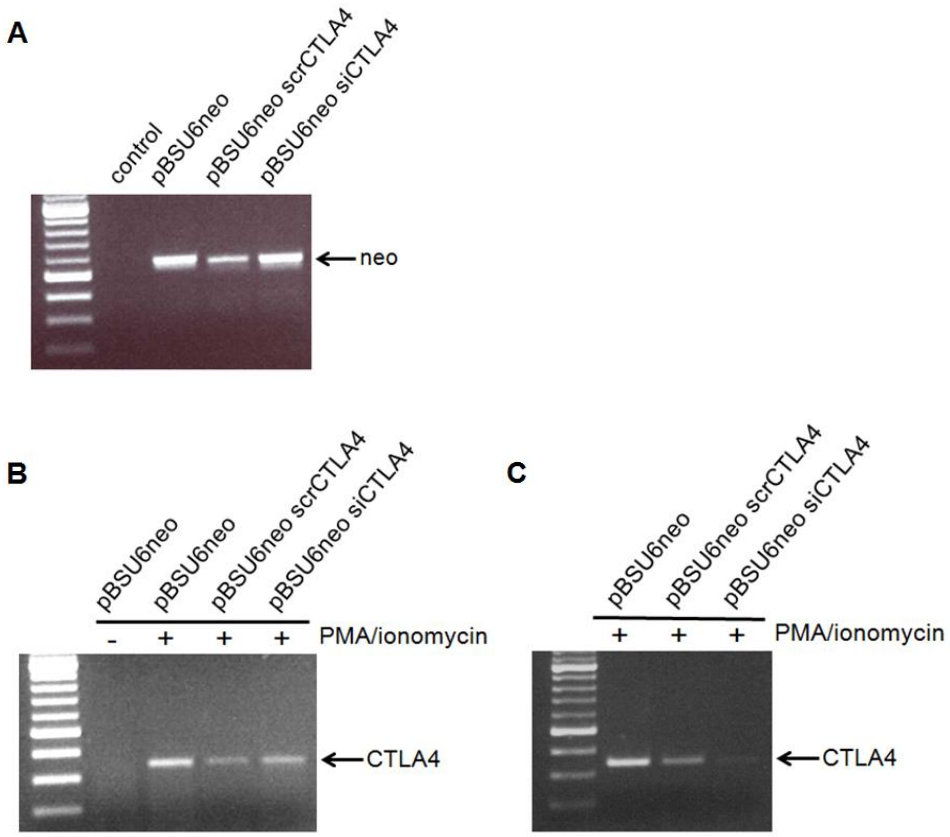

Figure 3.6. Silencing of CTLA4 in transiently transfected Jurkats.

WT Jurkat cells were transfected by electroporation with 2 µg of pBSU6neo siCTLA4, pBSU6neo scrCTLA4 or pBSU6neo. 24h post-transfection the cells were cultured for 3 days in the presence of PMA/ ionomycin or left untreated. (A) PCR analysis confirms the presence of the vectors pBSU6neo siCTLA4, pBSU6neo scrCTLA4 and pBSU6neo in the DNA samples of the transfected cells. (B), (C) CTLA4 expression was determined by RT-PCR.

3.2.4 Detection of expression of mature siCTLA4 and scrCTLA4 in transiently transfected Jurkats

Two different stem-loop RT primers designed according to Chen *et al*. bind sequence-specific to the 3' portion of the mature *siCTLA4* or *scrCTLA4* and are reverse transcribed. This results in 70 bp large RT products that then could be amplified with a forward

primer sequence-specific for the *siCTLA4* or *scrCTLA4* and a universal reverse primer. The expression was quantified using a conventional SYBR Green I assay. Fig. 3.7 A shows that we were able to detect the expression of the mature *siCTLA4* in the Jurkats transiently transfected with pBSU6neo siCTLA4 after 21 cycles using Fr siCTLA4 sl primer and Universal Rev primer in the real-time PCR reaction. As a control for the specificity of the stem-loop RT assay was used an RNA sample from Jurkats transfected with the empty vector pBSU6neo, that was reverse transcribed with the same set of primers. Surprisingly, for this sample a Ct value of 28.89 was observed. Another control "no RT primer" was included where no stem-loop primer was added in the reverse transcriptase reaction. A Ct value of 37.24 was measured in this sample. We observed a similar pattern in the assay for *scrCTLA4* detection. The highest Ct value of 24 was determined in the Jurkats transfected with pBSU6neo scrCTLA4 as shown in Fig. 3.8 A. However, fluorescence was detected also in the Jurkats transfected with the empty vector after 30 cycles and again in the "no RT primer" sample after 37 cycles. Melting curve analysis was performed to distinguish between the correct amplicons and non-specific products. In both assays was observed a single peak with Tm of 84°C in the samples of Jurkats transfected with pBSU6neo siCTLA4 or pBSU6neo scrCTLA4. In contrast, the melting curve for the sample of Jurkat transfected with the empty vector showed a peak with Tm of 86°C in the *siCTLA4* assay and multiple peaks (Tm 87°C and 90°C) in the *scrCTLA4* assay. A peak with Tm of 88°C was observed for the "no RT primer" samples in the *siCTLA4* assay and multiple peaks (Tm 86.5°C and 92°C) in the *scrCTLA4* assay. The amplification products were further visualised on an agarose gel (Fig 3.7 B, 3.8 B)

confirming the presence of the 61 bp desired PCR product and the non-specific products found in the control samples.

The results from the real-time quantification of siRNA by stem-loop RT-PCR show that it was able to detect the expression of mature *siCTLA4* and *scrCTLA4* in the transiently transfected Jurkats.

A) **B)**

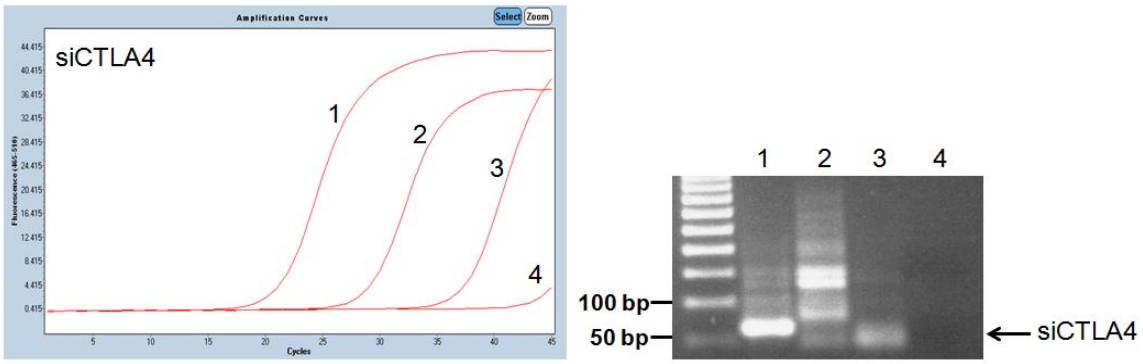

C)

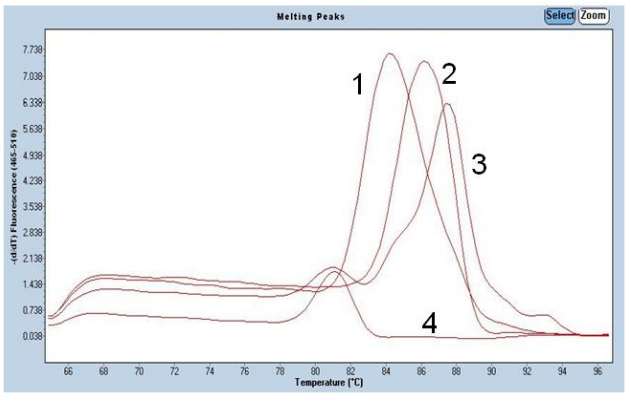

Figure 3.7. siRNA SYBR Green I assay for detection of *siCTLA4* expression.

Real-time PCR amplification profile of *siCTLA4*. 1. Jurkats transiently transfected with pBSU6neo siCTLA4; 2. Jurkats transiently transfected with pBSU6neo; 3. minus-RT control; 4. NTC-no template control. (A) *siCTLA4* SYBR Green I assay. (B) Gel blot analysis of the amplification products. (C) Melting curve analysis of the amplification products.

A) **B)**

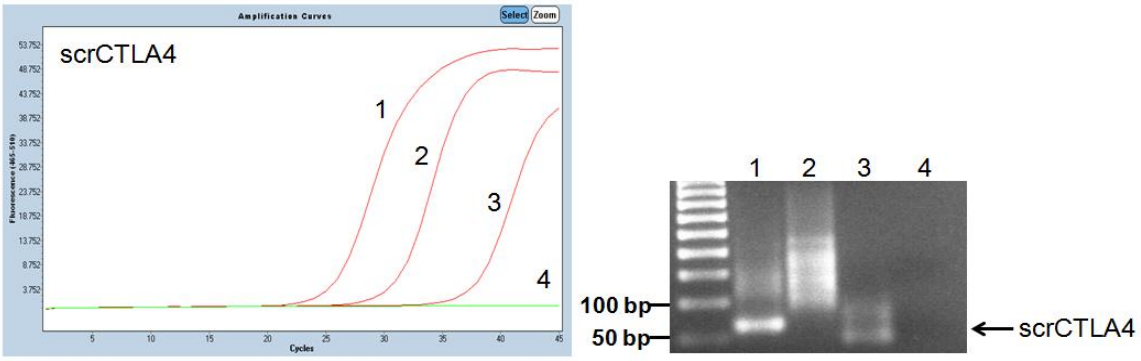

C)

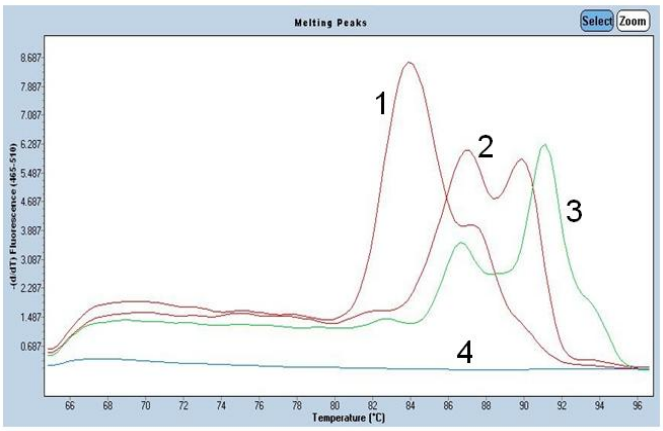

Figure 3.8. siRNA SYBR Green I assay for detection of *scrCTLA4* expression.

Real-time PCR amplification profile of *scrCTLA4* in: 1. Jurkats transiently transfected with pBSU6neo scrCTLA4; 2. Jurkats transiently transfected with pBSU6neo; 3. minus-RT control; 4. NTC-no template control. (A) *scrCTLA4* SYBR Green I assay. (B) Gel blot analysis of the amplification products. (C) Melting curve analysis of the amplification products.

3.2.5 Establishing of Jurkat stable cell lines transfected with pBSU6neo siCTLA4, pBSU6neo scrCTLA4 and pBSU6neo

To establish a Jurkat stable cell line with silenced CTLA4 expression, Jurkat cells were transfected with pBSU6neo siCTLA4 (si). As controls were used Jurkats that express the scrambled version of the siRNA specific for CTLA4 (scr) and Jurkats that express the empty vector pBSU6neo (ev). As described in materials and methods clonal lines were obtained by limited dilution and selected by growth in medium supplemented with G418. Only cells that incorporated the plasmid DNA that encodes the neomycin resistance gene could be further propagated. This was verified by PCR analysis of the selected clones using primers Neo Fr and Neo Rev (Table 2.3) designed to bind in the region of the CMV enhancer and the neomycin resistance gene in the generated constructs. As shown in Fig. 3.9 A most of the tested clones -si, -scr and -ev are positive for the expected 550 bp band. We also investigated the cell lines for the knockdown of CTLA4 expression. The expression was induced upon stimulation of the cells with PMA and ionomycin for 3 days and the extracted total RNA was analysed. The results from the RT-PCR presented on Fig. 3.9 B show that CTLA4 was downregulated in two of the –si samples. Compared to that CTLA4 expression was induced in all –ev clones transfected with the empty vector pBSU6neo. Upregulation was determined also in all but one –scr clone. Detection of GAPDH in the samples served as a loading control (Fig. 3.9 C).

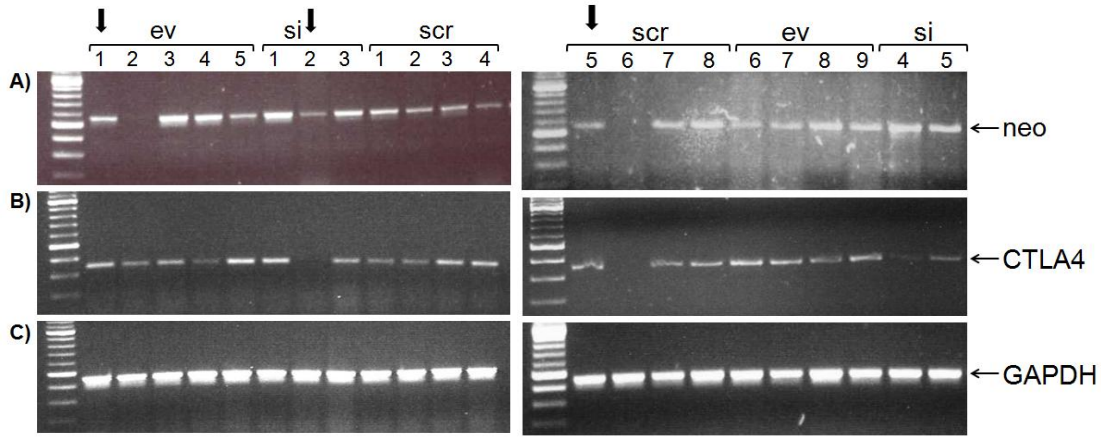

Figure 3.9. Selection of Jurkat stable cell lines that have incorporated pBSU6neo (ev), pBSU6neo scrCTLA4 (scr) and pBSU6neo siCTLA4 (si).

The cells were stimulated with PMA and ionomycin for 3 days. (A) The presence of the plasmid was detected by PCR in the DNA sampels. (B) CTLA-4 expression levels were detected by RT-PCR and (C) GAPDH was used as a loading control. Arrows indicate the selected clones Jurkat-ev1, Jurkat-scr5 and Jurkat-si2. Ev: clones transfected with pBSU6neo; Scr: clones transfected with pBSU6neo scrCTLA4; Si: clones transfected with pBSU6neo siCTLA4.

The production of the IL-2 cytokine is considered an excellent way to measure T cell activation. Since we wanted to use our model to study the role of CTLA4 in intracellular signaling in T cells and use IL-2 production as a potential marker for activation it was important to show that the selected clones were still able to secrete IL-2 upon induction. Figure 3.10 presents the IL-2 levels produced from the tested clones and compared to the levels measured in wild type Jurkats stimulated under the same conditions. The results show that all clones but –ev 3 secreted significant levels of the cytokine upon treatment with PMA and ionomycin for 3 days. PMA is a small molecule used to activate protein kinase C (PKC). Ionomycin is used to raise the intracellular level of Ca^{2+} and together with PMA is able to induce strong cytokine production in T cells. It was not expected to

see that the downregulation of CTLA4 in the stable cell clone would interfere with the IL-2 production induced by PMA/ionomycin stimulation since in this type of activation there is no crosslinking of the CTLA4 receptor. To be able to use the wild type Jurkat cells as an additional control in further experiments, the selected clones were the ones that produced IL-2 amount similar to the wild type Jurkat upon PMA/ionomycin stimulation.

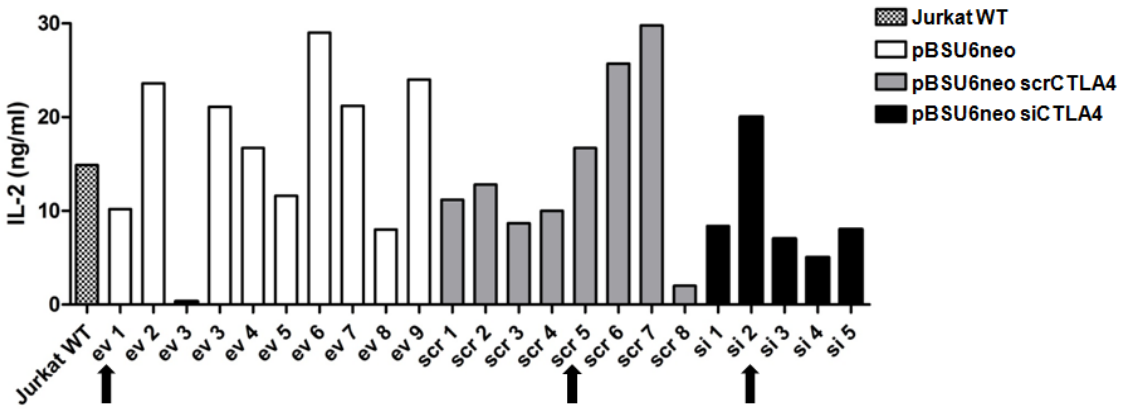

Figure 3.10. IL-2 levels produced upon stimulation in stable transfected cell lines.

The cells of selected clones and Jurkat WT were stimulated with PMA and ionomycin for 3 days. Supernatants were collected and the levels of secreted IL-2 were determined using IL-2 ELISA. Arrows indicate the selected clones Jurkat-ev1, Jurkat-scr5 and Jurkat-si2, which produce IL-2 amount similar to Jurkat WT.

Therefore, the clones used in further analyses were selected according to the following criteria: positive detection of the plasmid in the genomic DNA; levels of IL-2 production similar to the ones induced in Jurkat WT upon treatment with PMA/ionomycin; inhibition of CTLA4 expression for the –si clone and no inhibition of it for the –scr and –ev clones upon stimulation.

The clones –si 2 (further referred as Jurkat-si), -scr 5 (further referred as Jurkat-scr) and –ev 1 (further referred as Jurkat-ev) were further used in this study.

The downregulation of CTLA4 in the Jurkat-si cells upon stimulation was also confirmed by real-time PCR (Fig. 3.11). It was determined that the levels of expression were significantly increased upon activation in the controls Jurkat WT, Jurkat-ev and Jurkat-scr compared to the unstimulated Jurkat WT control. In contrast, no increase was observed in the Jurkat-si sample despite the treatment. To exclude the possibility that the CTLA4 gene might be knocked out a PCR was performed with primers designed to bind to an intron and an exon within the sequence of the CTLA4 gene. PCR amplification products at the expected size (595 bp) were detected in all three cell clones and the WT Jurkat control, thus confirming further the successful knockdown in the Jurkat-si cell line (Fig. 3.12).

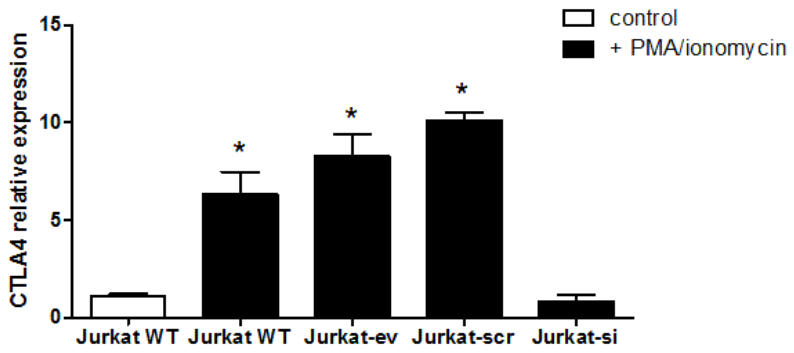

Figure 3.11. Downregulation of CTLA4 upon stimulation in stable transfected cell lines.

Jurkat WT cells and selected clones Jurkat-ev, Jurkat-scr and Jurkat-si were stimulated with PMA and ionomycin for 3 days. CTLA4 expression levels were determined by real-time PCR. The relative quantification of the target gene expression was determined using the $2^{-\Delta\Delta Ct}$ method and GAPDH was used for normalization. Statistical analysis was performed relative to controls of untreated WT Jurkat cells using one-way ANOVA followed by Tukey post- test. Columns represent the means of triplicates ± SEM. * $P< 0.05$, compared with untreated WT Jurkat cells.

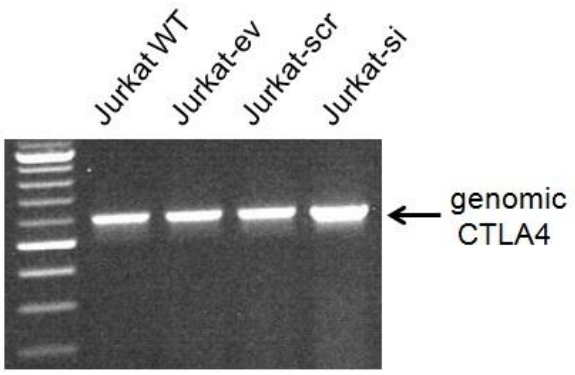

Figure 3.12. Detection of the CTLA4 gene by PCR analysis.

DNA samples were extracted from Jurkat WT, Jurkat-ev, Jurkat-scr and Jurkat-si and the CTLA4 gene was PCR amplified using primers gCTLA4 Fr and gCTLA4 Rev. Expected size of the product was 595bp.

The expression of CTLA4 upon induction was investigated by Western blot using an antibody from Santa Cruz. This time the detection was successful. Figure 3.13 shows expression of CTLA4 in the wild type Jurkats incubated with PMA and ionomycin for 3 days. Similar levels are observed also in the stable cell lines Jurkat-scr and Jurkat-ev. In contrast, barely any expression was detectable in Jurkat-si cells treated in the same way. As a positive control were used HeLa cells transfected with pCTLA4-Flag. The Western blot confirmed previous data from the real-time PCR showing that the expression induced by the CMV promoter in the transiently transfected HeLa is much stronger than endogenously induced expression in Jurkats.

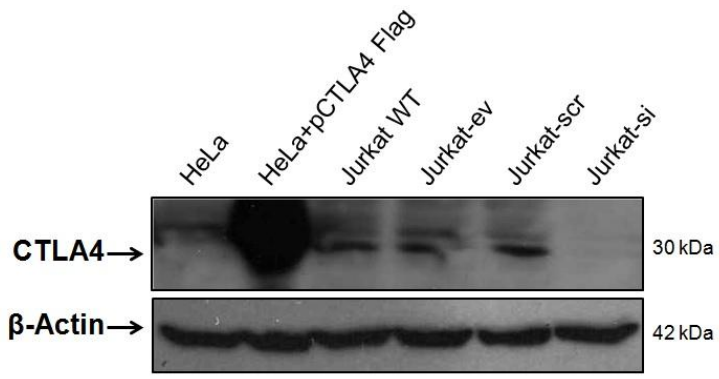

Figure 3.13. Detection of the CTLA4 expression by Western blot.

Jurkat WT, Jurkat-ev, Jurkat-scr and Jurkat-si cells were stimulated with PMA and ionomycin for 3 days. As a positive control HeLa cells were transfected with pCTLA4-Flag. As a negative control were used untransfected HeLa. 30 µg protein lysate were loaded in each lane and the membrane was probed for CTLA4. The membrane was stripped and re-probed for β-Actin, used as a loading control.

3.2.6 Detection of expression of mature siCTLA4 and scrCTLA4 in stable transfected Jurkats

Upon development of the Jurkat cell clones that have stably integrated pBSU6neo siCTLA4, pBSU6neo scrCTLA4 or pBSU6neo, it was important to determine that the selected clones expressed the siRNA of interest. The detection of the mature *siCTLA4* was performed using the stem loop RT-PCR with the stem loop siCTLA4 primer. This was followed by a real-time PCR quantification with Fr siCTLA4 sl primer and Universal Rev primer using the SYBR Green I assay. Figure 3.14 A shows the expression profile of *siCTLA4* in the selected clone Jurkat-si which was transfected with pBSU6neo siCTLA4. A Ct value of 20.91 was measured. As a control for the specificity of the stem-loop RT assay was used an RNA sample from Jurkat-ev transfected with the empty vector

pBSU6neo that was also reverse transcribed with the stem-loop siCTLA4 RT primer. A Ct value of 29.71 was observed for this sample. The melting curve analysis (Fig. 3.14 C) which showed a peak with Tm of 84°C together with the gel blot analysis (Fig. 3.14 B) indicated that only the amplification product from the Jurkat-si sample has the expected size of 61bp. Despite the fluorescence signal observed in the real-time PCR from the Jurkat-ev sample, the melting curve analysis showed that the amplification product has a peak with different Tm (87.5°C) and the gel blot analysis showed that no distinct amplification product was visible at the right size. These results confirmed the specificity of the assay and proved that only the Jurkat-si clone expresses constitutively the *siCTLA4.*

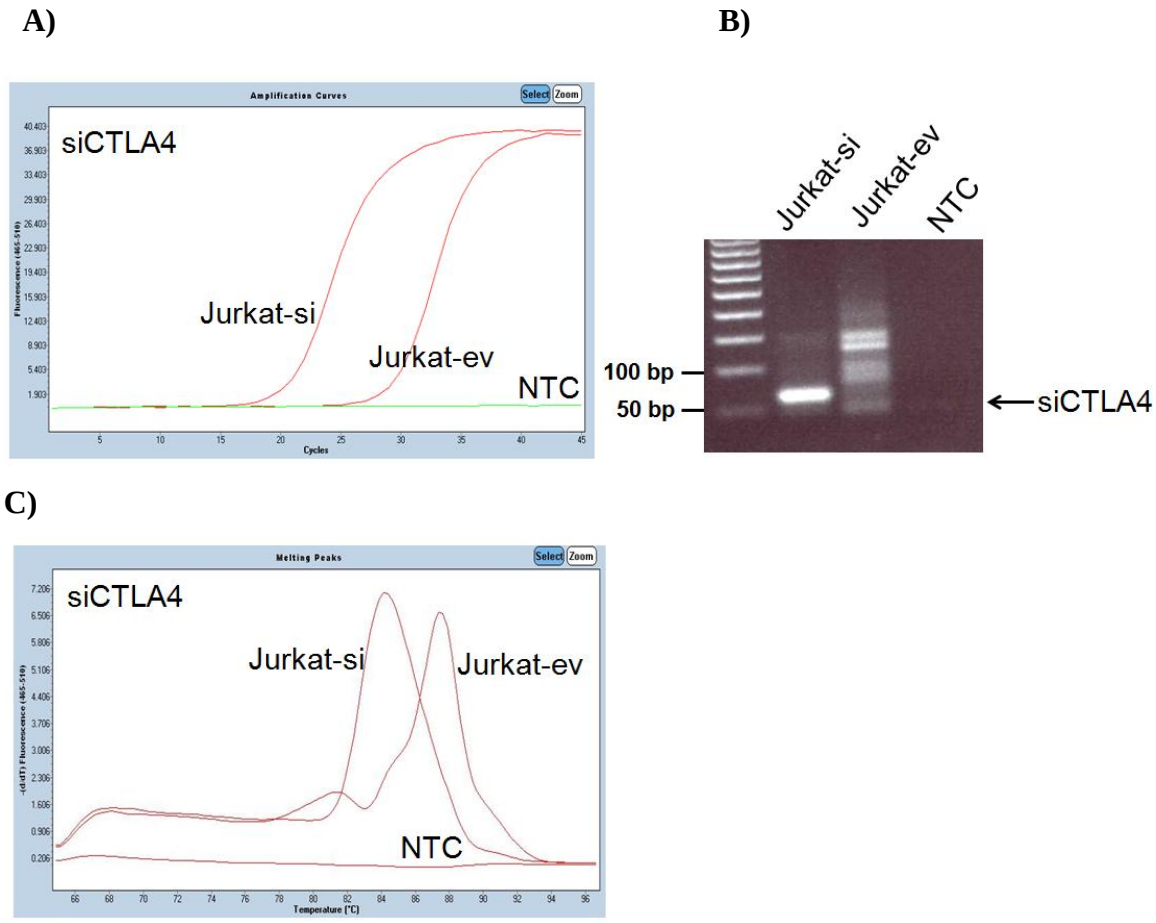

Figure 3.14. siRNA SYBR Green I assay for detection of *siCTLA4* expression.

(A) *siCTLA4* SYBR Green I assay. Real-time PCR amplification profile of *siCTLA4* in: Jurkats-si stable transfected with pBSU6neo siCTLA-4; Jurkats-ev stable transfected with pBSU6neo; NTC-no template control. (B) Gel blot analysis of the amplification products. (C) Melting curve analysis of the amplification products.

The expression of *scrCTLA4* was determined in the Jurkat-scr cell clone stable transfected with pBSU6neo scrCTLA4. The stem loop RT-PCR was performed with the stem loop scrCTLA4 primer. This was followed by a real-time quantification with FR scrCTLA4 sl primer and Universal Rev primer using the SYBR Green I assay. Figure 3.15 A shows the expression profiles of *scrCTLA4* in the selected clones Jurkat-scr and Jurkat-ev. A Ct value of 24.58 was measured in the Jurkat-scr samples compared to a Ct

value of 31.35 in the Jurkat-ev sample. Melting curve analysis showed a peak with Tm of 84°C (Fig.3.29 C) for the Jurkat-scr and the expected 61bp band in the gel blot (Fig.3.15 B) confirming the presence of the correct amplification product. In comparison to that, the melting curve analysis for the Jurkat-ev sample showed a peak with Tm of 87°C (Fig.3.15 C) and no distinct band represented the correct amplification product in the gel blot analysis (Fig.3.15 B).

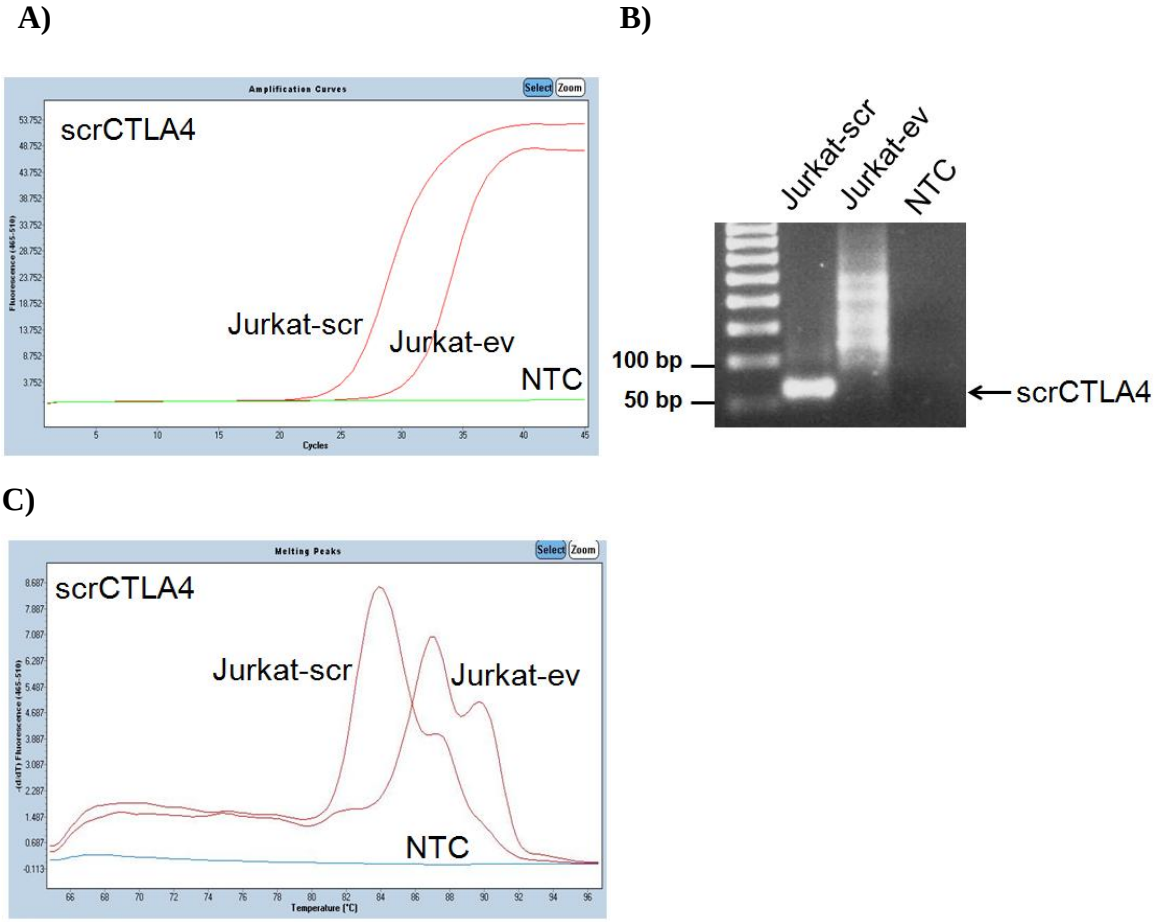

Figure 3.15. siRNA SYBR Green I assay for detection of *scrCTLA4* expression.

(A) *scrCTLA4* SYBR Green I assay. Real-time PCR amplification profile of *scrCTLA4* in: Jurkats-scr stable transfected with pBSU6neo scrCTLA4; Jurkats-ev stable transfected with pBSU6neo; NTC-no template control. (B) Gel blot analysis of the amplification products. (C) Melting curve analysis of the amplification products.

To confirm further that precisely *siCTLA4* and *scrCTLA4* are detected in this assay the PCR products were sequenced. The PCR products amplified from the Jurkat-si and Jurkat-scr samples were inserted into pCR2.1-TOPO vector (3931 bp) (Invitrogen) and the recombinant vector was transformed into competent XL-10 *E.coli*. Several colonies were selected and the plasmid DNA was isolated from the bacterial cultures. To identify the plasmids that contained the PCR product of interest, the DNA was subjected to a restriction digest with EcoRI and analysed on 1.5% agarose gel. Plasmids that have incorporated the PCR product successfully between the two EcoRI sites would show a 71 bp band upon restriction digest with this enzyme. Plasmid DNA tested in lane 2, positive for the PCR product for *siCTLA4* and in lane 3 and 4, positive for the PCR product for *scr CTLA4* (Fig.3.16 A) were sequenced (MWG Operon, UK). The sequence obtained from the sample originating from the Jurkat-si cells (lane 2) was aligned to the sequence originally designed for the small hairpin structure encoding the siCTLA4 (BioEdit software). It was confirmed that the sequence corresponding to the mature *siCTLA4* was present in the PCR product which was successfully cloned into pCR2.1-TOPO vector. The sequence obtained from the sample originating from the Jurkat-scr cells (lane 4) was aligned to the sequence originally designed for the small hairpin encoding the scrCTLA4. It was confirmed that the sequence corresponding to the mature *scrCTLA4* was present in the PCR product which was successfully cloned into pCR2.1-TOPO vector. (Fig. 3.16 B). In this way it was proven that the selected clones Jurkat-si and Jurkat-scr express the mature *siCTLA4* and *scrCTLA4*.

A)

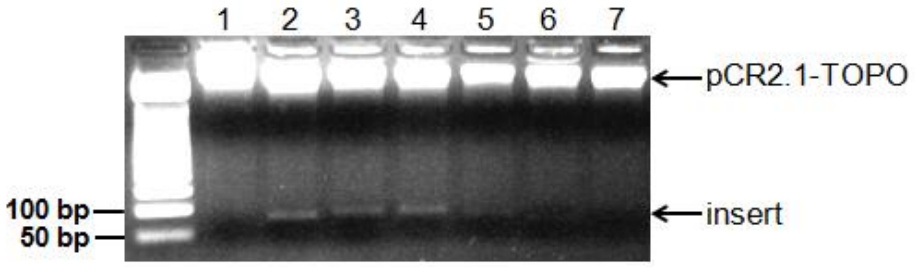

B)

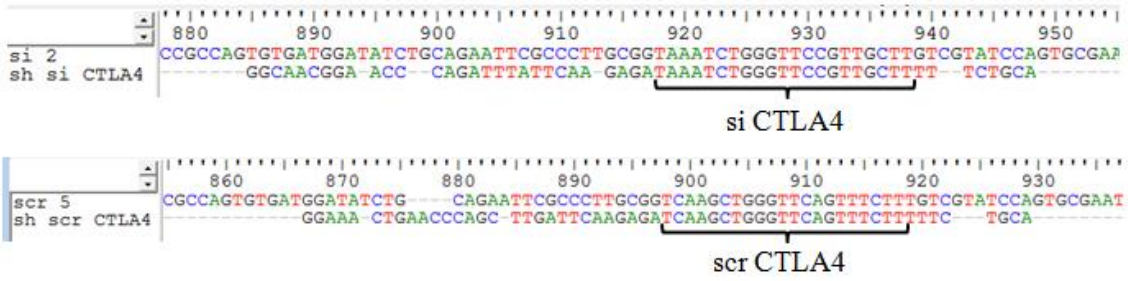

Figure 3.16. Analysis of recombinant pCR2.1-TOPO + *siCTLA4* or *scrCTLA4*.

(A) The PCR product of *siCTLA4* was inserted into pCR2.1-TOPO vector (lane 1 and 2). The PCR product of *scrCTLA4* was inserted into pCR2.1-TOPO vector (lane 3 - 7). Recombinant plasmids were analysed upon restriction digest with EcoRI. (B) Sequencing results obtained from the cloning from lane 2 and lane 4 were aligned to the sequences of the small hairpins encoding siCTLA4 and scrCTLA4. BioEdit software was used for analysis.

3.2.7 Analysis of the IL-2 production in the generated stable cell lines Jurkat-si, Jurkat-scr, Jurkat-ev and Jurkat WT

To evaluate the functionality of the novel cell lines the IL-2 production upon stimulation was examined. The cells were stimulated with plate bound anti-CD3, anti-CD28 and anti-CTLA4 antibodies and the IL-2 production was quantified for different periods of time. It was expected that the anti-CTLA4 antibody would crosslink the CTLA4 receptor on the surface and induce a signal opposing the CD3/CD28 mediated activation that resulted in IL-2 production. First, the anti-CTLA4 antibody was tested in two different concentrations in combination with anti-CD3 and anti-CTLA4 to find an optimal concentration for it. In this initial experiment the IL-2 production was determined in the cell supernatants of the different cell lines after 3 days of stimulation. In all cell lines the stimulation with anti-CD3 alone resulted in IL-2 production comparable to the unstimulated control. As expected, the addition of a costimulatory signal mediated by the anti-CD28 antibody resulted in a significant production of IL-2 in all cell lines. The results showed also that the levels of IL-2 were decreased in the Jurkat-WT (J WT), Jurkat-ev (J ev) and Jurkat-scr (J scr) when anti-CTLA4 was added to the stimulating anti-CD3 and anti-CD28 antibodies. As expected, in the Jurkat-si (J si) cell line such effect was not observed. Interestingly, for the J WT and J scr cell lines a bigger decrease was observed when less amounts of anti-CTLA4 were used. However, less IL-2 was produced in the J scr cell line when the amounts of anti-CTLA4 increased (Fig.3.17). In order to subject the different cell lines to the same experimental conditions, it was decided to use 0.01µg/µl anti-CTLA4 antibody solution corresponding to 0.65µg/well (96-well plate) for further assays.

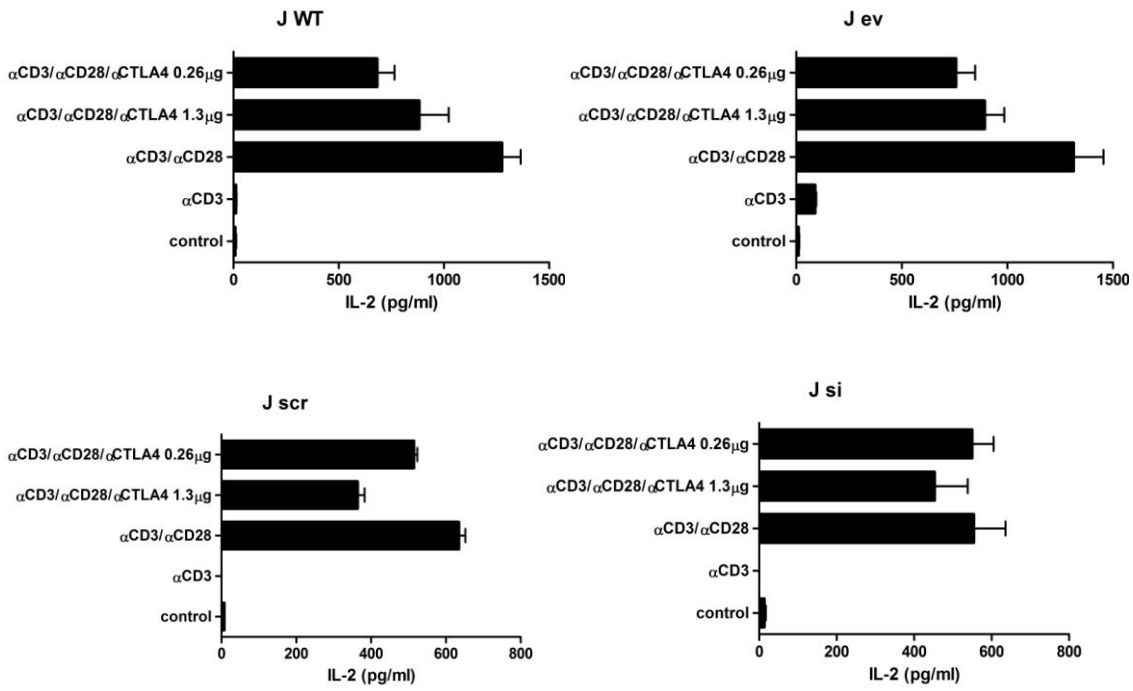

Figure 3.17. IL-2 production upon stimulation in Jurkat WT and Jurkat-ev, Jurkat-scr and Jurkat-si stable cell lines.

Jurkat WT, Jurkat-ev, Jurkat-scr and Jurkat-si cells were stimulated in triplicates with plate bound anti-CD3-, anti-CD28- and anti-CTLA4 antibodies for 3 days. Supernatants were collected and the amount of IL-2 in them was determined using ELISA. Columns represent the means of duplicates ± SEM.

Next, the kinetics of IL-2 production upon anti-CD3/CD28 stimulation in the presence or absence of anti-CTLA4 antibody over a period of 4 days was studied. It was observed that upon anti-CD3/CD28 stimulation all cell lines produced IL-2 which would peak at day 3 and levels remained high throughout day 4. In the presence of the anti-CTLA4 antibody such increase in the IL-2 production was not observed after day 2 of stimulation in the J WT, J ev and J scr cell cultures. The levels measured for day 3 and 4 in these cultures remained comparable to the levels detected on day 2 upon stimulation. The IL-2

production in the J-si cell line also peaked at day 3. The addition of anti-CTLA4 antibody during the activation did not show any opposing effect to the CD3/CD28 stimulation in the J si cell line, as IL-2 levels continued to rise throughout day 3 and 4 and the produced amounts were very similar to the ones measured in cultures stimulated in the absence of anti-CTLA4 (Fig. 3.18). The data supports the hypothesis for the inhibitory role of CTLA4, since the CTLA4 expression detected in stimulated cultures peaks at day 2- 3, which correlates with the time point of the observed decrease in IL-2 production in the J WT, J scr and J ev cells. These results indicate also that the generated Jurkat-si cell line expressing constitutively shRNA that targets CTLA4 could be used in functional assays to study the role of CTLA4 in T cell signaling.

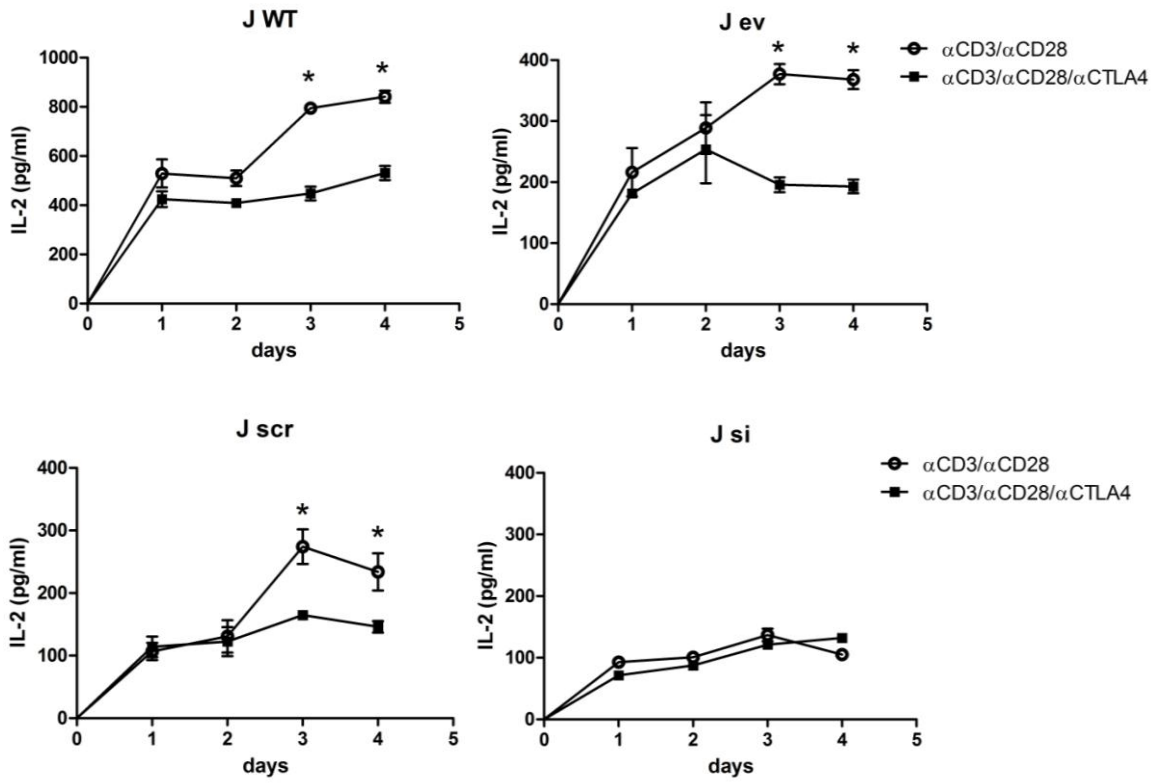

Figure 3.18. IL-2 production upon stimulation in Jurkat WT and Jurkat-ev, Jurkat-scr and Jurkat-si stable cell lines.

Jurkat WT, Jurkat-ev, Jurkat-scr and Jurkat-si cells were stimulated in triplicates with plate bound anti-CD3-, anti-CD28- and anti-CTLA4 antibodies for 4 days. Supernatants were collected at different time points and the amount of IL-2 in them was determined using ELISA. Statistical analysis was performed using two-way ANOVA followed by Bonferroni post-test. *P<0.05, compared to αCD3/αCD28/αCTLA4 values for each time point.

To further test the efficacy of the silencing in the generated Jurkat-si cell line in functional assays, the cells were transfected with pCTLA4-Flag to overexpress CTLA4 and stimulated with anti-CD3/CD28 or anti-CD3/CD28/CTLA4. The IL-2 production was analysed 24h and 48h later (Fig. 3.19). Since transient expression is usually analysed 1-2 days upon transfection, it was expected that a CTLA4-mediated alteration in the IL-2 production in the control cell line could be observed already after 24h upon stimulation

due to the crosslinking of the overexpressed CTLA4. No significant difference was determined in the IL-2 production between the Jurkat-si cells stimulated with anti-CD3/CD28 or anti-CD3/CD28/CTLA4 for 1 and 2 days. On the other hand, in the Jurkat WT cells decreased IL-2 levels were observed on the second day after stimulation when the anti-CTLA4 antibody was involved. It was expected that a significant difference in the IL-2 levels would be observed already after the first day of stimulation. However, this was not the case, probably due to effects caused by the transfection. Both Jurkat-si and Jurkat WT cells seemed to react more sensitive to stimulation and produce more IL-2 after the transfection compared to cells that were stimulated in the same way, but were not subjected to transfection before that. Overall, the results indicated that the expressed siRNA in the generated Jurkat-si cell line is efficient enough to silence overexpressed CTLA4 and modulate the inhibitory effect of CTLA4 on IL-2 production.

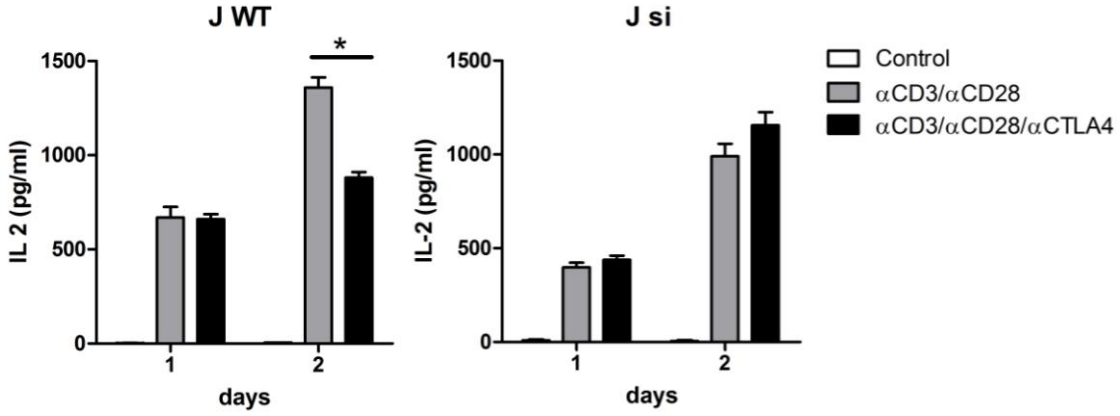

Figure 3.19. IL-2 production upon stimulation in Jurkat WT and Jurkat-si stable cell lines upon overexpression of CTLA4.

Jurkat WT and Jurkat-si cells were transfected with 2 μg of pCTLA4-Flag. After 24h the cells were stimulated in duplicates with plate bound antibodies for 1 and 2 days. Supernatants were collected at different time points and the amount of IL-2 in them was determined using ELISA. Statistical analysis was performed using two-way ANOVA followed by Bonferroni post- test. Columns represent the means ± SEM. * P< 0.05, compared with αCD3/αCD28 stimulated cells.

4. Chapter 3 - Analysis of the role of CTLA4 in T cell signaling using the generated Jurkat-si cell line

4.1 Methods

4.1.1 Dual-luciferase assay

Dual-luciferase assay (Promega) was used to investigate transgene Firefly luciferase and *Renilla* luciferase expression. Jurkat cells were stimulated for 48h, washed twice, resuspended in fresh media and rested for 6h. $1x10^6$ cells were transfected using electroporation with 1.8 µg pGL3-NF-κB (Firefly luciferase expressing reporter plasmid under the control of a NF-κB response element) and 0.5 µg phRL-TK (*Renilla* luciferase expressing normalizing plasmid (Promega)) (gifts from M. Castro, UCLA). The increase in Firefly luciferase expression would show the activation of NF-κB in the cells and the *Renilla* luciferase expression would be used to normalize transfection efficiency. The cells were rested overnight and stimulated with plate-bound antibodies (anti-CD3, anti-CD28, anti-CTLA4) in 96-well plates. After six hours the supernatant was removed. The assay was performed according to the manufacturers' instructions (Promega). The cells were resuspended in 25 µl 1xPBL (Passive lysis buffer) and incubated at room temperature with shaking for 15 min. 20 µl of cell lysate were transferred into a luminometer 96-well plate and 100 µl of LAR II reagent were added to each sample. The firefly luciferase activity was measured in a luminometer. Next 100 µl of Stop&Glo Reagent were added to each sample and the *Renilla* luciferase activity was measured in the luminometer. A sample with untransfected cells was used to estimate the background

of the dual-luciferase assay. The value of the background was subtracted from all measured values.

4.2 Results

The exact mechanism of CTLA4 function is still not well understood. In this study we tried to analyse what role CTLA4 plays in T cell activation using the generated cell models. The phosphorylation of several proteins involved in proximal and distal signaling events was investigated. We also wanted to estimate if the vector-mediated downregulation of CTLA4 in the Jurkat-si cell line would abrogate any effect that CTLA4 might have on signaling pathways.

4.2.1 Analysis of proximal T cell signaling events.

To investigate if CTLA4 interferes with proximal TCR- mediated signaling events, the cells were stimulated with a combination of αCD3/αCD28 or αCD3/αCD28/αCTLA4 antibodies for different periods of time between 0 and 60 min. Crosslinking of CD3, CD28 and CTLA4 using antibodies triggers T cell signaling at the plasma membrane. Before that the cells were stimulated with PMA/ionomycin for 48h to induce CTLA4 expression and rested overnight. The samples were analysed by immunoblotting using phosphospecific antibodies.

LAT is an adaptor protein that is being phosphorylated by ZAP-70 at several tyrosine sites which serve as docking sites for other proteins involved in T cell signaling. The phosphorylation of LAT at tyrosine 191 was very strong after 5 min stimulation with peak levels 15 and 30 min upon stimulation in the Jurkat WT, Jurkat-ev and Jurkat-scr cells (Fig.4.1). No difference was observed upon CTLA4 crosslinking. Overall a weaker signal was detected in the Jurkat-si samples. This data suggest that the binding capacity of LAT to other signaling proteins in the Jurkat-si cell line could be weaker compared to the control cell lines.

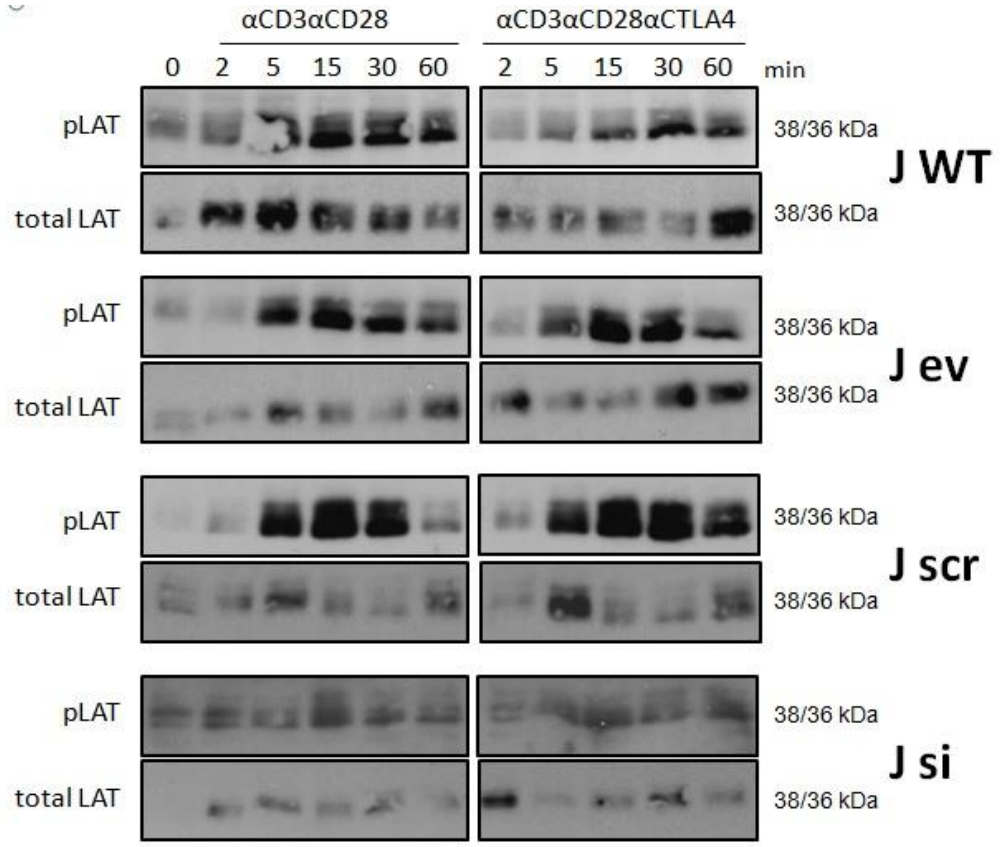

Figure 4.1 Analyses of LAT expression.

Restimulated Jurkat WT, Jurkat-ev, Jurkat-scr and Jurkat-si cells were incubated for different times (0-60 min) with αCD3/αCD28 and αCD3/αCD28/αCTLA4. 30 µg of whole cell lysates were immunobloted for phospho-LAT. The membranes were stripped and re-probed for LAT.

SLP-76 is another adaptor protein which expression was examined (Fig. 4.2). The expression of this protein in each of the cell lines was not affected by the experimental conditions: duration of the stimulation and CTLA4 crosslinking. However, an overall weaker expression was observed in the Jurkat-si samples compared to all the other control cell lines. The blots were probed for β-Actin to ensure equal loading.

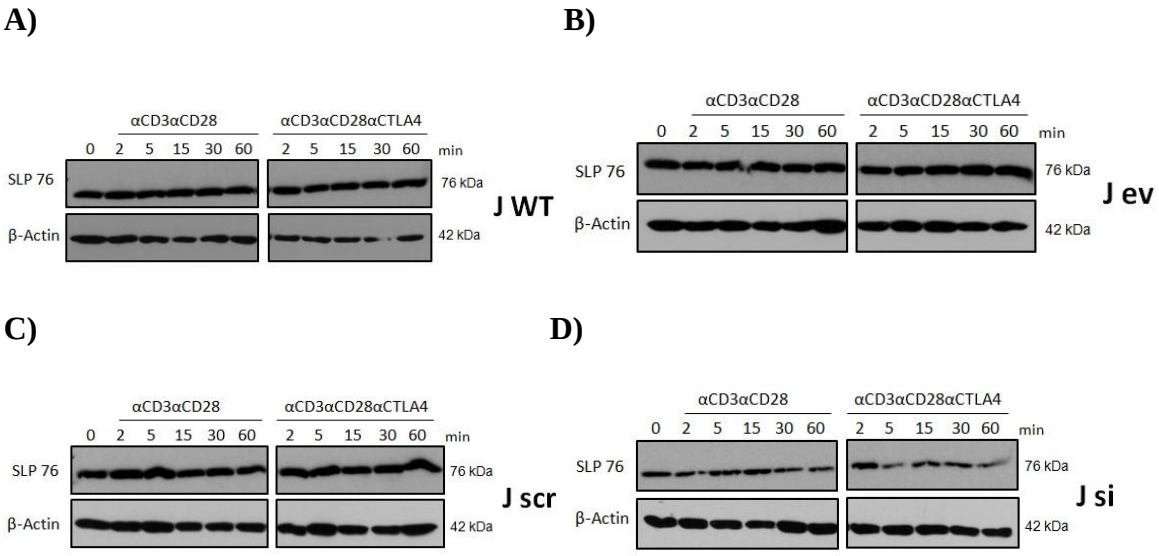

Figure 4.2 Analyses of SLP-76 expression.

Restimulated Jurkat WT, Jurkat-ev, Jurkat-scr and Jurkat-si cells were incubated for different times (0-60 min) with αCD3/αCD28 and αCD3/αCD28/αCTLA4. 30 µg of whole cell lysates were immunobloted for SLP-76. The membranes were re-probed for β-Actin.

Zap-70 is protein kinase involved in the very early stages of signaling transduction upon TCR engagement and is the kinase responsible for LAT and SLP-76 phosphorylation [105] [106]. It is rapidly phosphorylated on several tyrosine residues by the Src family

kinases Fyn and Lck [107]. A very weak signal was detected using the phospho- Zap-70 (Tyr319) antibody in all cell lines through the time course of stimulation (Fig. 4.3). An increase could be detected at time points 15 an 30 min in most samples, especially, in the Jurakt-scr cell line. Crosslinking of CTLA4 did not seem to have any impact on the phosphorylation of the protein. The amount of total Zap-70 in the samples was also analysed. The expression of Zap-70 was detected in all samples confirming equal loading of the samples.

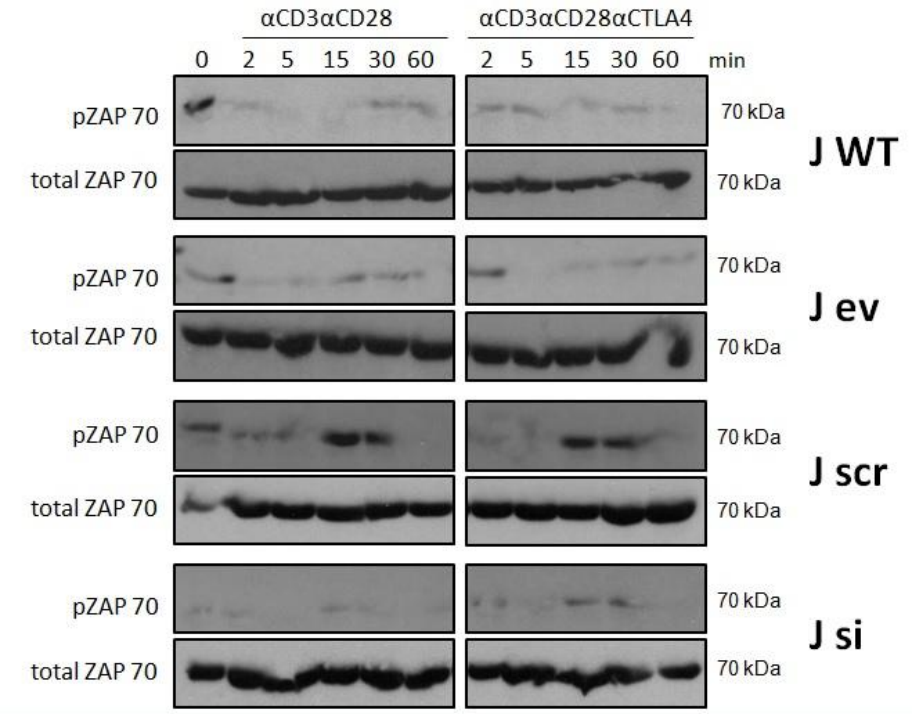

Figure 4.3 Analyses of Zap-70 expression.

Restimulated Jurkat WT, Jurkat-ev, Jurkat-scr and Jurkat-si cells were incubated for different times (0-60 min) with αCD3/αCD28 and αCD3/αCD28/αCTLA4. 30 µg of whole cell lysates were immunobloted for phospho-Zap-70. The membranes were stripped and re-probed for Zap-70.

It was surprising not to detect strong phosphorylation of Zap-70, therefore, it was of interest to examine the phosphorylation of Lck. In this study a very strong signal was observed in all cell lines including in the unstimulated controls (Fig. 4.4). The used antibody detects endogenous levels of Lck only when it is phosphorylated at Tyr505. It has been shown that the expression was detected even in unstimulated Jurkats unless the cells were serum starved and CIP (calf intestinal alkaline phosphatase) treated. Lck is a kinase that can be phosphorylated at two tyrosine residues: Y394, which is considered to mediate positive activation and Y505, which is considered to be inhibitory [108]. However, it has been reported that TCR-induced activation leads to simultaneous phosphorylation of both sites in Jurkat and primary T cells [109]. Therefore, it was difficult to use the analysis of Tyr505 phosphorylation of Lck alone to explain further downstream signaling events.

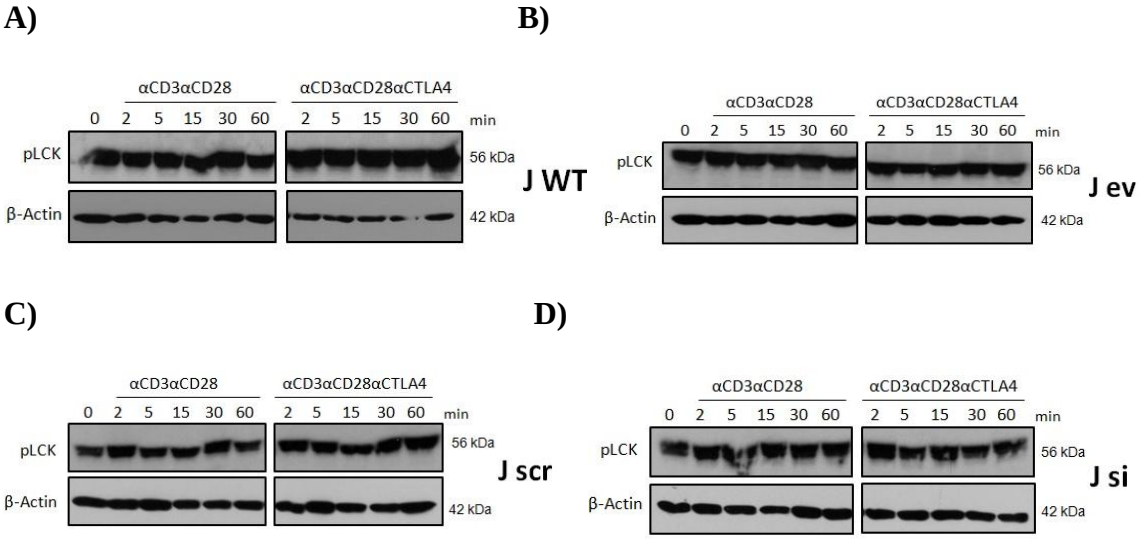

Figure 4.4 Analyses of pLCK expression.

Restimulated Jurkat WT, Jurkat-ev, Jurkat-scr and Jurkat-si cells were incubated for different times (0-60 min) with αCD3/αCD28 and αCD3/αCD28/αCTLA4. 30 µg of whole cell lysates were immunobloted for pLCK. The membranes were re-probed for β-Actin.

4.2.2 Analyses of distal T cell signaling events

The family of the mitogen-activated protein kinases (MAPK) regulates several transcription factors which are essential for T cell activation and survival. The extracellular signal-regulated kinase (ERK) and the c-Jun N-terminal kinase (JNK) play an important role for the activation of the transcription factor AP-1. Previous studies in murine T cells report that CTLA4 engagement inhibits ERK and JNK activation, however, others report that CTLA4 ligation upregulates JNK, but inhibits ERK activity [54, 55]. Therefore, the phosphorylation of the two kinases was examined using the model developed in this study. The increase in the phosphorylation of ERK1 and ERK2 was detected already 5 min upon stimulation, reaching its peak by 30-60 min and remained very strong throughout the whole time course of activation in all cell lines (Fig. 4.5). The observed results are consistent with other reports that have studied the αCD3/αCD28-induced activation of ERK1/2 in Jurkats [110]. A weaker phosphorylation of the kinase was detected also in the unstimulated controls. The high basal levels could be due to the preactivation and manipulation of the cells before the antibodies-mediated stimulation. In some studies it had been noted that extensive manipulation of Jurkat cells could result in high basal levels of Erk activation [111]. It has been also reported that Jurkat cells have hyperphosphorylated Itk and constitutively active PKB/AKT, which can influence downstream signalling and increase ERK1/2 activity in this cell line [112, 113]. Crosslinking of CTLA4 did not seem to interfere with the αCD3/αCD28-induced activation of this MAPK. The levels of phosphorylation in the Jurkat-si cell line were comparable with the ones in the control cell lines.

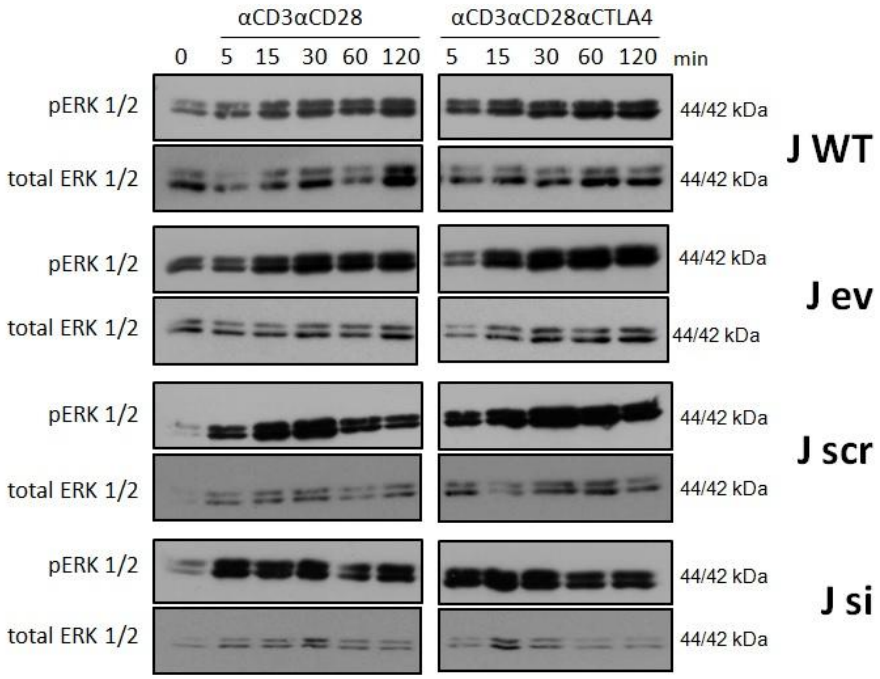

Figure 4.5 Analyses of ERK expression.

Restimulated Jurkat WT, Jurkat-ev, Jurkat-scr and Jurkat-si cells were incubated for different times (0-120 min) with αCD3/αCD28 and αCD3/αCD28/αCTLA4. 30 µg of whole cell lysates were immunobloted for phospho-ERK1/2. The membranes were stripped and re-probed for ERK1/2.

The members of the JNK family of MAPK are activated in response to cellular stress and inflammatory cytokines and activate the transcription factor c-Jun important for IL-2 induction [20]. In this study the αCD3/αCD28-stimulation induced a phosphorylation of JNK that peaked at 30-60 min in all cell lines and decreased at 120 min (Fig. 4.6). Interestingly, the crosslinking of CTLA4 seemed to enhance the JNK activity in the Jurkat WT samples at 30 and 60 min, in the Jurkat-scr sample at 60 min and a slightly increase it in the Jurkat-ev sample at 30 min. In contrast, no effect was observed in the Jurkat-si cells upon addition of the αCTLA4 antibody compared to the cells stimulated with αCD3/αCD28. As expected, due to the silencing of CTLA4 in these cells the

antibody could not crosslink the receptor on the cell surface and interfere with the αCD3/αCD28-stimulation. This confirmed the functionality of the generated Jurkat-si cell line. Immunoblotting of the cell lysates with anti-JNK showed that the same amount of protein was loaded in each lane. More than two bands can be seen at the blots incubated with the antibody against total JNK. It is possible that this antibody detects other isoforms of the protein, since alternative splicing of the three *Jnk* genes can result in ten different JNK protein kinases [114]. These results indicate that the engagement of CTLA4 potentiates JNK activation.

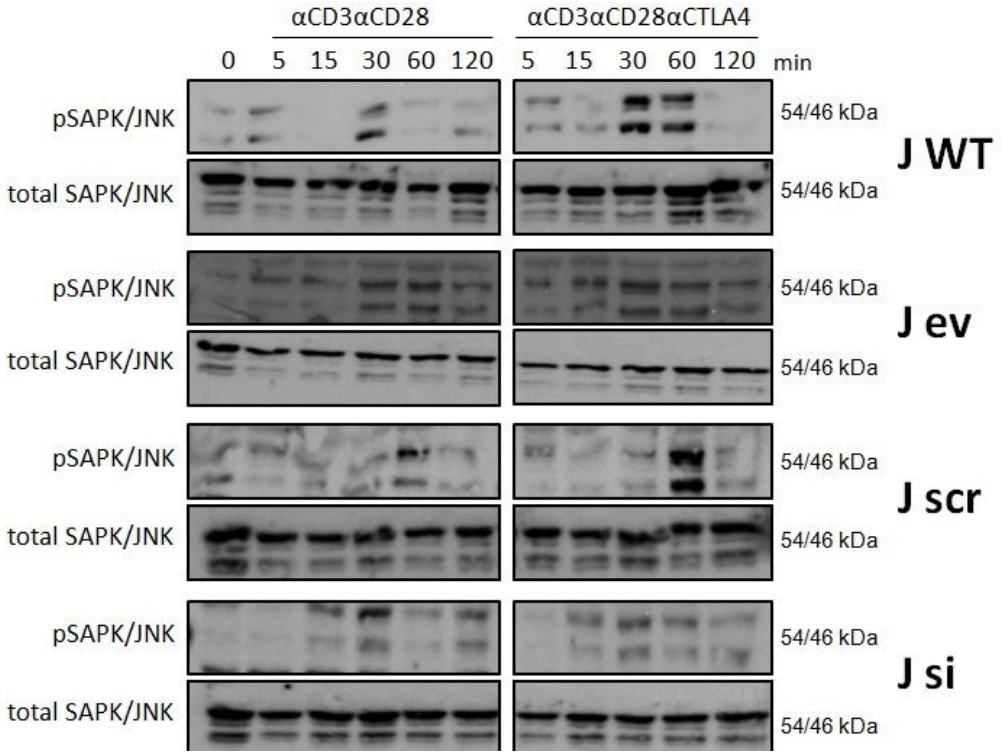

Figure 4.6 Analyses of SAPK/JNK expression.

Restimulated Jurkat WT, Jurkat-ev, Jurkat-scr and Jurkat-si cells were incubated for different times (0-120 min) with αCD3/αCD28 and αCD3/αCD28/αCTLA4. 30 µg of whole cell lysates were immunobloted for phospho-SAPK/JNK. The membranes were stripped and re-probed for SAPK/JNK.

Earlier in this study it was observed that crosslinking of CTLA4 seems to downregulate IL-2 expression after 2 days of activation with αCD3/αCD28. Therefore, it was of interest to examine the phosphorylation of SAPK/JNK under the same stimulation conditions and to check if there is a possible correlation between SAPK/JNK phosphorylation and the decreased IL-2 levels after 3 days of stimulation. However, no phosphorylation of SAPK/JNK was detected in any of the samples when the the Jurkat si and Jurkat scr cells were stimulated for longer periods of time (Fig. 4.7). The blots were probed also for β-Actin to ensure equal loading.

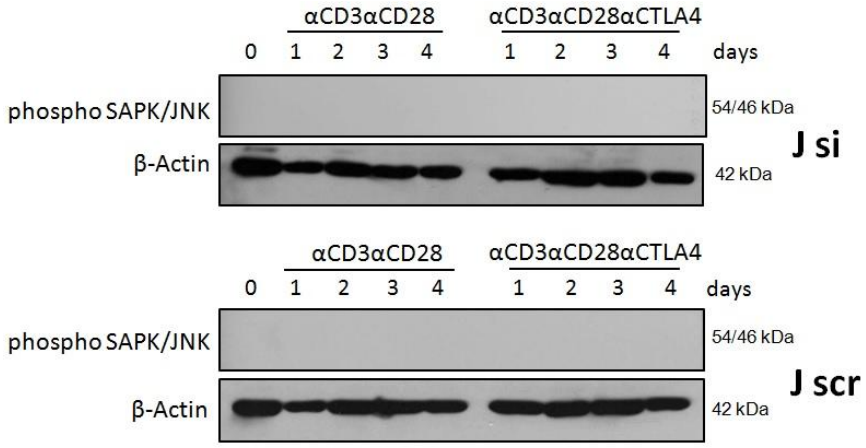

Figure 4.7 Analyses of SAPK/JNK expression.

Jurkat-scr and Jurkat-si cells were incubated for different times (0-4 days) with αCD3/αCD28 and αCD3/αCD28/αCTLA4. 30 µg of whole cell lysates were immunobloted for phospho-SAPK/JNK. The membranes were stripped and re-probed for β-Actin used as a loading control.

4.2.3 NF-κB activation in the generated Jurkat-si, Jurkat-scr and Jurkat-ev cell lines

NF-κB is one of the transcription factors that bind to the IL-2 promoter and is essential for IL-2 gene transcription. Fraser *et al*. reported that CTLA4 crosslinking reduced transcriptional activity of AP-1, NFAT and NF-κB in T cells isolated from transgenic mice containing the luciferase reporter constructs under the control of each transcription factor regulatory element [115]. Therefore, we tried to examine if NF-κB activity was affected in the models used in this study. Jurkat WT cells and the generated cell lines were prestimulated for 48h with phorbol ester (PMA) and calcium ionophore-ionomycin to induce CTLA4 expression. The cells were rested for 5-6 hours and transfected with pGL3-NF-κB (Firefly luciferase expressing reporter plasmid under the control of a NF-κB response element) and pRL-TK (*Renilla* luciferase expressing normalizing plasmid, gift from M. Castro, UCLA). The samples were rested overnight and subsequently stimulated with anti-CD3, anti-CD28 and anti-CTLA4 antibodies. After 6 hours the cells were lysed and luciferase activity was measured. On figure 4.8 A are presented the NF-κB activity fold changes normalized to *Renilla* luciferase compared to the unstimulated samples for each group of transfected cells. From this graph it seemed that the stimulation with CTLA4 ligation induced much higher NF-κB activity in the control cell lines compared to the αCD3/αCD28 activation. Surprisingly, in the J si cell line a very small fold change was determined between the stimulated and unstimulated samples. Because of these unexpected results following the usual data analysis, we looked further into the absolute luminescence values from the measurements of the Firefly luciferase (NF-κB) (Fig. 4.8 C) and *Renilla* luciferase (Fig. 4.8 D). Figure 4.8 C showed that NF-κB activity

was detected in all samples that were stimulated, in contrast to the unstimulated controls, indicating successful activation of the cells. The highest levels were observed in the Jurkat WT cells. However, no significant difference was detected in any of the cell lines upon CTLA4 ligation. More surprising were the results from the measurements of the *Renilla* luciferase activity that was supposed to be used for normalization. The detected levels of *Renilla* luciferase luminescence were overall quite low. The results showed that the highest luminescence (average: 76 RLU) was detected in the Jurkat WT cells. The average value in the Jurkat-si cell line was about 50 RLU and in the Jurkat-ev and Jurkat-scr cells less than 20 RLU. This indicated that transfection efficiency differed a lot in the different cell lines. It was expected that the levels of *Renilla* luciferase luminescence for each cell line would be similar within the three different experimental conditions: unstimulated control, αCD3/αCD28-stimulation and αCD3/αCD28/αCTLA4-stimulation since they originated from the same sample of transfected cells. However, this was not the case, thus indicating that the pRL-TK plasmid encoding *Renilla* luciferase was not a suitable control reporter gene. Because of its origin, a possible contamination and/or damage of the pRL-TK plasmid could not be excluded. Therefore, the normalized values of the pGL3-NF-κB Firefly luciferase reporter (Fig.4.8 A) could not be trusted. The IL-2 production that was secreted in the supernatant upon stimulation was also determined in the different samples. All cell lines produced IL-2 upon 6 hours stimulation and no significant difference was observed when CTLA4 was crosslinked. Considering previous results it was not expected to see a prominent difference upon CTLA4 ligation after such short period of stimulation. The results also indicated that the cells responded very sensitive to stimulation upon transfection, since only after 6 hours of incubation with the

antibodies between 300 and 600 pg/ml of IL-2 were produced. The detected IL-2 production further confirmed doubts about the accuracy of the luciferase assay.

In conclusion, all cell lines were successfully transfected with pGL3-NF-κB and NF-κB activity was detected upon stimulation. Unfortunately, it was not possible to determine whether the ligation of CTLA4 had any effect on the NF-κB activity. The luciferase values could not be normalized and analysed correctly because of the unreliable data obtained from the control reporter gene encoded in the pRL-TK plasmid.

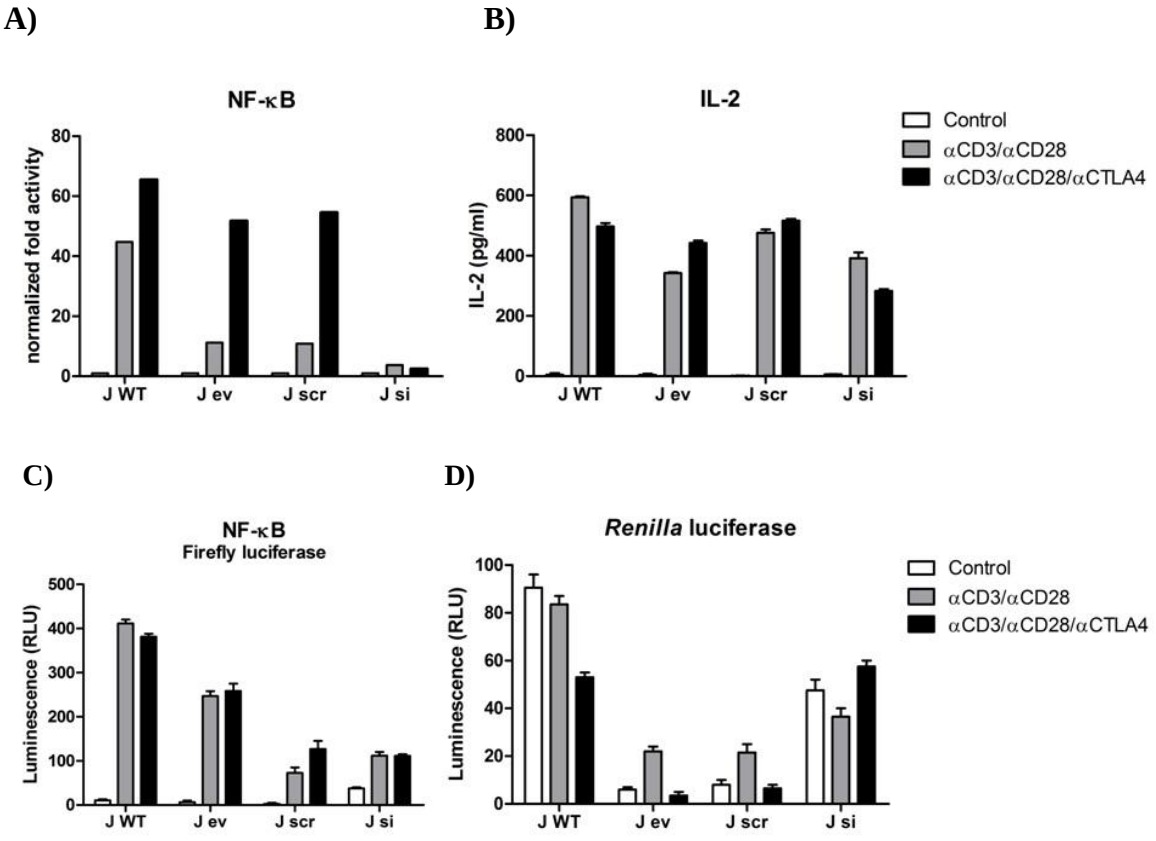

Figure 4.8 Detection of NF-κB transcriptional activity in stable cell lines.

(A) NF-κB Firefly luciferase data were normalized to Renilla luciferase activity and fold changes were calculated compared to the unstimulated controls in each group. (B) Supernatants were collected and the amount of IL-2 in them was determined using ELISA. (C) Firefly luciferase signal. (D) *Renilla* luciferase signal. Columns represent the means of duplicates ± SEM.

4.2.4 Analysis of the effects of SP600125 on IL-2 production

The inhibitor SP600125 was used to further investigate the role of SAPK/JNK in the IL-2 production in the CTLA4 model. SP600125 is a reversible ATP-competitive inhibitor selective for JNK-1, 2 and 3. It is known to inhibit the expression of inflammatory genes like IFN-γ, TNF-α and IL-2 in primary CD4+ T cells [116]. Previous results in this study suggested a potential role of CTLA4 in the increase of JNK phosphorylation in restimulated cells. Therefore, it was of interest to check if the inhibition of JNK would have any effect on the decreased IL-2 production observed when CTLA4 was crosslinked during stimulation.

Jurkat cells were treated with increasing concentration of SP600125 and stimulated with plate-bound αCD3/αCD28 antibodies to induce activation of the MAPK signaling pathways. It was estimated that already at a concentration of 5 µM SP600125 starts to inhibit the phosphorylation of c-Jun (Fig. 4.9). The phosphorylation of SAPK/JNK was also investigated. Interestingly, a slight decrease in the phosphorylation of SAPK/JNK was observed when the inhibitor was present. This might be due to the inhibition of autophosphorylation of the enzyme. Staining of the blot for total SAPK/JNK and β-Actin ensured the equal loading of the samples. For all further experiments with SP600125 a concentration of 20 µM was used since the inhibition at this concentration was more prominent.

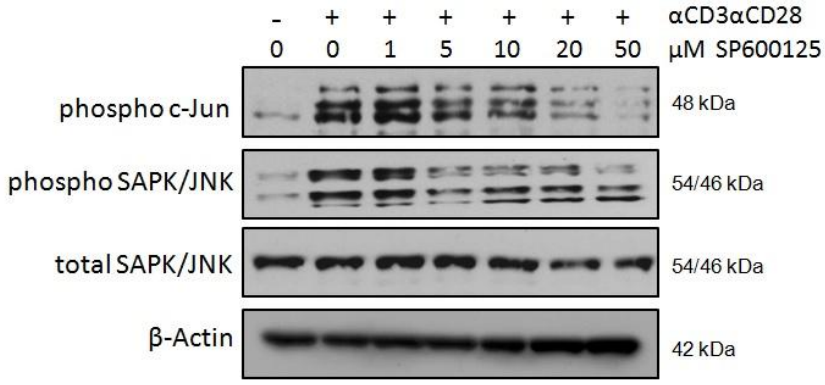

Figure 4.9 Inhibitory effect of SP600125 on Jurkat cells.

Jurkat cells were incubated for 1h with different concentrations of SP600125 and then transferred to αCD3/αCD28-coated plates. After 30 min of stimulation the proteins were extracted. 30 μg of whole cell lysates were immunobloted for phospho-c-Jun(Ser73), phospho-SAPK/JNK and SAPK/JNK. β-Actin was used as a loading control.

Next, the effect of SP600125 on the IL-2 secretion in cells activated with αCD3/αCD28 antibodies for 1-4 days in the presence or absence of CTLA4 was examined (Fig. 4.10). It was determined that crosslinking of CTLA4 inhibited the increase of IL-2 production on day 3 in the Jurkat-scr cells. This was followed by a slight increase of the IL-2 levels on day 4. When the cells were stimulated in the absence of anti-CTLA4 antibody, however, the IL-2 production continued to increase and reached more than 900 pg/ml on day 3 compared to an average of 500 pg/ml on day 2. The measured IL-2 levels remained high on day 4 despite a slight decrease. In the Jurkat-si cells similar levels of IL-2 were measured in the presence or absence of anti-CTLA4 antibody. The production of IL-2 continued to increase, peaking at day 3 and remaining high at day 4 for both stimulating conditions. This part of the results of this experiment confirmed the data of a previous investigation of the IL-2 production under the same conditions (Fig.3.18) as the curves

followed the same pattern over the time course in the two different cell lines Jurkat-scr and Jurkat-si. The treatment with the JNK inhibitor blocked completely IL-2 production in both cell lines for the first two days of stimulation. Detectable levels of the cytokine were not measured until day 3 of activation and they slightly increased at day 4. Crosslinking of CTLA4 had no effect in altering the IL-2 levels in both cell lines in the presence of SP600125.

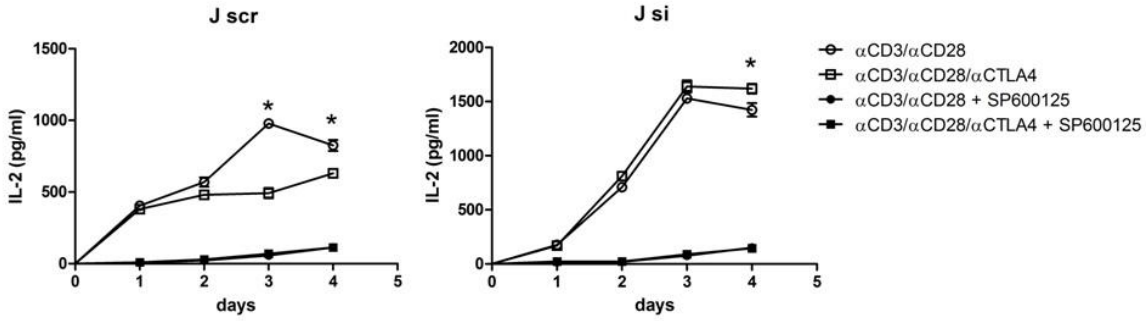

Figure 4.10 Inhibitory effect of SP600125 on Jurkat-si and Jurkat-scr stimulated for 4 days.

Jurkat-scr and Jurkat-si cells were stimulated with plate bound antibodies in the presence or absence of SP600125 for 1-4 days. Supernatants were collected at different time points and the amount of IL-2 in them was determined using ELISA. Statistical analysis was performed using two-way ANOVA followed by Bonferroni post-test. *P<0.001, αCD3/αCD28 values compared to αCD3/αCD28/αCTLA4 values or αCD3/αCD28+SP600125 values compared to αCD3/αCD28/αCTLA4+SP600125 values for each time point.

The levels of IL-2 were also examined in pre-activated cells. Activation with PMA and ionomycin for 2 days was used to induce CTLA4 expression. The cells were then stimulated with anti-CD3/anti-CD28 in the presence or absence of anti-CTLA4 antibody. The results from the re-stimulated cultures in the presence or absence of SP600125 are

presented on figure 4.11. In the Jurkat-scr cells the levels of produced IL-2 after 24h of re-stimulation reached an average of 13000 pg/ml. This represented a 30-fold increase compared to the levels measured in the primary stimulation for the same time point. When CTLA4 was crosslinked considerably lower levels of IL-2 were detected with an average of 8200 pg/ml. After 2 days of stimulation the cytokine levels in the samples stimulated with anti-CD3/anti-CD28 peaked at an average of 65000 pg/ml. In the presence of anti-CTLA4 antibody the levels of IL-2 reached an average of 42500pg/ml. A substantial decrease of the cytokine production was observed on day 3 under both conditions, which was followed by a slight increase at day 4. For all four days the IL-2 production remained distinctly lower when CTLA4 was crosslinked in the Jurkat-scr samples. Very high levels of IL-2 were detected also in the Jurkat-si samples upon re-stimulation. After day 1 an average of around 15000 pg/ml was measured, which is about an 80-fold increase compared to the primary stimulation. On the second day IL-2 levels peaked around 60000pg/ml. Also in the Jurkat-si samples the levels of IL-2 on day 3 dropped almost to the ones detected on day 1. A slight increase was observed on day 4. A distinct difference was not detected when anti-CTLA4 antibody was present in the Jurkat-si cultures. In both cell lines the treatment with SP600125 decreased substantially the IL-2 production with an average of 3200 pg/ml in the Jurkat-scr cells and 2900 pg/ml in the Jurkat-si cells after 24h of stimulation. Over the time course a slight increase was observed throughout day 4. Similar levels of IL-2 were measured in the cultures of both cell lines where CTLA4 was crosslinked compared to the ones stimulated with anti-CD3/anti-CD28. The results from the re-stimulation in the presence of SP600125 confirmed the data from the primary stimulation indicating the remarkable potential of

SP600125 to inhibit IL-2 production. They also suggest that any possible effect that CTLA4 might have via JNK on the IL-2 production is abrogated when JNK is inhibited. Different kinetics in IL-2 production was observed in the primary and secondary stimulation. Whereas in the primary stimulated cells the cytokine production peaked at day 3, in the re-stimulated cells it was at day 2. The peak levels in the re-stimulated cultures exhibited a 60-fold higher values compared to the ones in the primary stimulation.

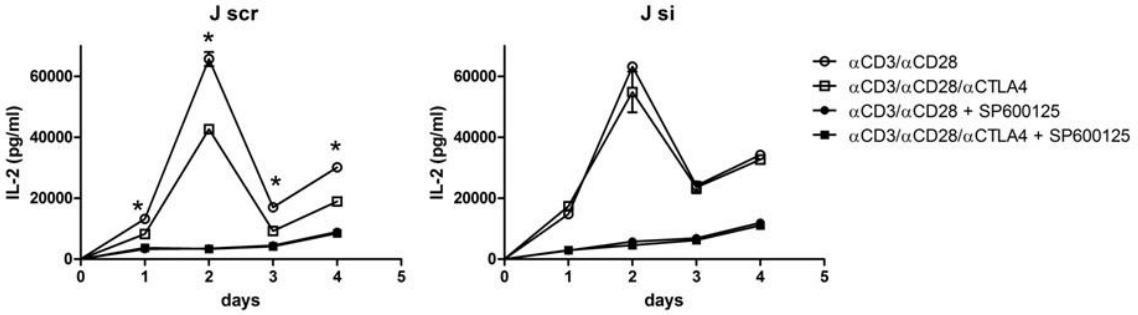

Figure 4.11 Inhibitory effect of SP600125 on Jurkat-si and Jurkat-scr re-stimulated for 4 days.

Jurkat-scr and Jurkat-si were stimulated for 2 days with PMA/ionomycin and rested overnight. The cells were re-stimulated with plate bound antibodies in the presence or absence of SP600125 for 1-4 days. Supernatants were collected at different time points and the amount of IL-2 in them was determined using ELISA. Statistical analysis was performed using two-way ANOVA followed by Bonferroni post-test. *P<0.001, αCD3/αCD28 values compared to αCD3/αCD28/αCTLA4 values or αCD3/αCD28+SP600125 values compared to αCD3/αCD28/αCTLA4+SP600125 values for each time point.

5. Discussion

The cells of the innate immune system are able to detect pathogens via invariant receptors and eliminate infection in a non-specific manner. Another important function is the activation of naive antigen-specific T cells by antigen presenting cells, which is essential for the initiation and direction of the adaptive immunity. However, some pathogens and viruses have developed mechanisms to escape immune surveillance and defeat immune responses. One promising approach to overcome immunological tolerance involves augmenting endogenous T cell mediated immunity by interrupting the T cell down-regulatory pathway. CTLA4 has been identified as one of the major negative regulators of T cell response. However, the highly endocytotic behavior of this receptor makes it a difficult target to study and the exact mechanism of function is not well understood yet. Despite that CTLA4 is already considered a potential target for the development of immunotherapy. Antibodies against CTLA4 have been developed and are being tested in several clinical trials against melanoma [76]. Although immunoglobulin-based therapies appear to be promising there are several disadvantages using an antibody against CTLA4. Since it is stored intracellular and only expressed transiently on the cell membrane, the protein is an ‘invisible’ target for antibodies. Antibodies must be administrated regularly to the patients to maintain an effective concentration. However, this is related to high costs for the patient. Another negative point is that toxicity and adverse immune responses are often related to the systematic administration of high doses [76].

Using RNA interference to knock down CTLA4 and eventually modulate T cell activation seems to be a promising alternative to the immunoglobulin-based therapy. The silencing of CTLA4 should reduce both extracellular and intracellular expression and

should not be cytotoxic to T cells. The application of this approach should also contribute to the knowledge about the role of CTLA4 in T cell receptor signaling. Three types of small RNA can be used to perform RNA interference in mammalian cells: chemically synthesized siRNA, short hairpin RNA (shRNA) cloned into a plasmid or viral vector and microRNA adapted short hairpin RNA (shRNAmir) also cloned into a plasmid or viral vector [80, 89, 99].

Introduction of siRNA is easy to use but results in transient silencing of the gene target, which makes it unsuitable for the analysis of long-term effects. Another limitation is associated with the variability of the transfection efficiency of siRNA molecules in different cell lines. shRNA, on the other hand, relies on the cell machinery for expression and offers several advantages compared to siRNA. The most commonly utilized plasmids used to express shRNA contain an RNA-polymerase-III-based promoter such as U6 or H1. These induce high levels of shRNA expression and mediate highly efficacious silencing. Another advantage is that the resulting construct is small and simple which makes it easy to clone in different plasmid and viral vectors [117]. In shRNAmir the hairpin structure is derived from an endogenous miRNA gene in which the mature miRNA sequence in the pri-miRNA is replaced with the target gene sequence. In this case the shRNAmir utilizes the RNAi pathway at the pri-miRNA stage, whereas the shRNA does this at the pre-miRNA level. Another difference is that shRNA-mir can be placed under the regulation of Polymerase II promoters, which can provide more flexibility in designing the construct. Thus a coding gene, like a reporter gene or regulatory systems can be expressed simultaneously with the shRNA-mir hairpin structure [89].

CTLA4 silencing with synthetic siRNA in PBMC has already been reported [118]. For this project we looked for a suitable vector to incorporate the siRNA that would allow long term and stable expression and facilitate the development of a stable cell line. In the first stage of this study we identified and validated a target sequence in human CTLA4 mRNA that can be silenced. Oligonucleotides that coded for shRNA specifically against the coding region in the second exon of CTLA4 or scrambled controls were cloned in the MCS of a Bluescript vector containing a U6 promoter downstream of a CMV enhancer element. Initially, the generated plasmids were tested in co-transfection experiments with a vector encoding the cDNA for CTLA4 (pCTLA4-Flag) in HeLa cells. HeLa cells are easy to handle and show consistent high transfection efficiency when transfected with liposome-based reagents. They do not express endogenous CTLA4, so that the co-transfection experimental set up offers a more convenient and controlled way to test the potency of the generated shRNA containing constructs, since it is considered that these constructs would be expressed with the same efficiency as the co-transfected CTLA4-encoding plasmid. This was a way to overcome the difficulties of the low transfection efficiency observed in Jurkats when liposome-based reagents were used. Despite reports in the literature about the application of liposome-based reagents for the successful transfection of Jurkat cells, all attempts to use this method failed and no expression of the reporter genes β-galactosidase and GFP was detected [119].

The Western blot analysis of the co-transfected HeLa showed a good silencing effect of pBSU6siCTLA4 compared to controls (pBSU6scrCTLA4) (Fig.2.5). These results indicated that the chosen shRNA is sequence-specific and can induce significant reduction in CTLA4 expression. An alternative approach to study the silencing of

endogenous CTLA4 and its effects on T cell signaling using Jurkat as a model was to develop a stable transfected clone that expresses the shRNA. One way of developing such a clone is to co-transfect the cells with a plasmid encoding a gene for drug resistance (e.g. neomycin) and the pBSU6siCTLA4. However, this approach was not used since the screening for a siCTLA4 expressing cell clone may be too difficult and time consuming. Instead, the shRNA expressing cassette (shRNA and U6 promoter) was inserted into a pCIneo vector expressing the neomycin resistance gene and the successful cloning was confirmed by restriction digest and sequencing. After a Western blot analysis using the same HeLa model employed to evaluate the pBSU6siCTLA4 construct, CTLA-4 expression was not detected either in the samples transfected with pCIneo siCTLA4 or in the controls (Fig.2.7). Therefore, these results did not verify that the new construct pCIneo siCTLA4 is suitable for the development of a stable transfected cell line that would exhibit CTLA4 knock-down. A further attempt to confirm the silencing effect of the shRNA sequence observed initially was made by generating pCTLA4-Flag siCTLA4 and the control pCTLA4-Flag scrCTLA4, where the shRNA cassette was inserted into a vector encoding the coding sequence for CTLA4. This time strong CTLA4 expression was observed upon the Western blot analysis of the transfected HeLa, regardless which construct was used: the one encoding the siCTLA-4 or the one encoding the scrambled control sequence (Fig.2.9). The failure to see any reduction in the expression could be due to the fact that the selected shRNA sequence does not mediate strong RNA interference. The same sequence, however, inserted in the Bluescript backbone demonstrated a good silencing effect. An important modification of the pBSU6 vector was the placement of an enhancer from the cytomegalovirus (CMV) upstream of the U6

promoter. This enhanced the promoter activity and increased the shRNA synthesis, thereby strengthening the silencing of the target. In the pCTLA4-Flag plasmid the expression of CTLA4 is driven by the CMV promoter which is one of the strongest promoters used to induce expression. In order to avoid any possible plasmid recombination caused by the presence of two CMV elements in the same plasmid, only the U6 promoter and the following shRNA were inserted into the pCTLA4-Flag. The obtained results indicate that this might have resulted in the reduction of the synthesized shRNA that would be insufficient to silence the amount of overexpressed CTLA4 transcripts induced by the CMV promoter. Transcriptional interference between strong and weak promoters has already been studied and can explain the observed results in the transfection with the modified pCTLA4-Flag vectors [120]. Considering the results gained from the experiments with the different constructs, it was decided to use the pBSU6 vector backbone and insert a neomycin cassette in pBSU6siCTLA4 and pBSU6scrCTLA4. The new construct combined two important features: it increased the amount of synthesized shRNA induced by the CMV enhancer and allowed the generation of a stable transfected cell line expressing the shRNA. Analyses of the Western blot using co-transfected HeLa showed a good silencing effect of the vector encoding siCTLA4. Strong CTLA4 expression was detected when the scrambled control (scrCTLA4) and the empty vector were used, thus confirming the sequence-specificity of the designed shRNA (Fig.2.11). Another confirmation of the successfully induced RNAi was delivered by the results obtained from the real-time PCR experiments. The application of this quantitatively more sensitive method made it possible to estimate that the suppressive effect of shRNA to CTLA4 in the co-transfected cells can reach more than 75%

(Fig.2.12). Another interesting observation was made by comparing the mRNA levels of CTLA4 expression in Jurkats to the ones in transfected HeLa. It was estimated that the CMV promoter driven expression in the HeLa is much stronger than the one detected in stimulated Jurkats. This suggests that the silencing of endogenous CTLA4 in Jurkats using the pBSU6neo siCTLA4 would be even more efficient than the RNA interference observed in co-transfected HeLa.

Various model systems have been developed to investigate CTLA4 such as primary human T cells, leukaemia cell lines, stable transfected cell lines and different mouse models [24, 40, 104, 121]. In this study it was decided to use the Jurkat leukaemia cell line. This cell line has been used for decades to investigate T cell biology and a lot of T cell signaling proteins were characterized due to the development of sublines that are deficient in these signaling molecules [122]. We expected that Jurkats can be utilized as a useful model for the investigation of the effects of CTLA4 downregulation in functional assays and signaling pathways.

Silencing of the endogenous expression of CTLA4 induced upon stimulation was tested in Jurkats using transient transfection via electroporation. The electroporation and the Nucleofector technology have been applied for difficult to transfect cells and in the present project were chosen as the method that successfully introduced foreign DNA in Jurkat cells. Despite the detection of the plasmid in the DNA samples, indicating effective transfection, a clear downregulation could not be reproduced. A possible reason for that could be that the cells were analysed 4 days post-transfection and at that time point a lot of them were not expressing the plasmid any more. Transient expression of transfected genes is usually analysed 24-48h post-transfection. An additional reason

could be that the transfection efficiency in the Jurkat cell line is not very high. This would result in that only a fraction of the cells that are subsequently stimulated to induce CTLA4 expresson would express also the siRNA against CTLA4. These data suggested that the establishment of a Jurkat stable cell line expressing the shRNA against CTLA4 would be a more suitable and reliable model for the investigation of the role of this receptor. Such a stable cell line would ensure a reproducible and consistent shRNA expression and would allow the set up of long-term experiments.

On the other hand, the results obtained from the generated different constructs suggested that the use of co-transfection for the characterisation of the shRNA expressing plasmids might introduce too many variables that could impede the estimation of silence efficiency and/or gene expression. Back in 1992 it was established that the introduction of different types of plasmids to control transfection efficiency could affect the expression of the gene of interest [123]. To minimize the variables, a HeLa cell lines stably expressing CTLA4 was generated. A constitutive expression of CTLA4 in this cell line will allow an easier and more accurate evaluation of other constructs generated to induce suppressive effects against this receptor using transient transfection.

In order to investigate the long-term and reproducible effect of the shRNA mediated CTLA4 silencing three Jurkat cell lines were developed that stably integrated pBSU6neo siCTLA4, pBSU6neo scrCTLA4 and pBSU6neo in the cellular genome. DNA samples extracted from the stable cell lines were evaluated by a PCR amplification of a sequence that is specific for the vectors. It was demonstrated that the expression of endogenous CTLA4 induced upon treatment with PMA and ionomycin was successfully downregulated in the Jurkat cell line expressing the silencing shRNA compared to the

controls. Another ‘criteruim’ for selection was the ability of the cells to produce IL-2 upon stimulation. Foreign DNA can be integrated in different sites of the genome and effect the transcription of the gene of interest [124]. Since we were interested to studying the possible effects of CTLA4 silencing on IL-2 production, it was of importance to ensure that the selected clones have not lost the ability to produce this cytokine. Another important issue was the detection of the ‘presence’ of the actual mature small interfering RNA. The expression of the mature small interfering RNA was detected successfully in the transiently transfected cells as well as in the stable cell lines using stem-loop RT followed by real time quantification with SYBR Green I assay. This method offers a convenient way of confirming the expression of the small interfering RNA without the need to include additional reporter genes in the vectors encoding the shRNA. Compared to other methods for detection of small interfering RNAs, such as northern blotting [125], the quantitative stem-loop RT-PCR demonstrates better specificity and requires less material. Besides it is a much faster way of detection compared to methods based on cloning. Originally, when this assay was developed, miRNA expression was detected using stem-loop RT followed by TaqMan PCR analysis [97]. Chen *et al.* suggest that the use of the TaqMan PCR assay for quantification increases specificity needed when primer dimers produce a background and facilitates the detection of less abundant miRNA. However, the use of the TaqMan PCR assay requires individual fluorescence probes for each small RNA target, which makes the detection quite costly. Therefore, we chose to optimize the quantification using a SYBR Green I assay. Combined with melting curve analysis and visualization of the product by gel electrophoresis, the SYBR Green I assay provided good specificity and allowed the detection of the *siCTLA4* and *scrCTLA4*.

It was confirmed that these sequences were *siCTLA4* and *scrCTLA4* by using sequencing of the PCR products.

In conclusion, the cell clones used for further functional analyses were selected according to the following criteria:

- Presence of the plasmid in the DNA;
- Downregulation of CTLA4 on the mRNA and protein level in the samples transfected with pBSU6neo siCTLA4 and presence of CTLA4 in the samples transfected with the scrambled control or empty vector;
- Presence of CTLA4 in the genomic DNA;
- Presence of the mature small RNA sequences;
- Ability to produce IL-2.

It was as early as in 1996 when the inhibitory function of CTLA4 was associated with downregulation of IL-2 production in T cells [104]. Therefore, the kinetics of IL-2 production was examined over a period of 4 days in response to CD3 and CD28 ligation and CTLA4 crosslinking. A reduction in the IL-2 production was observed after day 3 of stimulation when CTLA4 was crosslinked in the generated control cell lines and Jurkat WT cells. The change of the cytokine production correlated with the CTLA4 expression which was detectable 48h upon activation. These results correspond to previous studies that report the same inhibitory effect but employed other models such as stable cell lines or human PBMC [102, 126]. No change of the kinetics of the IL-2 production was observed in the Jurkat-si cells when CTLA4 was crosslinked, which confirmed the functionality of the generated cell line. Pandiyan *et al.* pre-activated mouse splenocytes to induce CTLA4 expression and investigate its role in apoptosis upon secondary

stimulation [127]. Schneider *et al.* also used the same approach to study the involvement of the receptor in anergy induction in human PBMCs [128]. Therefore, it was of interest to examine the IL-2 production in secondary stimulation using the generated models. It was expected that the IL-2 levels would be lower in the presence of anti-CTLA4 antibody already after 24h upon stimulation since the receptor would be present at the surface at the moment of activation. Under these conditions a consistent decreased IL-2 production was detected in the course of time (1-4 days) of stimulation in the generated control cell line Jurkat-scr. On the contrary, in the Jurkat-si cells the levels of IL-2 measured in the presence or absence of anti-CTLA4 antibody were very similar, indicating as expected no involvement of CTLA4 in the downstream signaling pathways due to the successful silencing. Interestingly, a significant difference was observed in the absolute levels of IL-2 between the primary and secondary stimulation. In both cell lines Jurkat-scr and Jurkat-si there was 30-60-fold increase in cytokine production upon secondary stimulation compared to the primary stimulation for the same points. After the first activation the cells were transferred into new medium, rested overnight and no IL-2 was detected in the unstimulated control samples, which should exclude any possible involvement of basal cytokine levels from the primary stimulation. Another interesting observation is the different kinetics of IL-2 production under the two conditions during the time course. Whereas in the primary stimulation the cytokine levels in response to anti-CD3/anti-CD28 activation increase steadily throughout the first and second day and peak on day 3, in the secondary stimulation the levels peak on day 2, decrease notably on day 3 and increase slightly again throughout the fourth day. To our knowledge, a comparison for a longer time course of stimulation has not been sufficiently studied yet. In previous studies

the IL-2 response upon antibodies-mediated activation was reported only for one time point either under conditions of primary or secondary stimulation [128, 129]. CTLA4 did not seem to affect the kinetics in the time course. The crosslinking of the receptor resulted in a lower cytokine production under both conditions in the control cell lines but it still followed the same pattern of the kinetics that was observed with anti-CD3/anti-CTLA4 stimulation. It seems more likely that phosphotases like SHP-1 and SHP-2 could be involved and, in the case of the secondary stimulation, mediate earlier dephosphorylation of the kinases triggering signaling pathways that result in IL-2 production. SHP-1 is known to associate with Vav1, Grb2 and Sos1 which are involved in the intracellular pathways during T cell activation [130].

Investigations of the phosphorylation of some signaling proteins in response to anti-CD3/anti-CD28 and anti-CD3/anti-CD28/anti-CTLA4 revealed that the decrease of IL-2 production in the presence of anti-CTLA4 antibody could be mediated by an increased phosphorylation of JNK. The JNK signaling pathway leads to phosphorylation of the c-Jun proteins that associate with c-Fos proteins to form the AP-1 transcrition factor for the IL-2 gene. An inhibitor of JNK (SP600125) was implemented to investigate whether abrogation of this signaling pathway would alter the IL-2 production in response to CTLA4 crosslinking. It was assumed that in the presence of the inhibitor and CTLA4 crosslinking a decrease in IL-2 production will not occur any more. However, this turned out not to be the case. In both cell lines Jurkat-scr and Jurkat-si the IL-2 production was dramatically inhibited in the presence of the JNK inhibitor in primary and secondary stimulation for the time course of stimulation. Crosslinking of CTLA4 under these conditions did not have any effect on cytokine production. SP600125 is a small molecule

that is cell permeable and selectively inhibits c-Jun phosphorylation by binding to the JNK kinase [116]. The inhibitory effect of SP600125 on IL-2 production observed in this study with the generated models is consistent with other reports that show inhibited IL-2 gene expression [131]. One explanation for the lack of a CTLA4 mediated effect could be the fact that the cells are incubated with the inhibitor in advance before the stimulation. Thus, any role that CTLA4 crosslinking would have on the IL-2 production would be masked and 'covered' by the already existing inhibition mediated by SP600125. This would not exclude the potential role of JNK in CTLA4-mediated signaling suggested by the results of the immunoblotting performed earlier in the project.

CTLA4 is also known to inhibit NF-kB activation [56, 115]. Unfortunately, it was not possible to confirm this in the present study. To determine NF-kB activity the pre-activated cells were transfected with a plasmid containing a NF-kB luciferase reporter together with a control plasmid and activated with plate-bound antibodies. Despite successful detection of the NF-kB activation an accurate evaluation of the luciferase reporter was not possible due to the controversial results from the control plasmid used for normalization.

We tried to investigate the involvement of CTLA4 in some proximal and distal signaling events using the pre-activated stable cell lines. The results did not indicate that CTLA4 interferes with the phosphorylation of any of the following proteins: Lck, ZAP-70, LAT, SLP-76 or ERK. Only the phosphorylation of JNK seemed to be increased upon CTLA4 ligation in the Jurkat WT and control cell lines. In contrast, Guntermann *et al.* report that CTLA4 inhibits ZAP-70 phosphorylation of the Y319 site and ERK phosphorylation [126]. This difference could be due to the choice of model and experimental set up. In

that report human CD4+ T lymphocytes isolated from peripheral blood were used in primary stimulation for 5 min with anti-CD3/anti-CTLA4 antibodies. However, the natural ligands of CTLA4 CD80 and CD86 also bind to CD28, triggering also this signaling pathway. Therefore an exclusion of CD28 during the activation, which does not naturally occur, could influence the results. The other interesting result reported in the above-quoted publication is the detection of low surface and high intracellular CTLA4 expression in resting human T lymphocytes. This could be due to the presence of regulatory CD4+/CD25+ T cells in the cell suspension as these express constitutively also CTLA4 on the surface and could affect further the results from the functional studies. During the preparation and isolation of the cells the CD25 marker was not considered. Other research groups focused on the investigation of distal signaling event like the ERK and JNK pathways. In 1997 Calvo *et al.* reported reduced ERK and JNK kinase activity in response to anti-CD3/anti-CD28/anti-CTLA4 stimulation in pre-activated mouse T-lymphocytes [54]. A couple of years later in 2002 Schneider *et al.* published a paper reporting that CTLA4 ligation inhibited ERK activity, while up-regulating and sustaining JNK activation in mouse T lymphocytes activated with a combination of antibodies and APCs [55]. Our data also indicated up-regulation of JNK phosphorylation upon CTLA4 involvement. However, the levels of ERK phosphorylation were not altered. Jurkat is a leukaemia cell line that does not express the phosphotases PTEN and SHIP which results in high basal levels of PtdIns $(3,4,5)P_3$ and constitutive activation of Akt [113]. Previous studies report hyperphosphorylation of several downstream signaling proteins including ERK1/2 in the Jurkat cell line compared to HuT78 and peripheral blood T cells [129]. Our results confirm the presence of a basal ERK activity, followed by a strong increase in

the phosphorylation of this MAPK in response to stimulation. Comparing the results from various research groups, it becomes clear that different models and experimental set up can sometimes lead to controversial conclusions while trying to define the mechanism of CTLA4 signaling. Therefore, the specificity and limitation deriving from the Jurkat cell model should be well considered to avoid misinterpretation of results.

Hoff *et al.* suggest that CTLA4 signaling transduction activates the ubiquitin ligase Itch which in turn enhances the ubiquitination of the Jun proteins resulting in inhibition of T cell activity [132]. Another study reports that the activation of the JNK pathway in T cells activates the ubiquitin ligase Itch which then leads to increase of degradation of c-Jun and JunB and in this way can modulate cytokine production [133]. Linking the activation of the JNK pathway with the ubiquitination and subsequent degradation of proteins could explain the increased phosphorylation of JNK mediated by CTLA4 and the downregulated IL-2 production observed in the Jurkat WT model used in this study. Ligation of CTLA4 in the Jurkat WT and Jurkat-scr cells mediates stronger activation of the JNK pathway which could activate the ubiquitin ligase Itch. Subsequently, the phosphorylated c-Jun proteins, that are part of one of the AP-1 transcription factors of the IL-2 gene, are targeted by Itch and subjected to degradation which would result in reduction of IL-2 production. This hypothesis is supported by the results obtained from the generated Jurkat-si cell line with silenced CTLA4 expression where no increase of JNK activity is observed and the levels of IL-2 production remain similar to the ones induced in the absence of anti-CTLA4 antibody.

In conclusion, the study revealed a sequence that can successfully silence human CTLA4 expression, which was identified and evaluated. Integrating the shRNA in a plasmid

guaranteed strong expression and facilitated the generation of a cell line with downregulated CTLA4 expression – Jurkat-si. The Jurkat-si and the generated control cell lines Jurkat-scr and Jurkat-ev were tested in functional assays under two different conditions: primary and secondary stimulation. The obtained data suggest that increased JNK activity plays a role in the CTLA4-mediated inhibition of IL-2 production. Based on the data obtained with the generated models figure 5.1 illustrates the possible role of CTLA4 in the T cell signaling pathway that triggers IL-2 production. The generated stable cell lines could be used for further investigations of the role of CTLA4 in T cell biology.

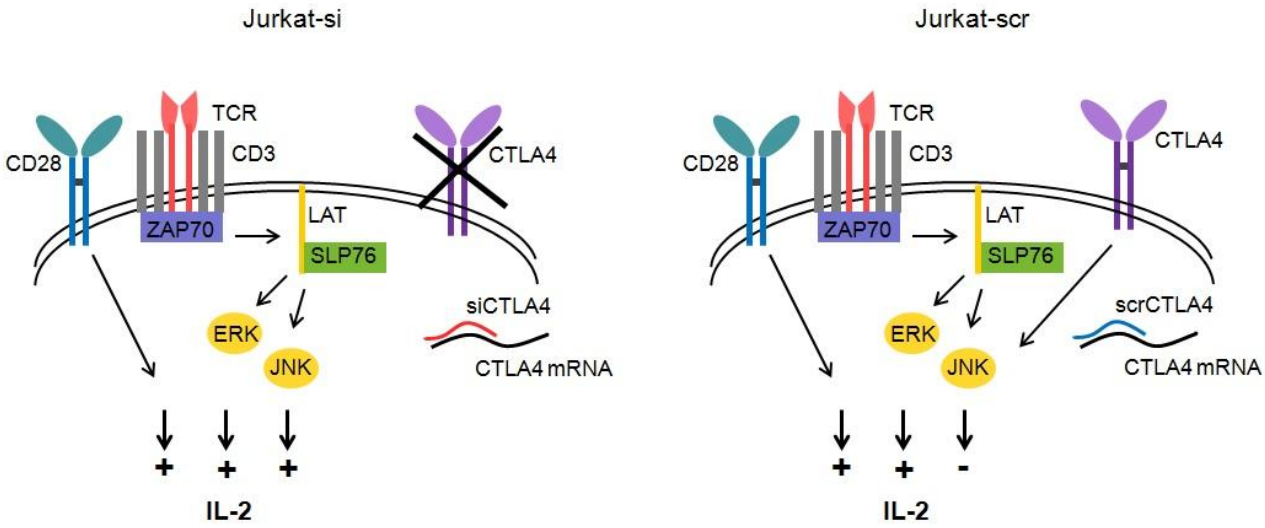

Fig. 5.1. The role of CTLA4 in the regulation of IL-2 production.

Upon activation of the cells through the TCR complex and co-stimulatory molecules (CD28) ZAP-70 kinase is recruited to the TCR complex. Among other proteins ZAP-70 phosphorylates the adaptor proteins LAT and SLP-76. The signaling pathways that are triggered result in activation of MAPK ERK and JNK which take part in the regulation of IL-2 production. Crosslinking of CTLA4 leads to increased JNK activation and inhibits IL-2 production. Silencing of CTLA4 in the Jurkat-si model leads to unaltered JNK activation and sustained IL-2 production.

6. References

1. Matsuda, F., et al., *The complete nucleotide sequence of the human immunoglobulin heavy chain variable region locus.* J Exp Med, 1998. **188**(11): p. 2151-62.
2. Itano, A.A. and M.K. Jenkins, *Antigen presentation to naive CD4 T cells in the lymph node.* Nat Immunol, 2003. **4**(8): p. 733-9.
3. McKinstry, K.K., T.M. Strutt, and S.L. Swain, *The potential of CD4 T-cell memory.* Immunology, 2010. **130**(1): p. 1-9.
4. Grakoui, A., et al., *The immunological synapse: a molecular machine controlling T cell activation.* Science, 1999. **285**(5425): p. 221-7.
5. Dustin, M.L. and D. Depoil, *New insights into the T cell synapse from single molecule techniques.* Nat Rev Immunol, 2011. **11**(10): p. 672-84.
6. Monks, C.R., et al., *Three-dimensional segregation of supramolecular activation clusters in T cells.* Nature, 1998. **395**(6697): p. 82-6.
7. Gaffen, S.L. and K.D. Liu, *Overview of interleukin-2 function, production and clinical applications.* Cytokine, 2004. **28**(3): p. 109-23.
8. Weiss, A. and D.R. Littman, *Signal transduction by lymphocyte antigen receptors.* Cell, 1994. **76**(2): p. 263-74.
9. Reth, M., *Antigen receptor tail clue.* Nature, 1989. **338**(6214): p. 383-4.
10. Di Bartolo, V., et al., *Tyrosine 319, a newly identified phosphorylation site of ZAP-70, plays a critical role in T cell antigen receptor signaling.* J Biol Chem, 1999. **274**(10): p. 6285-94.
11. Samelson, L.E., *Signal transduction mediated by the T cell antigen receptor: the role of adapter proteins.* Annu Rev Immunol, 2002. **20**: p. 371-94.
12. Rao, A., C. Luo, and P.G. Hogan, *Transcription factors of the NFAT family: regulation and function.* Annu Rev Immunol, 1997. **15**: p. 707-47.
13. Monks, C.R., et al., *Selective modulation of protein kinase C-theta during T-cell activation.* Nature, 1997. **385**(6611): p. 83-6.
14. Sedwick, C.E. and A. Altman, *Perspectives on PKCtheta in T cell activation.* Mol Immunol, 2004. **41**(6-7): p. 675-86.
15. Prasad, K.V., et al., *T-cell antigen CD28 interacts with the lipid kinase phosphatidylinositol 3-kinase by a cytoplasmic Tyr(P)-Met-Xaa-Met motif.* Proc Natl Acad Sci U S A, 1994. **91**(7): p. 2834-8.
16. Ward, S.G. and D.A. Cantrell, *Phosphoinositide 3-kinases in T lymphocyte activation.* Curr Opin Immunol, 2001. **13**(3): p. 332-8.
17. Nel, A.E., et al., *Ligation of the T-cell antigen receptor (TCR) induces association of hSos1, ZAP-70, phospholipase C-gamma 1, and other phosphoproteins with Grb2 and the zeta-chain of the TCR.* J Biol Chem, 1995. **270**(31): p. 18428-36.
18. Schneider, H., et al., *T cell antigen CD28 binds to the GRB-2/SOS complex, regulators of p21ras.* Eur J Immunol, 1995. **25**(4): p. 1044-50.
19. Jain, J., C. Loh, and A. Rao, *Transcriptional regulation of the IL-2 gene.* Curr Opin Immunol, 1995. **7**(3): p. 333-42.

20. Weiss, L., et al., *Regulation of c-Jun NH(2)-terminal kinase (Jnk) gene expression during T cell activation.* J Exp Med, 2000. **191**(1): p. 139-46.
21. Khoshnan, A., et al., *Primary human CD4+ T cells contain heterogeneous I kappa B kinase complexes: role in activation of the IL-2 promoter.* J Immunol, 1999. **163**(10): p. 5444-52.
22. Khoshnan, A., et al., *The NF-kappa B cascade is important in Bcl-xL expression and for the anti-apoptotic effects of the CD28 receptor in primary human CD4+ lymphocytes.* J Immunol, 2000. **165**(4): p. 1743-54.
23. Su, B., et al., *JNK is involved in signal integration during costimulation of T lymphocytes.* Cell, 1994. **77**(5): p. 727-36.
24. Waterhouse, P., et al., *Lymphoproliferative disorders with early lethality in mice deficient in Ctla-4.* Science, 1995. **270**(5238): p. 985-8.
25. Valk, E., C.E. Rudd, and H. Schneider, *CTLA-4 trafficking and surface expression.* Trends Immunol, 2008. **29**(6): p. 272-9.
26. Ling, V., et al., *Complete sequence determination of the mouse and human CTLA4 gene loci: cross-species DNA sequence similarity beyond exon borders.* Genomics, 1999. **60**(3): p. 341-55.
27. Oaks, M.K., et al., *A native soluble form of CTLA-4.* Cell Immunol, 2000. **201**(2): p. 144-53.
28. Wong, C.K., et al., *Aberrant production of soluble costimulatory molecules CTLA-4, CD28, CD80 and CD86 in patients with systemic lupus erythematosus.* Rheumatology (Oxford), 2005. **44**(8): p. 989-94.
29. Tector, M., et al., *Biochemical analysis of CTLA-4 immunoreactive material from human blood.* BMC Immunol, 2009. **10**: p. 51.
30. Ueda, H., et al., *Association of the T-cell regulatory gene CTLA4 with susceptibility to autoimmune disease.* Nature, 2003. **423**(6939): p. 506-11.
31. Kouki, T., et al., *CTLA-4 gene polymorphism at position 49 in exon 1 reduces the inhibitory function of CTLA-4 and contributes to the pathogenesis of Graves' disease.* J Immunol, 2000. **165**(11): p. 6606-11.
32. Maszyna, F., et al., *Diversity of clonal T cell proliferation is mediated by differential expression of CD152 (CTLA-4) on the cell surface of activated individual T lymphocytes.* J Immunol, 2003. **171**(7): p. 3459-66.
33. Takahashi, T., et al., *Immunologic self-tolerance maintained by CD25(+)CD4(+) regulatory T cells constitutively expressing cytotoxic T lymphocyte-associated antigen 4.* J Exp Med, 2000. **192**(2): p. 303-10.
34. Leung, H.T., et al., *Cytotoxic T lymphocyte-associated molecule-4, a high-avidity receptor for CD80 and CD86, contains an intracellular localization motif in its cytoplasmic tail.* J Biol Chem, 1995. **270**(42): p. 25107-14.
35. Valk, E., et al., *T cell receptor-interacting molecule acts as a chaperone to modulate surface expression of the CTLA-4 coreceptor.* Immunity, 2006. **25**(5): p. 807-21.
36. Kolsch, U., et al., *Normal T-cell development and immune functions in TRIM-deficient mice.* Mol Cell Biol, 2006. **26**(9): p. 3639-48.
37. Beraud-Dufour, S. and W. Balch, *A journey through the exocytic pathway.* J Cell Sci, 2002. **115**(Pt 9): p. 1779-80.

38. Bonifacino, J.S. and E.C. Dell'Angelica, *Molecular bases for the recognition of tyrosine-based sorting signals.* J Cell Biol, 1999. **145**(5): p. 923-6.
39. Schneider, H., et al., *Cytolytic T lymphocyte-associated antigen-4 and the TCR zeta/CD3 complex, but not CD28, interact with clathrin adaptor complexes AP-1 and AP-2.* J Immunol, 1999. **163**(4): p. 1868-79.
40. Teft, W.A., T.A. Chau, and J. Madrenas, *Structure-Function analysis of the CTLA-4 interaction with PP2A.* BMC Immunol, 2009. **10**: p. 23.
41. Schneider, H., et al., *CTLA-4 binding to the lipid kinase phosphatidylinositol 3-kinase in T cells.* J Exp Med, 1995. **181**(1): p. 351-5.
42. Zoller, K.E., I.A. MacNeil, and J.S. Brugge, *Protein tyrosine kinases Syk and ZAP-70 display distinct requirements for Src family kinases in immune response receptor signal transduction.* J Immunol, 1997. **158**(4): p. 1650-9.
43. Miyatake, S., et al., *Src family tyrosine kinases associate with and phosphorylate CTLA-4 (CD152).* Biochem Biophys Res Commun, 1998. **249**(2): p. 444-8.
44. Lenschow, D.J., et al., *Expression and functional significance of an additional ligand for CTLA-4.* Proc Natl Acad Sci U S A, 1993. **90**(23): p. 11054-8.
45. Collins, A.V., et al., *The interaction properties of costimulatory molecules revisited.* Immunity, 2002. **17**(2): p. 201-10.
46. Manzotti, C.N., et al., *Integration of CD28 and CTLA-4 function results in differential responses of T cells to CD80 and CD86.* Eur J Immunol, 2006. **36**(6): p. 1413-22.
47. Qureshi, O.S., et al., *Trans-endocytosis of CD80 and CD86: a molecular basis for the cell-extrinsic function of CTLA-4.* Science, 2011. **332**(6029): p. 600-3.
48. Hwu, P., et al., *Indoleamine 2,3-dioxygenase production by human dendritic cells results in the inhibition of T cell proliferation.* J Immunol, 2000. **164**(7): p. 3596-9.
49. Schmidt, E.M., et al., *Ctla-4 controls regulatory T cell peripheral homeostasis and is required for suppression of pancreatic islet autoimmunity.* J Immunol, 2009. **182**(1): p. 274-82.
50. Marengere, L.E., et al., *Regulation of T cell receptor signaling by tyrosine phosphatase SYP association with CTLA-4.* Science, 1996. **272**(5265): p. 1170-3.
51. Chikuma, S., J.B. Imboden, and J.A. Bluestone, *Negative regulation of T cell receptor-lipid raft interaction by cytotoxic T lymphocyte-associated antigen 4.* J Exp Med, 2003. **197**(1): p. 129-35.
52. Martin, M., et al., *Cytotoxic T lymphocyte antigen 4 and CD28 modulate cell surface raft expression in their regulation of T cell function.* J Exp Med, 2001. **194**(11): p. 1675-81.
53. Schneider, H. and C.E. Rudd, *Tyrosine phosphatase SHP-2 binding to CTLA-4: absence of direct YVKM/YFIP motif recognition.* Biochem Biophys Res Commun, 2000. **269**(1): p. 279-83.
54. Calvo, C.R., D. Amsen, and A.M. Kruisbeek, *Cytotoxic T lymphocyte antigen 4 (CTLA-4) interferes with extracellular signal-regulated kinase (ERK) and Jun NH2-terminal kinase (JNK) activation, but does not affect phosphorylation of T cell receptor zeta and ZAP70.* J Exp Med, 1997. **186**(10): p. 1645-53.
55. Schneider, H., et al., *Cutting edge: CTLA-4 (CD152) differentially regulates mitogen-activated protein kinases (extracellular signal-regulated kinase and c-*

Jun N-terminal kinase) in CD4+ T cells from receptor/ligand-deficient mice. J Immunol, 2002. **169**(7): p. 3475-9.
56. Olsson, C., et al., *CTLA-4 ligation suppresses CD28-induced NF-kappaB and AP-1 activity in mouse T cell blasts.* J Biol Chem, 1999. **274**(20): p. 14400-5.
57. Janes, P.W., S.C. Ley, and A.I. Magee, *Aggregation of lipid rafts accompanies signaling via the T cell antigen receptor.* J Cell Biol, 1999. **147**(2): p. 447-61.
58. Hodi, F.S., *Cytotoxic T-lymphocyte-associated antigen-4.* Clin Cancer Res, 2007. **13**(18 Pt 1): p. 5238-42.
59. Sakaguchi, S., et al., *Immunologic tolerance maintained by CD25+ CD4+ regulatory T cells: their common role in controlling autoimmunity, tumor immunity, and transplantation tolerance.* Immunol Rev, 2001. **182**: p. 18-32.
60. Walker, L.S., *Treg and CTLA-4: Two intertwining pathways to immune tolerance.* J Autoimmun, 2013.
61. Brunkow, M.E., et al., *Disruption of a new forkhead/winged-helix protein, scurfin, results in the fatal lymphoproliferative disorder of the scurfy mouse.* Nat Genet, 2001. **27**(1): p. 68-73.
62. Edinger, M., et al., *CD4+CD25+ regulatory T cells preserve graft-versus-tumor activity while inhibiting graft-versus-host disease after bone marrow transplantation.* Nat Med, 2003. **9**(9): p. 1144-50.
63. Belkaid, Y. and B.T. Rouse, *Natural regulatory T cells in infectious disease.* Nat Immunol, 2005. **6**(4): p. 353-60.
64. Fallarino, F., et al., *Modulation of tryptophan catabolism by regulatory T cells.* Nat Immunol, 2003. **4**(12): p. 1206-12.
65. Paust, S., et al., *Engagement of B7 on effector T cells by regulatory T cells prevents autoimmune disease.* Proc Natl Acad Sci U S A, 2004. **101**(28): p. 10398-403.
66. Wing, K., et al., *CTLA-4 control over Foxp3+ regulatory T cell function.* Science, 2008. **322**(5899): p. 271-5.
67. Munn, D.H., et al., *Inhibition of T cell proliferation by macrophage tryptophan catabolism.* J Exp Med, 1999. **189**(9): p. 1363-72.
68. Manches, O., et al., *HIV-activated human plasmacytoid DCs induce Tregs through an indoleamine 2,3-dioxygenase-dependent mechanism.* J Clin Invest, 2008. **118**(10): p. 3431-9.
69. Ravanfar, P., et al., *Existing antiviral vaccines.* Dermatol Ther, 2009. **22**(2): p. 110-28.
70. Leach, D.R., M.F. Krummel, and J.P. Allison, *Enhancement of antitumor immunity by CTLA-4 blockade.* Science, 1996. **271**(5256): p. 1734-6.
71. Peggs, K.S., et al., *Blockade of CTLA-4 on both effector and regulatory T cell compartments contributes to the antitumor activity of anti-CTLA-4 antibodies.* J Exp Med, 2009. **206**(8): p. 1717-25.
72. Curran, M.A. and J.P. Allison, *Tumor vaccines expressing flt3 ligand synergize with ctla-4 blockade to reject preimplanted tumors.* Cancer Res, 2009. **69**(19): p. 7747-55.
73. Mocellin, S. and D. Nitti, *CTLA-4 blockade and the renaissance of cancer immunotherapy.* Biochim Biophys Acta, 2013. **1836**(2): p. 187-196.

74. Hodi, F.S., et al., *Improved survival with ipilimumab in patients with metastatic melanoma.* N Engl J Med, 2010. **363**(8): p. 711-23.
75. Beck, K.E., et al., *Enterocolitis in patients with cancer after antibody blockade of cytotoxic T-lymphocyte-associated antigen 4.* J Clin Oncol, 2006. **24**(15): p. 2283-9.
76. Ribas, A., et al., *Antitumor activity in melanoma and anti-self responses in a phase I trial with the anti-cytotoxic T lymphocyte-associated antigen 4 monoclonal antibody CP-675,206.* J Clin Oncol, 2005. **23**(35): p. 8968-77.
77. Hoos, A., et al., *Improved endpoints for cancer immunotherapy trials.* J Natl Cancer Inst, 2010. **102**(18): p. 1388-97.
78. Chen, Z., et al., *Modeling CTLA4-linked autoimmunity with RNA interference in mice.* Proc Natl Acad Sci U S A, 2006. **103**(44): p. 16400-5.
79. Fire, A., et al., *Potent and specific genetic interference by double-stranded RNA in Caenorhabditis elegans.* Nature, 1998. **391**(6669): p. 806-11.
80. Elbashir, S.M., et al., *Duplexes of 21-nucleotide RNAs mediate RNA interference in cultured mammalian cells.* Nature, 2001. **411**(6836): p. 494-8.
81. Bernstein, E., et al., *Role for a bidentate ribonuclease in the initiation step of RNA interference.* Nature, 2001. **409**(6818): p. 363-6.
82. Gregory, R.I., et al., *Human RISC couples microRNA biogenesis and posttranscriptional gene silencing.* Cell, 2005. **123**(4): p. 631-40.
83. Jinek, M. and J.A. Doudna, *A three-dimensional view of the molecular machinery of RNA interference.* Nature, 2009. **457**(7228): p. 405-12.
84. Cai, X., C.H. Hagedorn, and B.R. Cullen, *Human microRNAs are processed from capped, polyadenylated transcripts that can also function as mRNAs.* Rna, 2004. **10**(12): p. 1957-66.
85. Lee, Y., et al., *The nuclear RNase III Drosha initiates microRNA processing.* Nature, 2003. **425**(6956): p. 415-9.
86. Yi, R., et al., *Exportin-5 mediates the nuclear export of pre-microRNAs and short hairpin RNAs.* Genes Dev, 2003. **17**(24): p. 3011-6.
87. Ohler, U., et al., *Patterns of flanking sequence conservation and a characteristic upstream motif for microRNA gene identification.* Rna, 2004. **10**(9): p. 1309-22.
88. Xia, H., et al., *siRNA-mediated gene silencing in vitro and in vivo.* Nat Biotechnol, 2002. **20**(10): p. 1006-10.
89. Yue, J., et al., *A miR-21 hairpin structure-based gene knockdown vector.* Biochem Biophys Res Commun, 2010. **394**(3): p. 667-72.
90. Lagos-Quintana, M., et al., *New microRNAs from mouse and human.* Rna, 2003. **9**(2): p. 175-9.
91. Reinhart, B.J., et al., *MicroRNAs in plants.* Genes Dev, 2002. **16**(13): p. 1616-26.
92. Sood, P., et al., *Cell-type-specific signatures of microRNAs on target mRNA expression.* Proc Natl Acad Sci U S A, 2006. **103**(8): p. 2746-51.
93. Jay, C., et al., *miRNA profiling for diagnosis and prognosis of human cancer.* DNA Cell Biol, 2007. **26**(5): p. 293-300.
94. Valoczi, A., et al., *Sensitive and specific detection of microRNAs by northern blot analysis using LNA-modified oligonucleotide probes.* Nucleic Acids Res, 2004. **32**(22): p. e175.

95. Ramkissoon, S.H., et al., *Nonisotopic detection of microRNA using digoxigenin labeled RNA probes.* Mol Cell Probes, 2006. **20**(1): p. 1-4.
96. Barad, O., et al., *MicroRNA expression detected by oligonucleotide microarrays: system establishment and expression profiling in human tissues.* Genome Res, 2004. **14**(12): p. 2486-94.
97. Chen, C., et al., *Real-time quantification of microRNAs by stem-loop RT-PCR.* Nucleic Acids Res, 2005. **33**(20): p. e179.
98. Lorenzo Malquori, L.C., Giovina Ruberti, *The 3′ UTR of the human CTLA4 mRNA can regulate mRNA*
stability and translational efficiency. Biochimica et Biophysica Acta, 2007. **1779**(1).
99. Xia, X.G., et al., *An enhanced U6 promoter for synthesis of short hairpin RNA.* Nucleic Acids Res, 2003. **31**(17): p. e100.
100. Freeley, M., et al., *Stimulus-induced phosphorylation of PKC theta at the C-terminal hydrophobic-motif in human T lymphocytes.* Biochem Biophys Res Commun, 2005. **334**(2): p. 619-30.
101. Elmarghani, A., H. Abuabaid, and P. Kjellen, *TOM1L is involved in a novel signaling pathway important for the IL-2 production in Jurkat T cells stimulated by CD3/CD28 co-ligation.* Mediators Inflamm, 2009. **2009**: p. 416298.
102. Baroja, M.L., et al., *The inhibitory function of CTLA-4 does not require its tyrosine phosphorylation.* J Immunol, 2000. **164**(1): p. 49-55.
103. Pistillo, M.P., et al., *CTLA-4 is not restricted to the lymphoid cell lineage and can function as a target molecule for apoptosis induction of leukemic cells.* Blood, 2003. **101**(1): p. 202-9.
104. Krummel, M.F. and J.P. Allison, *CTLA-4 engagement inhibits IL-2 accumulation and cell cycle progression upon activation of resting T cells.* J Exp Med, 1996. **183**(6): p. 2533-40.
105. Zhang, W., et al., *LAT: the ZAP-70 tyrosine kinase substrate that links T cell receptor to cellular activation.* Cell, 1998. **92**(1): p. 83-92.
106. Isakov, N., et al., *ZAP-70 binding specificity to T cell receptor tyrosine-based activation motifs: the tandem SH2 domains of ZAP-70 bind distinct tyrosine-based activation motifs with varying affinity.* J Exp Med, 1995. **181**(1): p. 375-80.
107. Kong, G., et al., *Distinct tyrosine phosphorylation sites in ZAP-70 mediate activation and negative regulation of antigen receptor function.* Mol Cell Biol, 1996. **16**(9): p. 5026-35.
108. Hermiston, M.L., Z. Xu, and A. Weiss, *CD45: a critical regulator of signaling thresholds in immune cells.* Annu Rev Immunol, 2003. **21**: p. 107-37.
109. Nyakeriga, A.M., H. Garg, and A. Joshi, *TCR-induced T cell activation leads to simultaneous phosphorylation at Y505 and Y394 of p56(lck) residues.* Cytometry A, 2012. **81**(9): p. 797-805.
110. Freeley, M., et al., *Loss of PTEN expression does not contribute to PDK-1 activity and PKC activation-loop phosphorylation in Jurkat leukaemic T cells.* Cell Signal, 2007. **19**(12): p. 2444-57.
111. Griffith, C.E., W. Zhang, and R.L. Wange, *ZAP-70-dependent and -independent activation of Erk in Jurkat T cells. Differences in signaling induced by H2o2 and Cd3 cross-linking.* J Biol Chem, 1998. **273**(17): p. 10771-6.

112. Shan, X., et al., *Deficiency of PTEN in Jurkat T cells causes constitutive localization of Itk to the plasma membrane and hyperresponsiveness to CD3 stimulation.* Mol Cell Biol, 2000. **20**(18): p. 6945-57.
113. Astoul, E., et al., *PI 3-K and T-cell activation: limitations of T-leukemic cell lines as signaling models.* Trends Immunol, 2001. **22**(9): p. 490-6.
114. Gupta, S., et al., *Selective interaction of JNK protein kinase isoforms with transcription factors.* Embo J, 1996. **15**(11): p. 2760-70.
115. Fraser, J.H., et al., *CTLA4 ligation attenuates AP-1, NFAT and NF-kappaB activity in activated T cells.* Eur J Immunol, 1999. **29**(3): p. 838-44.
116. Bennett, B.L., et al., *SP600125, an anthrapyrazolone inhibitor of Jun N-terminal kinase.* Proc Natl Acad Sci U S A, 2001. **98**(24): p. 13681-6.
117. Rao, D.D., et al., *siRNA vs. shRNA: similarities and differences.* Adv Drug Deliv Rev, 2009. **61**(9): p. 746-59.
118. Yu, Y., et al., *CTLA4 silencing with siRNA promotes deviation of Th1/Th2 in chronic hepatitis B patients.* Cell Mol Immunol, 2009. **6**(2): p. 123-7.
119. Mazurov, D., et al., *Role of O-glycosylation and expression of CD43 and CD45 on the surfaces of effector T cells in human T cell leukemia virus type 1 cell-to-cell infection.* J Virol, 2012. **86**(5): p. 2447-58.
120. Callen, B.P., K.E. Shearwin, and J.B. Egan, *Transcriptional interference between convergent promoters caused by elongation over the promoter.* Mol Cell, 2004. **14**(5): p. 647-56.
121. Laurent, S., et al., *CTLA-4 expressed by chemoresistant, as well as untreated, myeloid leukaemia cells can be targeted with ligands to induce apoptosis.* Br J Haematol, 2007. **136**(4): p. 597-608.
122. Abraham, R.T. and A. Weiss, *Jurkat T cells and development of the T-cell receptor signalling paradigm.* Nat Rev Immunol, 2004. **4**(4): p. 301-8.
123. Farr, A. and A. Roman, *A pitfall of using a second plasmid to determine transfection efficiency.* Nucleic Acids Res, 1992. **20**(4): p. 920.
124. Wurm, F.M., *Production of recombinant protein therapeutics in cultivated mammalian cells.* Nat Biotechnol, 2004. **22**(11): p. 1393-8.
125. Lagos-Quintana, M., et al., *Identification of novel genes coding for small expressed RNAs.* Science, 2001. **294**(5543): p. 853-8.
126. Guntermann, C. and D.R. Alexander, *CTLA-4 suppresses proximal TCR signaling in resting human CD4(+) T cells by inhibiting ZAP-70 Tyr(319) phosphorylation: a potential role for tyrosine phosphatases.* J Immunol, 2002. **168**(9): p. 4420-9.
127. Pandiyan, P., et al., *CD152 (CTLA-4) determines the unequal resistance of Th1 and Th2 cells against activation-induced cell death by a mechanism requiring PI3 kinase function.* J Exp Med, 2004. **199**(6): p. 831-42.
128. Schneider, H., et al., *CTLA-4 activation of phosphatidylinositol 3-kinase (PI 3-K) and protein kinase B (PKB/AKT) sustains T-cell anergy without cell death.* PLoS One, 2008. **3**(12): p. e3842.
129. Bartelt, R.R., et al., *Comparison of T cell receptor-induced proximal signaling and downstream functions in immortalized and primary T cells.* PLoS One, 2009. **4**(5): p. e5430.
130. Kon-Kozlowski, M., et al., *The tyrosine phosphatase PTP1C associates with Vav, Grb2, and mSos1 in hematopoietic cells.* J Biol Chem, 1996. **271**(7): p. 3856-62.

131. Han, Z., et al., *c-Jun N-terminal kinase is required for metalloproteinase expression and joint destruction in inflammatory arthritis.* J Clin Invest, 2001. **108**(1): p. 73-81.
132. Hoff, H., et al., *CTLA-4 (CD152) inhibits T cell function by activating the ubiquitin ligase Itch.* Mol Immunol, 2010. **47**(10): p. 1875-81.
133. Gao, M., et al., *Jun turnover is controlled through JNK-dependent phosphorylation of the E3 ligase Itch.* Science, 2004. **306**(5694): p. 271-5.

7. Appendix I

1 x TBE Buffer

Add 1000 ml of 10xTBE buffer (Invitrogen) to 9000 ml of distilled H_2O.

1% agarose gel

Add 1 g agarose (Invitrogen) to 100 ml of 1xTBE buffer and boil until the agarose has dissolved. Let to cool to 60°C and add 7 µl of ethidium bromide (10 mg/ml). Mix and pour into gel tray.

6xloading buffer

0.25% bromphenol blue (BDH)

0.25% xylene cyanol (BDH)

30% glycerol (BDH)

In distilled H_2O

Phenol/chloroform/isoamyl alcohol

49 ml phenol (Sigma)

49 ml chloroform (Sigma)

2 ml isoamyl alcohol (Sigma)

Mix, aliquot and freeze at -20°C

70% Ethanol

70 ml 100% ethanol (Sigma)

30 ml of distilled H_2O

TE buffer

10 mM Tris (appendix I)

1mM EDTA (appendix I)

pH 8

1M Tris

12.1 g Tris (BDH)

100 ml of distilled H_2O; adjust pH to 7 using HCl; autoclave

0.5M EDTA

18.1 g EDTA (Sigma)

100 ml of distilled H_2O; adjust pH to 7 using NaOH; autoclave

5M NaCl

73 g NaCl (Sigma)

250 ml of distilled H_2O; autoclave

Cell lysis solution

25mM EDTA

2% SDS

In distilled H_2O

Protein precipitation solution

10M ammonium acetate

In distilled H_2O

1M Sodium carbonate

10.5 g sodium carbonate (BDH)

100 ml distilled H_2O; autoclave

0.1M $CaCl_2$

5.5 g $CaCl_2$

250 ml of distilled H_2O; autoclave

LB broth

10 g Bacto-Tryptone (Lab M Limited)

10 g NaCl (Sigma)

5 g Yeast (Lab M Limited)

1L of distilled H_2O; autoclave

LB agar

3 g Bacto-Tryptone (Lab M Limited)

3 g NaCl (Sigma)

1.5 g Yeast (Lab M Limited)

4.5 g agar (Lab M Limited)

300 ml of distilled H_2O; autoclave; cool to 60°C and add 150 µl of ampicillin (100 mg/ml)

100 mg/ml Ampicillin

100 mg ampicillin

1 ml of sterile H_2O; filter solution and freeze at -20°C

SOC medium

4 g Bacto-Tryptone (Lab M Limited)

0.1 g NaCl (Sigma)

1 g Yeast (Lab M Limited)

2 ml 250mM KCl

1 ml 2M $MgCl_2$

Add 196 ml of distilled H_2O; adjust pH to 7 with 1M NaOH; autoclave

Add 4 ml of sterile filtered 1 M glucose under sterile conditions

2M $MgCl_2$

19 g $MgCl_2$ (Sigma)

100 ml of distilled H_2O

1M Glucose

18 g glucose (Sigma)

100 ml of distilled H_2O; sterile filtered

10xTBS

12.1 g Tris

87.6 g NaCl

1 L distilled H_2O; adjust pH to 7.6 with HCl

1xTBST

100 ml 10xTBS

1 ml Tween 20 (Sigma)

900 ml of distilled H_2O

10% APS

0.1 g ammonium persulfate (Sigma)
1 ml of distilled H_2O

10xRunning buffer

30 g Tris (Sigma)

144 g glycine (Sigma)

10 g SDS (Sigma)

1L of distilled H_2O

4xUpper buffer

12.11 g Tris (Sigma)

0.8 g SDS (Sigma)

200 ml of distilled H_2O; adjust pH to 6.8 with HCl

4xLower buffer

36.34 g Tris (Sigma)

0.8 g SDS (Sigma)

200 ml of distilled H_2O; adjust pH to 8.8 with HCl

12% Trenn gel

2.5 ml Lower buffer

4 ml 30% acrylamide/Bis solution (Biorad)

0.1 ml 10% APS

8 µl TEMED (Sigma)

3.3 ml of distilled H_2O

5% Sammel gel

0.4 ml Upper buffer

0.5 ml 30% acrylamide/Bis solution (Biorad)

30 µl 10% APS

5 µl TEMED (Sigma)

2.1 ml of distilled H_2O

6x loading buffer

0.242 g Tris (Sigma)

8 ml 10% SDS

6 mg bromphenol blue

4 ml glycerol (Sigma)

Add water up to 20 ml; aliquot 1 ml and freeze at -20°C; before use add 50 µl 1M (DTT)

10xTransfer buffer

30.3 g Tris (Sigma)

144.1 g glycine (Sigma)

1L of of distilled H_2O; adjust pH to 8.3

5% blocking solution

5g skimmed milk (Dunnes)

100 ml 1xTBST

RIPA buffer

50mM Tris, pH 7.4

150 mM NaCl

1mM NaF

1mM EDTA

1% NP-40

In distilled H_2O; aliquot in 1 ml tubes and freeze at -20°C; add 1 µl of protease inhibitors cocktail (Calbiochem) before use

Stripping buffer

1% w/v SDS

62.5 mM Tris-HCl (pH 6.8)

100 mM β-mercaptoethanol (14.3M)

In distilled H_2O

0.02% EDTA in PBS

7.4 g EDTA (Sigma)

1L of sterile PBS

X-gal staining solution

0.2% X-gal

2mM $MgCl_2$

5mM $K_4Fe(CN)_6x3H_20$

5mM $K_3Fe(CN)_6$ in PBS

Appendix II

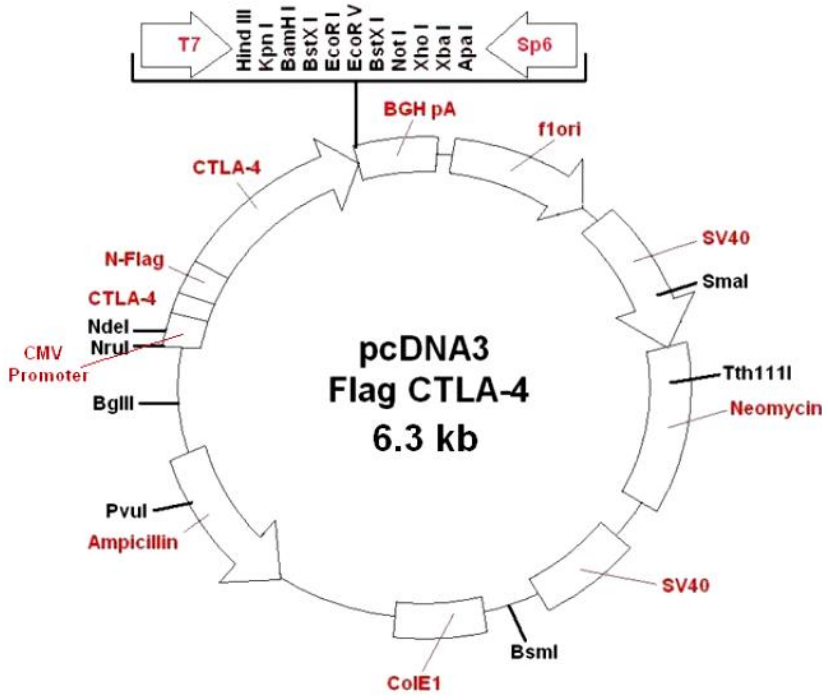

Fig.6.1. Vector map of pCTLA4-Flag (a gift from G. Ruberti [98])

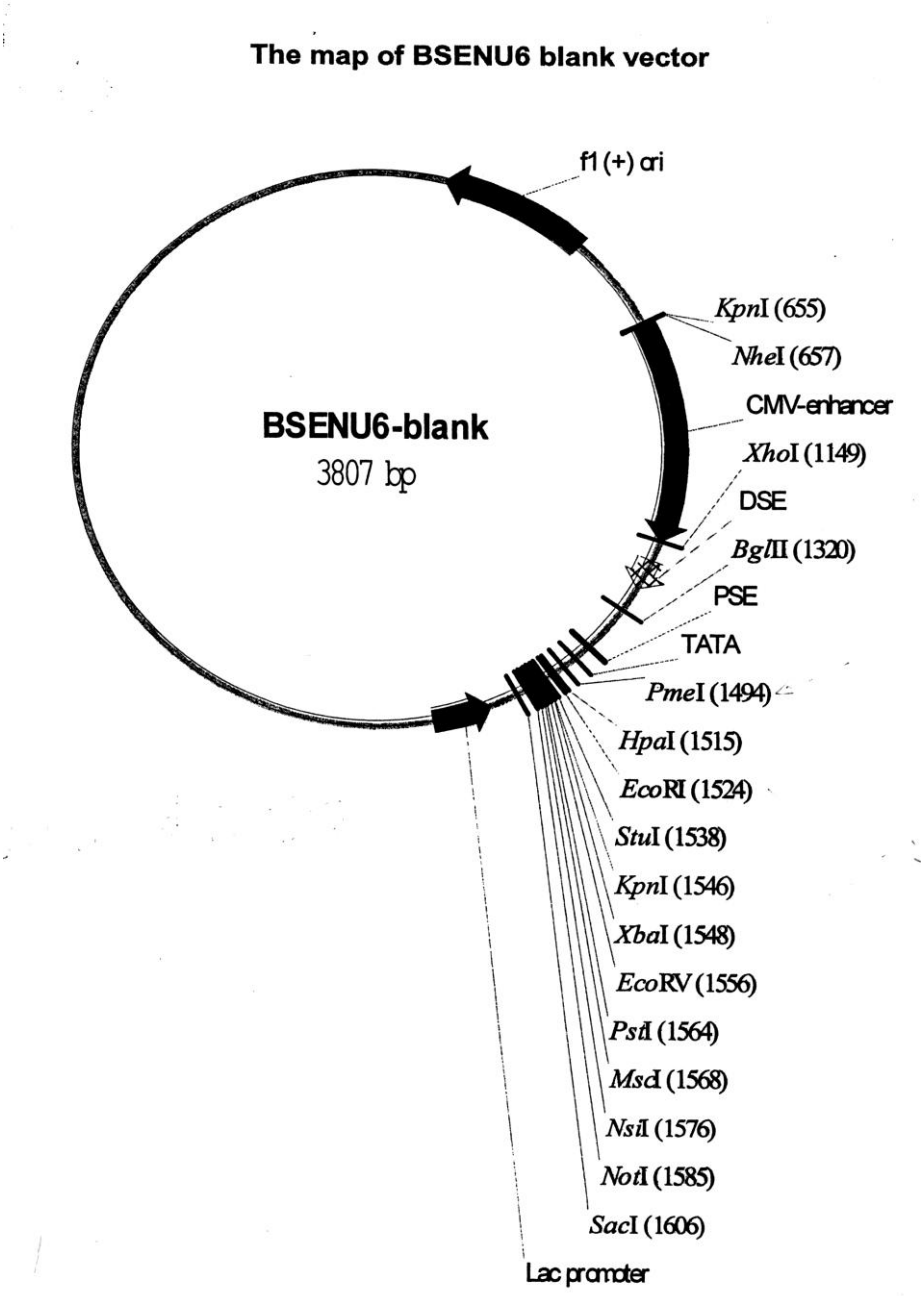

Fig.6.2. Vector map of pBSU6, a gift from Xu, Z [99].

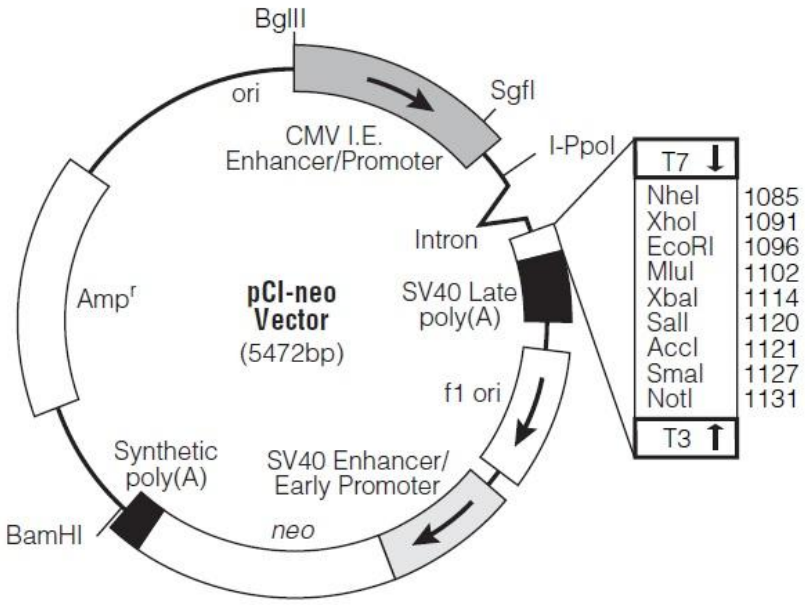

Fig.6.3. Vector map of pCIneo (Promega)

A)

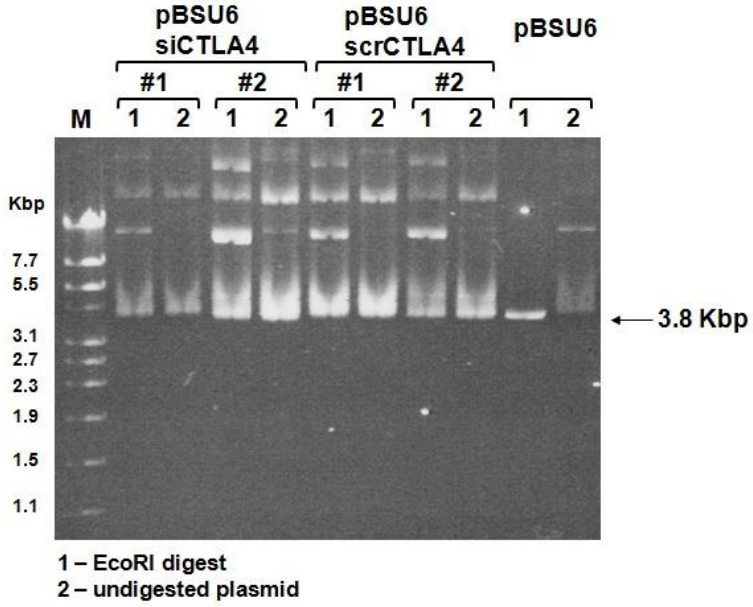

B)

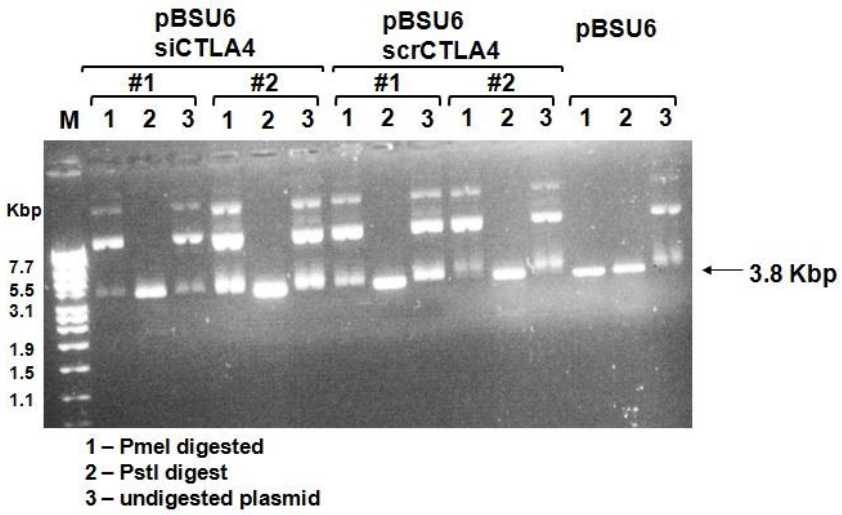

Fig.6.4. Restriction digest of different clones that express the pBSU6 siCTLA4, pBSU6 scrCTLA4 and pBSU6 vector.

Two clones #1 and #2 were tested for each plasmid pBSU6 siCTLA4 and pBSU6 scrCTLA4, and compared to the control vector pBSU6. (A) DNA samples were digested with EcoRI (1) or left untreated (2). Upon successful introduction of the insert, the EcoRI restriction site should be destroyed. (B) DNA samples were digested with PmeI (1), PstI (2) or left untreated (3). Upon successful introduction of the insert, the PmeI restriction site should be destroyed but the PstI restriction site should remain.

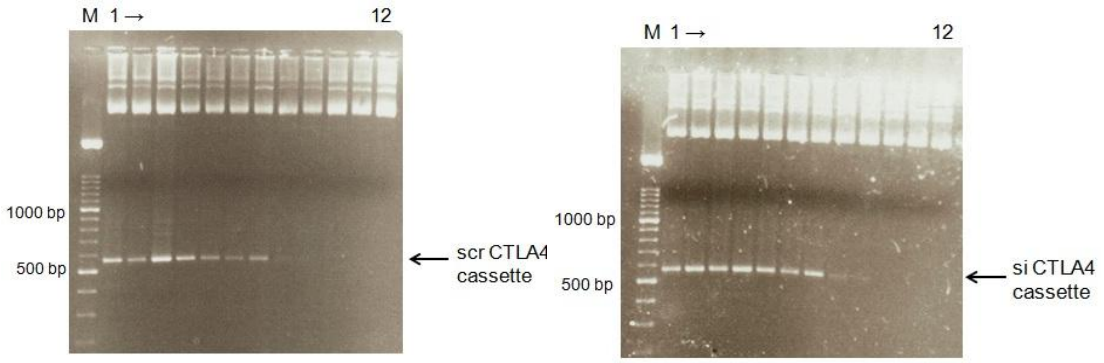

Fig. 6.5. PCR amplification of the shRNA cassette from pBSU6siCTLA4 and pBSU6scrCTLA4 using primers shCTLA4 Fr and shCTLA4 Rev (Table 2.2).

The optimal annealing temperature for the shCTLA4 Fr and the shCTLA4 Rev primers was tested in PCR amplification reactions using pBSU6siCTLA4 or pBSU6scrCTLA4 plasmid DNA as a template. The annealing temperature varied increasing from 55°C for lane 1 to 66°C for lane 12.

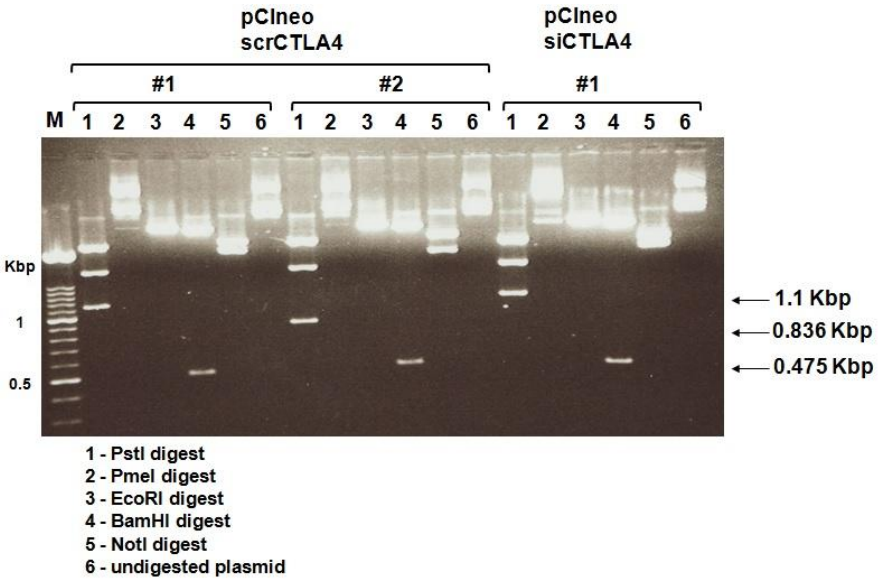

Fig. 6.6. Restriction digest of different clones that express pCIneo scrCTLA4 and pCIneo siCTLA4.

Two clones #1 and #2 were tested for pCIneo scrCTLA4 and one #1 for pCIneo siCTLA4. Depending on the direction of the insert the size of the resulting bands upon restriction with

some of the enzymes could be slightly different. Expected sizes are shown in the table below (Orientation A vs Orientation B). The results show that the insert is incorporated in the original pCIneo plasmid in all three clones. In all three clones the digestion with BamHI (lane 4 for each clone), which site was used for the cloning of the shRNA cassette, results in restriction of the newly generated plasmids into two pieces: 5472 bp band (representing the original pCIneo vector) and 475 bp band (representing the insert). The PstI digest (lane 1 for each clone) gives information about the orientation of the insert. It shows that for clone #1 with pCIneo scrCTLA4 and clone #1 with for pCIneo siCTLA4 the insert has 'Orientation A'. Clone #2 incorporating the pCIneo scrCTLA4 contains the insert with 'Orientation B'. This is also confirmed by the results from the NotI digest (lane 5). Better separation of the two resulting bands in clone #2 (pCIneo scrCTLA4) is visible on the gel due to the bigger difference between the expected sizes (Orientation B), compared to the other two clones (Orientation A).

Enzyme	Orientation A (bp)	Orientation B (bp)
PstI	1806 + 1121 + 3020	1806 + 836 + 3305
PmeI	No digest	No digest
EcoRI	5947	5947
BamHI	475 + 5472	475 + 5472
NotI	2655 + 3292	2328 + 3619

For further experiments and transfection of cells plasmid DNA from clone #1 containing pCIneo scrCTLA4 and clone #1 containing pCIneo siCTLA4 were used.

A) B)

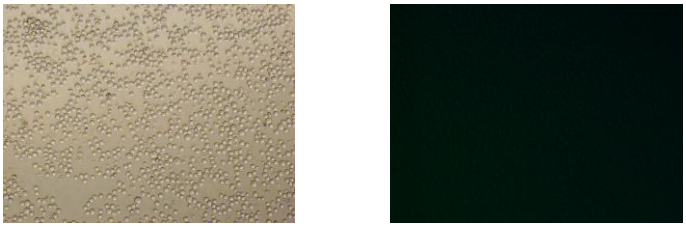

Fig. 6.7. Transient transfection of Jurkats.

Jurkats were transiently transfected with FuGENE (Roche) and pmaxGFP plasmid DNA. Transgene expression of GFP was analysed after 24h. A) Brightfield. B) GFP expression. Magnification 100x.

HeLa + pBSU6neo		HeLa + pBSU6neo scrCTLA4		HeLa + pBSU6neo siCTLA4	
CTLA4	GAPDH	CTLA4	GAPDH	CTLA4	GAPDH
19.73	14.56	19.82	14.3	23.48	14.71
19.97	14.92	19.96	14.35	23.22	14.85
19.77	14.8	19.94	14.48	23.12	14.9

Table 6.1. Ct values used to calculate the relative expression of CTLA4 for figure 2.12.

HeLa		HeLa F1		HeLa F2		HeLa F3	
CTLA4	GAPDH	CTLA4	GAPDH	CTLA4	GAPDH	CTLA4	GAPDH
39.36	14.38	36.05	14.43	37.24	13.91	35.84	14.3
39.84	14.53	35.51	14.27	36.72	14.05	35.53	14.23
40.03	14.62	35.58	14.52	36.63	14.25	35.92	14.14

HeLa F4		HeLa F5		HeLa F6	
CTLA4	GAPDH	CTLA4	GAPDH	CTLA4	GAPDH
33.89	14.04	34.87	14.48	34.19	14.28
33.69	14.07	34.8	14.29	33.95	13.96
33.83	14.12	35.17	14.56	34.27	14.13

Table 6.2. Ct values used to calculate the relative expression of CTLA4 for figure 2.13

HeLa F4+ pBSU6neo		HeLa F4+ pBSU6neo scrCTLA4		HeLa F4 + pBSU6neo siCTLA4	
CTLA4	GAPDH	CTLA4	GAPDH	CTLA4	GAPDH
33.32	14.68	33.96	14.97	35.49	14.89
33.87	14.96	33.78	14.82	35.67	15.26
33.41	14.62	34.11	14.87	35.64	15.38

Table 6.3. Ct values used to calculate the relative expression of CTLA4 for figure 2.14

HeLa		HeLa + pCTLA4 Flag		PBMC + PMA/ionomycin		Jurkat + PMA/ionomycin	
CTLA4	GAPDH	CTLA4	GAPDH	CTLA4	GAPDH	CTLA4	GAPDH
36.9	16.8	24.54	16.3	29.04	17.03	34.22	16.5
36.93	16.7	24.52	16.37	28.74	17.05	33.9	16.7
36.54	16.9	24.9	16.5	28.84	17.2	33.75	16.75

Table 6.4. Ct values used to calculate the relative expression of CTLA4 for figure 3.2 B

0 h		6 h		12 h		24 h	
CTLA4	GAPDH	CTLA4	GAPDH	CTLA4	GAPDH	CTLA4	GAPDH
39.5	14.4	39.17	13.84	35.12	15.38	33	17.08
40.79	14.78	39.1	14	36.48	14.98	35.24	17.33
39.61	14.28	38.61	14.23	35.91	15.43	34.55	17.56
2 d		3 d		4 d		5 d	
CTLA4	GAPDH	CTLA4	GAPDH	CTLA4	GAPDH	CTLA4	GAPDH
31.45	17.2	30.88	16.91	32.96	17.85	33.08	16.12
32.5	16.84	32.44	16.88	32.05	16.91	33.9	16.26
31.7	16.93	31.3	16.83			32.82	16.04

Table 6.5. Ct values used to calculate the relative expression of CTLA4 for figure 3.3. Jurkats were stimulated with PMA/ionomycin for different periods of time.

Jurkat WT		Jurkat WT + PMA/ionomycin		Jurkat-ev + PMA/ionomycin		Jurkat-scr + PMA/ionomycin		Jurkat-si + PMA/ionomycin	
CTLA4	GAPDH	CTLA4	GAPDH	CTLA4	GAPDH	CTLA4	GAPDH	CTLA4	GAPDH
36.84	16.84	34.22	16.5	34.24	17.08	33.44	16.84	37.7	16.72
36.54	16.9	33.9	16.7	33.97	17.2	33.53	16.8	37	17.2
36.53	16.8	34.1	16.8	33.85	17.1	33.68	16.9	37.31	17.65

Table 6.6. Ct values used to calculate the relative expression of CTLA4 for figure 3.11.